A STUDY OF SETTLEMENT OF STONE COLUMNS
BY FINITE ELEMENT MODELING
THROUGH CASE HISTORIES

A THESIS SUBMITTED TO
THE GRADUATE SCHOOL OF NATURAL AND APPLIED SCIENCES
OF
MIDDLE EAST TECHNICAL UNIVERSITY

BY

CEMRE HARZEM YARDIM

IN PARTIAL FULFILLMENT OF THE REQUIREMENTS
FOR
THE DEGREE OF THE MASTER OF SCIENCE
IN
CIVIL ENGINEERING

JANUARY 2013

Approval of the thesis:

A STUDY OF SETTLEMENT OF STONE COLUMNS BY FINITE ELEMENT MODELING THROUGH CASE HISTORIES

submitted by **CEMRE HARZEM YARDIM** in partial fulfillment of the requirements for the degree of **Master of Science in Civil Engineering Department, Middle East Technical University** by,

Prof. Dr. Canan Özgen
Dean, Graduate School of **Natural and Applied Science** ______________

Prof. Dr. Ahmet Cevdet Yalçıner
Head of Department, **Civil Engineering** ______________

Prof. Dr. Mehmet Ufuk Ergun
Supervisor, **Civil Engineering** ______________

Examining Committee Members:

Prof. Dr. Bahadır Sadık Bakır
Civil Engineering Dept., METU ______________

Prof. Dr. Mehmet Ufuk Ergun
Civil Engineering Dept., METU ______________

Asst. Prof. Dr. Nejan Huvaj Sarıhan
Civil Engineering Dept., METU ______________

Dr. Onur Pekcan
Civil Engineering Dept., METU ______________

Dr. Maral Tekin
Geomed Geotechnical Consultancy,
Investigation, Supervision & Trd. Co. Inc. ______________

Date: ______________

I hereby declare that all information in this document has been obtained and presented in accordance with academic rules and ethical conduct. I also declare that, as required by these rules and conduct, I have fully cited and referenced all material and results that are not original to this work.

Name, Last name : Cemre Harzem Yardım

Signature :

ABSTRACT

A STUDY OF SETTLEMENT OF STONE COLUMNS BY FINITE ELEMENT MODELING THROUGH CASE HISTORIES

Yardım, Cemre Harzem
M.Sc., Department of Civil Engineering
Supervisor: Prof. Dr. Mehmet Ufuk Ergun

January 2013, 106 pages

Stone column technique is mostly used to reinforce soft cohesive soils. Settlements are decreased under foundations and bearing capacity is increased. This study initially focuses on a comprehensive review of literature about stone column reinforced soils. Afterwards, numerical modeling of stone column reinforced soft clays is done. Three different cases are chosen on different foundation soils mainly soft clays. Parametric studies are done to determine influence of parameters on settlement reduction ratio under three different foundation conditions. Analyses are converted to two dimensional conditions and this conversion is also compared within the scope of this study. Settlement reduction ratio response to variation in parameters revealed similar results under three different foundation conditions.

Keywords: Finite Element Analysis, Settlement Reduction Ratio, Soft Clay, Stone column

ÖZ

VAKA ANALİZLERİ ÜZERİNDEN SONLU ELEMAN MODELLEMESİYLE TAŞ KOLONLARIN OTURMASINA İLİŞKİN BİR ÇALIŞMA

Yardım, Cemre Harzem
Yüksek Lisans, İnşaat Mühendisliği Bölümü
Tez Yöneticisi: Prof. Dr. Mehmet Ufuk Ergun

Ocak 2013, 106 sayfa

Taş kolon uygulaması genellikle yumuşak kohezyonlu zeminleri güçlendirmek için kullanılmaktadır. Temellerin oturma miktarı azaltılmakta ve taşıma gücü artırılmaktadır. Bu çalışma öncelikle, taş kolon ile güçlendirilmiş zeminler hakkındaki literatürün kapsamlı olarak incelenmesi üzerine odaklanmıştır. Daha sonra, taş kolonlarla güçlendirilmiş zayıf kil zeminlerin sayısal modellemesi yapılmıştır. Esas olarak yumuşak killerden oluşan değişik temel zeminlerinde üç vaka seçilmiştir. Bu üç farklı zemin koşulu altında parametrelerin oturma azaltma oranı üzerindeki etkileri parametrik çalışma yapılarak incelenmiştir. Analizler iki boyuta dönüştürülmüş ve bu dönüşüm de çalışma kapsamında karşılaştırılmıştır. Oturma azaltma oranının parametre değişimine gösterdiği tepkilerin üç farklı zemin koşulu altında benzerlik gösterdiği saptanmıştır.

Anahtar Kelimeler: Sonlu Elemanlar Analizi, Oturma Azaltma Oranı, Zayıf Kil, Taş Kolon

To My Family

ACKNOWLEDGEMENTS

I would like to thank my advisor Prof. Dr. Mehmet Ufuk Ergun for his guidance and support throughout the preparation of this thesis.

My next appreciation goes to Salih Aksoy and Dr. Maral Tekin from Geomed Co. Inc. I believe this thesis would not be completed without their contributions.

I respectfully commemorate my grandfathers Hasan Hüsnü Yardım and Nihat Demirel and my grandmother Fatma İkbal Yardım, who we have lost in the last five years.

I am very grateful to my beloved family Ahmet Hamdi Yardım, Serpil Yardım, Berna Hande Yardım and Sevim Demirel, who continuously supported me, provided guidance and understanding at any time in my life.

Last but not the least, sincere thanks to my colleagues Melih Türkoğlu, Mert Levendoğlu, Gökhan Özyurt, Serhan Ergin and Tolga Kurt for their endless help and support at even the most difficult times during the preparation of this thesis.

TABLE OF CONTENTS

LIST OF TABLES

TABLES

LIST OF FIGURES

FIGURES

LIST OF ABBREVIATIONS

α_m	CPT Correlation Coefficient
a_r	Area Replacement Ratio
β	Shear strength – Modulus Coefficient
c’	Apparent Cohesion
C_c	Compression Index
C_r	Recompression Index
c_u	Undrained Shear Strength
c_v	Coefficient of Consolidation
D	Diameter of Stone Column
d_e	Domain of Influence
E’	Drained Modulus of Elasticity
e_0	Initial Void Ratio
E_{50}^{ref}	Secant Stiffness in Standrad Drained Triaxial Test
E_{oed}^{ref}	Tangent Stiffness for Primary Oedometer Loading
E_u	Undrained Modulus of Elasticity
E_{ur}^{ref}	Unloading / Reloading Stiffness
ϕ'	Effective Internal Angle of Shearing Resistance
γ_{bulk}	Bulk Unit Weight
γ_{dry}	Dry Unit Weight
G_s	Specific Gravity
γ_{sat}	Saturated Unit Weight
γ_w	Unit Weight of Water
H	Thickness
HS	Hardening Soil
K	Modulus Number
K_0	Coefficient of Earth Pressure at Rest
k_h	Horizontal Permeability

k_v	Vertical Permeability
LL	Liquid Limit
m	Power for Stress-Level Dependency of Stiffness
MC	Mohr Coulomb
m_v	Coefficient of Volume Compressibility
n	Modulus Exponent
ν'	Drained Poisson's Ratio
ν_{ur}	Poisson's Ratio for Unloading-Reloading
P_a	Atmospheric Pressure
PI	Plasticity Index
PL	Plastic Limit
p^{ref}	Reference Stress for Stiffnesses
q_c	CPT Tip Resistance
R_f	Failure Ratio
S	Spacing of Stone Column
s	Settlement
σ'_0	Initial Effective Overburden Pressure
σ'_3	Effective Confining Pressure
σ'_c	Preconsolidation Pressure
S_d	Degree of Saturation
S_r	Settlement Reduction Ratio
w	Equivalent Strip Width
w_n	Water Content
ψ	Angle of Dilation
$\Delta\sigma$	Additional Load

CHAPTER 1

INTRODUCTION

Stone column (i.e., granular pile) reinforcement method consists of partial replacement of loose and/or soft soil with vertical columns composed of compacted stone or granular material. Stone Columns (SCs) have been extensively used under large raft foundations and embankments.

SC installation was first utilized in 1830 by French military engineers (Hughes & Withers, 1974). About 100 years later, this technique was further developed in Germany by employing vibration (Baumann and Bauer (1974) and Greenwood and Kirsch (1984)). In 1955, Japanese engineers rediscovered the method called “Compozer” which uses a similar technique. Technique is comprised of large diameter sand columns which are used to form a composite foundation (Aboshi et al.,1979).

SCs reinforce the soft soil by reducing compressibility and increasing bearing capacity, the mechanism of which is different from that of rigid piles as rigid piles bypass the soft ground. SC installation can reduce the settlements up to 50% compared to untreated case for both cohesive and cohesionless soils under large areas (Bachus & Barksdale, 1989). Other advantages of SCs can be classified as; allow faster consolidation in cohesive soils, mitigate liquefaction and improve stability.

1.1 Problem Statement

Based on the close examination of the literature, the following points require further evaluation.

There exist two types of SC. If SC penetrates firm strata, it is called end-bearing type SC. When SC partially penetrates firm strata, it is known as floating type SC. Effects of soil parameters on settlement reduction ratio (settlement of treated ground over untreated one) are investigated for end-bearing type SC reinforced foundation.

Analyzed cases are simplified into 2D conditions. In addition, three dimensional analyses are undertaken to discuss and compare 2D and 3D models. Concern is raised from dissipation path differences that may occur between 2D and 3D FE models.

Two different material models are used to model the soft soil foundation behavior. These two models are also compared in this study.

1.2 Research Objectives

This study mainly focuses on three issues presented below.

To investigate settlement reduction ratio variation for end-bearing SC reinforced foundation, effect of soil parameters need to be studied by using finite element (FE) modeling.

To compare conversion of the problem, two dimensional and three dimensional FE analyses are undertaken.

To compare two different material models that are planned to model the soft soil foundation.

1.3 Scope

The main scope of this thesis is described as; investigation of effect of soil parameters on settlement reduction ratio (S_r), comparison of simplification of three dimensional problem into two dimensional one and comparison of two different material models that are planned to model the soft soil.

Based on the nature of the study and due to time constraints, FE analyses are limited only to the clay foundation reinforced with SC. Soft clay (c_u>15-25 kPa), very soft clay (c_u<15-25 kPa) and interlayered soft clay cases are covered in this study.

Study is limited to the data of the case histories. This limitation narrowed the investigation to the case of end-bearing type SC case histories.

As the static loading conditions are considered, seismically induced loading is also excluded from this study.

1.4 Method

In this study, a widespread loading and a tank foundation loading of soft soil reinforced with stone columns are investigated throughout FE modeling. This modeling technique is explained in detail later in Chapter 3. Plane strain or axisymmetric condition is assumed and simulated under 2D conditions. In addition, three dimensional analyses are done.

CHAPTER 2

BEHAVIOR OF STONE COLUMNS

The behavior of stone columns (SCs) has been well studied in the literature. This chapter highlights the previous works that contributed to the development of knowledge related SCs at various stages. These are (i) design, (ii) installation, (iii) field performance, (iv) studies performed in the laboratory and (v) modeling works.

2.1 Design

The design of SCs can be performed using either analytical or empirical approaches. With time, the empirical portion of the design has diminished and the analytical approaches have become more popular. In both approaches, the bearing capacity and settlement are considered together with the consolidation rate of SC reinforced foundation.

The "unit cell" concept was used in most of the previous studies. In this concept, area of one single column together with the area of corresponding soil (depending on the distribution and spacing of columns) is considered for the analysis.

2.1.1 Bearing Capacity of Stone Column Reinforced Foundation

Different failure mechanisms for SC have to be considered in design phase, such as bulging (Hughes & Withers, 1974), general shear failure (Madhav & Vitkar, 1978), and sliding (Aboshi et al.,1979).

Drained tests were performed in laboratory to investigate the behavior of single stone column by Hughes and Withers (1974). Assuming the soil as an elasto-plastic material, Gibson and Anderson (1961) formulated the limiting radial stress as given in Eq. (2.1).

$$\sigma_{rL} = \sigma_{r0} + c\left(1 + ln\frac{E}{2c(1+\upsilon)}\right) \tag{2.1}$$

where σ_{r0} is the total in-situ lateral stress, c is the undrained cohesion, E is the elastic modulus and ν is the Poisson's ratio of the soil. This equation, with the evaluation of quick expansion pressuremeter test data, can be approximated to the Eq. (2.2).

$$\sigma_{rL} = \sigma_{r0} + 4c + u \tag{2.2}$$

where u is the pore pressure. Pore pressure is taken as zero due to the drainage into the column (Hughes et al.,1976). The effective vertical stress at which the column can carry as it bulges is given in Eq. (2.3).

$$\sigma'_V = \frac{(1 + sin\emptyset_c{}')}{(1 - sin\emptyset_c{}')}(\sigma_{r0} + 4c) \tag{2.3}$$

where ϕ_c' is the effective angle of shearing resistance of the column.

Axial capacity of the single column was calculated using the minimum value of limiting radial stress which would possibly occur at critical length of the column as described in Hughes et al. (1976). Critical length is defined as the occurrence of bulging failure and end bearing failure simultaneously. It can be found from Eq. (2.4).

$$p = cA_s + N_c \bar{c} A_c \tag{2.4}$$

Where p is the ultimate column load, c is the average shaft cohesion, A_s (=πDL_c) is the surface area of the column with diameter D, N_c is the bearing capacity factor (usually taken as 9 for long columns), $\bar{c}$ is the cohesion at the bottom of the column and A_c (=πD^2/4) is the column area with diameter D. Ultimate column load is then calculated from the effective vertical stress that column can carry as it bulges (Hughes & Withers, 1974).

Madhav and Vitkar (1978) presented a solution for the ultimate bearing capacity of a strip footing on a granular trench, the extension of granular piles by constructing them along one dimension, based on the general shear failure mechanism. Upper bound theorem was used to obtain the bearing capacity and charts were given in the paper as a result of the parametric studies.

Bachus and Barksdale (1989) calculated the ultimate bearing capacity of a single column from the Eq. (2.5).

$$q_{ult} = c.N_c' \tag{2.5}$$

where c is the undrained shear strength of the soil and N'_c is a bearing factor varies from 18 to 25. Lower limit of N'_c is for soils with PI is greater than 30 or organic soils. Other bearing capacity factor may be added to the above equation in the case of treating cohesionless soils. Value of factor of safety generally varies from 1.5 to 2.0 depending on field test is conducted or not, respectively.

According to Greenwood and Kirsch (1984), 5 degrees deviation of friction angle of SC has small effect on ultimate capacity of column.

Datye (1982) stated that, practical failure problem reduces to bulging by constructing a granular mat above stone columns and selecting suitable diameter and depth for stone columns. It is not necessary to construct end bearing columns when the major concern is the ultimate capacity of stone columns. Ultimate capacity values ranging between 65 c_u to 95 c_u and, 50 c_u to 62 c_u were reached at Kandla site and Raoli Hill site, respectively, as opposed to the values given elsewhere as 25 c_u.

Bouassida et al. (1995) indicated that bearing capacity enhancement factor (ratio of the treated bearing capacity to that of untreated) value falls between 1.0 and 1.5 for footing reinforced by group of columns with ϕ_c=35°-40° and a_r=0.2.

Bouassida et al. (2009) presented the lower bound of bearing capacity for a foundation resting on a soil extending very deep reinforced by a group of floating columns. Unit weight was not taken into account in the analysis. The soil and column were assumed to be isotropic, homogeneous and perfect adhesion was assumed between soil and column interface. This is illustrated with an example for stone column case where H_{max}=14.2m from limit analysis and H_{min}=3.7m (very small) from Brauns (1978) method in which the minimum length is found from equaling external force effect to zero.

Frikha et al. (2008) presented the ultimate bearing capacity of a single isolated column (based on cavity expansion) constructed in purely cohesive clay. Soft clay was assumed to behave as an elastoplastic material governed by a thin dilatant zone around column.

Calibration of the presented formula was done with the load tests of Bergado and Lam (1987). As a result of the calibration, dilatancy angle of the thin dilatant zone should be between 8 and 15 degrees.

Kurka and Zavoral (2009) presented an analytical method for the determination of stresses and strains in soft soil reinforced with stone columns. Change of Poisson's ratio in soil at the vicinity of the columns affected the outcome remarkably.

2.1.2 Settlement of Stone Column Reinforced Foundation

As stated in McCabe et al. (2007), European practice mostly preferred to use Priebe's method. Sometimes, Baumann and Bauer (1974) method is also used in the Europe. In the United States, Goughnour and Bayuk (1979a) approach is preferred. Approach of Goughnour and Bayuk (1979a) requires additional tests.

The "unit cell" concept was used by Priebe (1995). Solution was given for end-bearing type columns assuming column material was incompressible with both soil and column bulk densities were neglected. This solution was named as basic improvement factor (n_0) as given in Eq. (2.6). Priebe assumed a reasonable value of 1/3 for Poisson's ratio of the soil. After that, column compressibility and effect of bulk densities were also introduced in n_1 and n_2 solutions, respectively.

$$n_0 = 1 + \frac{A_C}{A} . \left[\frac{\frac{1}{2} + \frac{(1-\mu_s).\left(1-\frac{A_c}{A}\right)}{1-2\mu_s+\frac{A_c}{A}}}{\tan^2\left(45-\frac{\phi_c}{2}\right).\frac{(1-\mu_s).\left(1-\frac{A_c}{A}\right)}{1-2\mu_s+\frac{A_c}{A}}} - 1 \right] \tag{2.6}$$

Where A is the area of a unit cell consisting of a single column with an area of A_c, μ_s is the Poisson's ratio of the soil and ϕ_c is the angle of shearing resistance of the stone.

Priebe (2005) outlined the application of Priebe's method to extremely soft soils, floating foundations and proof against slope or embankment failure. In case of soft soils, soil improvement is attained by faster consolidation rather than by reinforcement. Priebe's method gives a ratio of improvement with respect to unimproved ground, so the method is applicable in the case of soft soils. In case of floating columns, balances of stress in the upper treated zone and in the underlying untreated zone are discussed. Latter one is suggested by the author. Embankment or slope failure is discussed at the end.

The boundaries of stress concentration ratio at yield (n_y) were established from the Eq. (2.7) (Aboshi et al., 1979).

$$\frac{1+\sin\phi'_c}{1-\sin\phi'_c} \leq n_y \leq \frac{1+\sin\phi'_c}{1-\sin\phi'_c} * \frac{1+\sin\phi'_s}{1-\sin\phi'_s} \tag{2.7}$$

Where ϕ'_c and ϕ'_s are the effective angle of shearing resistance of the column and soil respectively. At the beginning of the consolidation prior to the composite foundation loading n would be equal to unity and as consolidation progresses it would reach the value n_y. Authors recommend using residual parameter for effective angle of shearing resistance of the column as the yield strain of sand is less than that of clay.

Settlement reduction ratio (S_r) was estimated from the Eq. (2.8) (Aboshi et al., 1979).

$$S_r = \frac{1}{(1 + (n - 1)a_r} \quad (2.8)$$

where a_r is the area replacement ratio. In the case of 30%≪a_r, S_r is overestimated due to the replacement effect of sand columns.

Analytical solution was given by Balaam and Booker (1981) assuming elastic behavior for soft clay and stone. The “unit cell” concept was used. Increase of rate of settlement using Biot’s equations of consolidation with numerical solution was found in the case of granular piles. It was mentioned that in some cases, usage of a sand mat under raft foundation allowed also for vertical drainage. The effect of vertical drainage was negligible and as a result, only radial flow solution was considered also in that case. Interface between stone and soil was assumed to be rigid and smooth. Just after the load application, load was carried only by the soft clay because of the materials incompressibility under undrained conditions. As excess pore water pressures dissipated, stress on the column increased and exceeded the value on the soft clay.

Balaam and Booker (1985) added the yield of stone column to their previous publication. Major principal direction was assumed to be vertical and the rigid base was assumed to be perfectly smooth. Main parameters affecting settlement were found to be column spacing ratio, angle of shearing resistance of stone column, dilatancy angle, load level, modular ratio and Poisson’s ratio of the clay. Correction to the elastic solution was more pronounced when the column spacing ratio was less than or equal to 3, the modular ratio was high as much as 40 and the dilation angle of column was equal to zero.

Balaam and Poulos (1983) described a loading path analysis for estimation of a single stone column assuming clay column interface was adhesive. They also showed that for depth to column diameter ratios of 10 to 20, rigid and flexible foundations could be obtained in the same way as described in Balaam and Booker (1981) for rigid foundations. However, for depth to column diameter ratios smaller than 5, reduction in settlement was not much as a rigid foundation.

The “unit cell” concept was used at the immediate settlement calculations. Consolidation settlement is also given by Baumann and Bauer (1974).

Goughnour and Bayuk (1979a) indicated that field tests performed were under undrained conditions. On the other hand, most projects loading rate occurs in drained conditions. Authors also indicated that, test loading was only applied on the column which is different than the application method, in which loading was shared between column and soil. The “unit cell” concept was used, which was described with the thickness of the soil layer relatively small compared to the loading area. Equal strain was assumed regarding no shear stress at the boundary of the unit cell or at the interface between soil and column. In a field study conducted by Goughnour and Bayuk (1979b), these shear stresses are measured as 9.6 kPa which could be neglected for most soft soils.

A vertical incremental analysis was proposed to solve the vertical strain and average vertical stress in the clay for both elastic and plastic behavior of the stone. For each increment, larger of the calculated from elastic and plastic behavior of stone would be taken as the actual strain. This was an iterative procedure (Goughnour & Bayuk, 1979a). Compatible results were obtained between predicted and measured stress distributions and settlement magnitudes (Goughnour & Bayuk, 1979b).

Goughnour (1983) simplified the application of settlement analysis of Goughnour and Bayuk (1979a).

Comparison of case studies with various analytical studies on settlement improvement ratio (inverse of settlement reduction ratio) is shown in Figure 2.1.

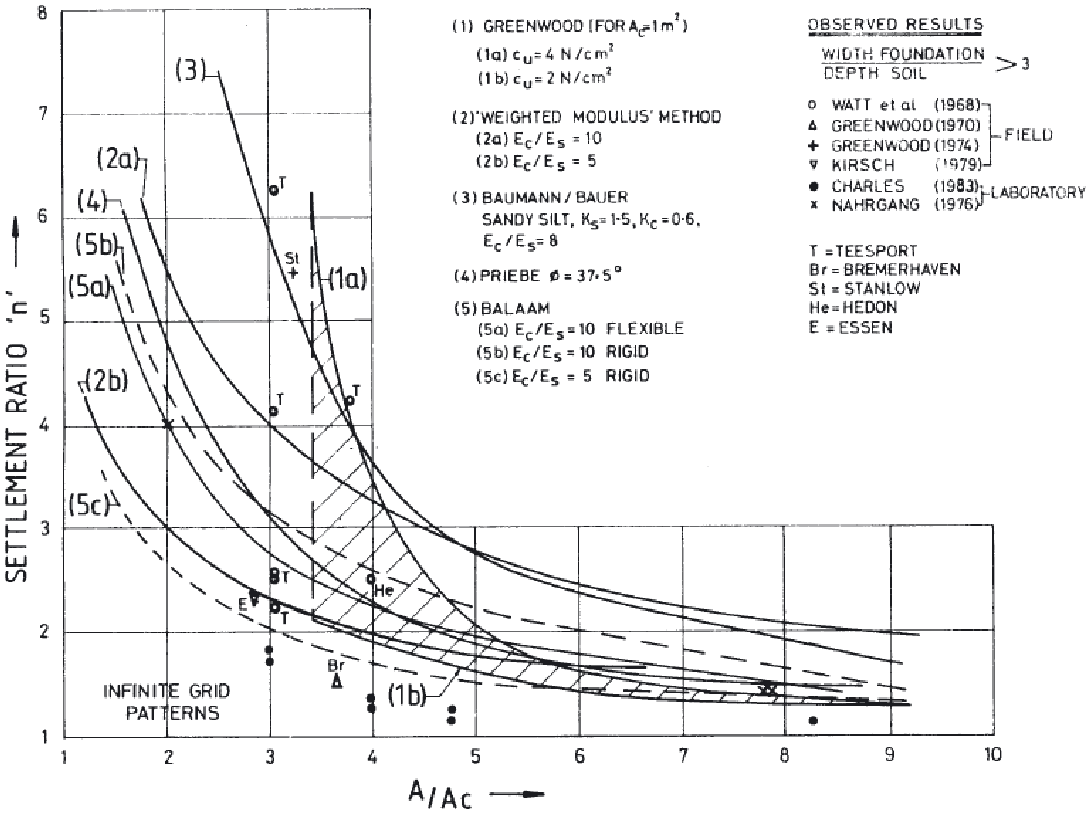

Figure 2.1 Comparison of elastic theories and field observations (reproduced from Greenwood and Kirsch, 1984)

W. F. Van Impe and De Beer (1983) proposed a method to analyze the settlement behavior of a granular trench.

Van Impe et al. (1997) mentioned of a combined bulging – pile failure mechanism for stone column.

Poorooshasb and Meyerhof (1997) considered rigid mat resting on end bearing stone column reinforced foundation. The “unit cell” concept was used. Small strain theory was assumed. Spacing with more than 4 times the diameter of the column has a little influence on settlement reduction ratio (referred as performance ratio in the paper). Settlement reduction ratio was affected mostly by column spacing and compaction of columns. Ultimate load capacity for a stone column was said to be between 100-500 kPa.

Alamgir et al. (1996) presented a theoretical solution for settlement of a reinforced flexible (such as flexible raft or embankment) foundation with end bearing columns. The “unit cell” concept was used for the “equal stress” problem with assuming elastic behavior for both soil and column. No slip condition was assumed at the soil column interface and shear stresses were assumed to be zero at the unit cell boundary. Radial strains were assumed to be very small. It was found that the modulus ratio influences settlement reduction notably but, the effect of Poisson's ratio was insignificant.

Saha and De (1994) recommended to use non-linear parabolic vertical strain function for stone column analysis. The "unit cell" concept was used and volume of stone column was assumed to be constant and radial deformation took place only at a depth equal to 4 times the diameter of the column. However, deformed shape of a full scale load test was different than the assumed deformed shape.

Madhav and Miura (1994) reflected the effect of dilation angle of stone columns. Settlement reduction ratio increases even with a dilation of 0.5% of the stone column material. This concept was first introduced by Poorooshasb and Madhav (1985).

Borges et al. (2009) proposed a new design method for embankments on soft soil reinforced with stone columns using finite element analysis. "Unit cell" concept was used. It was concluded that, area replacement ratio and compressibility ratio are the major factors affecting the settlement of treated ground. Formula is given in the Eq. (2.9).

$$S_r = \left(0.125\frac{C_{c,soil}}{C_{c,column}} + 0.7742\right) * \left(\frac{1}{a_r}\right)^{\left(-0.0038*\frac{C_{c,soil}}{C_{c,column}} - 0.3423\right)} \tag{2.9}$$

Madhav and Van Impe (1994) presented a study on the rigidity of the gravel mat used above the stone column reinforced foundations. Pasternak type model was used. A simple formula proposed by Juillie and Sherwood (1983) was also presented in this paper as given in Eq. (2.10).

$$\left(C - d_p\right) < 4H_f < H + H_f \tag{2.10}$$

Where C is the spacing, d_p is the diameter of stone column, H_f is the thickness of gravel mat and H is the thickness of the soft soil. Results were given for granular trench (plane strain) and other type loading separately. In granular trench case, for $\alpha_c \leq 0.1$, gravel bed can be considered as rigid in which α_c can be found from the Eq. (2.11).

$$\alpha_c = \sqrt{\frac{K_c . a^2}{G_f H_f}} \tag{2.11}$$

Where K_c is the subgrade modulus of stone column, a is the radius of the column, G_f is the shear modulus of gravel mat and H_f is the thickness of gravel mat. In other loading conditions, for $\lambda_c < 0.2$, gravel bed can be considered as rigid in which λ_c can be found from the Eq. (2.12).

$$\lambda_c = \frac{K_c . a^2}{G_f H_f} \tag{2.12}$$

Ellouze et al. (2010) analyzed the settlement of stone column reinforced foundation and criticized Priebe's method. Inconsistencies in Priebe's method were outlined and the critiques were reinforced with 3 case histories.

Zhang et al. (2012) presented an analytical solution for the settlement of foundations reinforced with stone columns. Equal strain was assumed, column was assumed to be an elastic material, confining pressure of the soil was assumed to be earth pressure at rest. Brauns (1978) formula was used to determine bulging depth: $h=2\ r_p \tan(\pi/4 + \phi_p/2)$ (r_p is the radius of the column and ϕ_p is the angle of shearing resistance of the column material). As stress concentration ratio increases, bulging depth increases and settlement decreases. Column modulus has no effect on bulging depth.

Liquefaction mitigation by stone columns was discussed by Engelhardt and Golding (1975) and by Baez and Martin (1992).

2.1.3 Consolidation Rate of Stone Column Reinforced Foundation

Castro and Sagaseta (2009) presented an analytical solution considering both the radial and vertical deformations either in elastic or elastoplastic material behavior, for the radial consolidation at the perimeter of stone columns under constant uniform load. “Unit cell” concept was used and equal strain was assumed. Average equivalent pore pressure along the radius was assumed. Radial coefficient of consolidation was formulated for elastic and elastoplastic behavior then, average degree of consolidation was found from Hansbo’s solution. After that, stresses and strains were calculated. Elastic strains were neglected in elastoplastic case. Distinction was made between two material behaviors such that; generation of plastic strain at the surface was assessed and decision was made for the type of behavior. Stress concentration ratio must be almost equal to constrained modular ratio. But stress concentration ratio was much higher than modular ratio in the most of the practical design guidelines where vertical deformation is considered only. Ratios were getting closer in the case where column elastic radial deformation was also considered. Stress concentration ratio was further decreased by considering plastic strains as in the case of real applications.

Xie et al. (2009) presented an analytical solution for the consolidation of a clay foundation reinforced with stone columns. Despite most of the studies which were assumed that the deformation occurs only in the soil, this paper assumed that the amount of water flowing in and out from the column are not even and this difference is equal to the deformation of the column. “Unit cell” concept was used and following assumptions are made: radial strain is neglected and equal strain is assumed, Darcy’s law is assumed, a uniform load is applied instantaneously and the load is sustained and amount of water flowing in and out from the column are not even and this difference is equal to the deformation of the column. Three different horizontal permeability patterns (namely; constant (I), linear (II) and parabolic (III) distribution pattern) are used for the disturbed zone. Average degree of consolidation by pattern I is smaller than II, and II is smaller than III. Consideration of column consolidation resulted in decrease of average degree of consolidation of reinforced foundation.

2.2 Installation

Greenwood (1970) presented a milestone work on reinforcement of ground with stone columns. Author suggested to use backfill material (uniform grading in the range of 20-70 mm size) in the case of soils with permeability value lower than 1E-5 m/s. Backfill is almost always compacted with water or compressed air which are known as wet top or dry top technique, respectively. While a soil with undrained shear strength of 7.5 kPa can be reinforced by wet technique, a soil with undrained shear strength of 20-25 kPa cannot be reinforced by dry technique. Dry technique can only be suitable for fine grained soils or mixed fill materials above the water table or in coarse cohesionless ground. A diameter of 0.9-1.04 m is achieved by wet technique and a diameter of 0.6-0.7 m is achieved by dry technique.

Applicability of the vibro-compaction and vibro-replacement methods in a grain size distribution chart is given in Figure 2.2. Single boulder with sizes larger than 50 cm stops the vibrator (Baumann & Bauer, 1974).

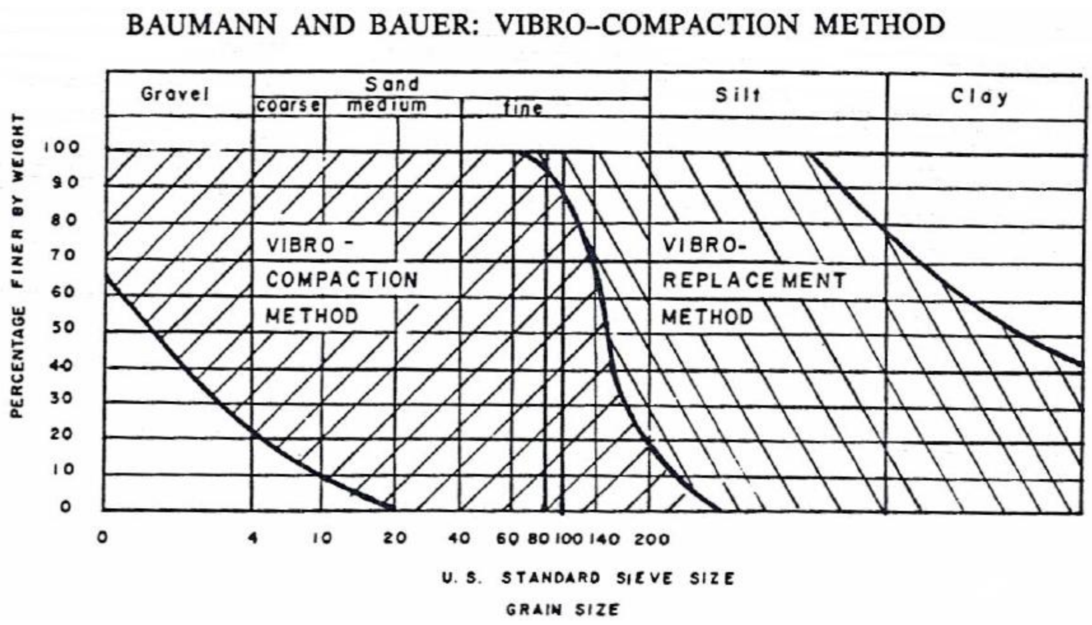

Figure 2.2 Range of soils suitable for stabilization (Reproduced from Baumann and Bauer, 1974)

As stated in Baumann and Bauer (1974), vibratory compaction machine contains three parts: the vibrator, extension tubes, and support rig or crane. Vibrator is a hollow cylindrical element up to 30 to 35 cm in diameter and 5 m in length. Eccentric weights are situated at the lower part of the vibrator, an electrical (380 or 550 V a.c) or a hydraulic motor at the upper part with a speed up to 3600 revolutions per minute. There is an elastic coupling where the extension tubes are attached to the vibrator. A vibrator approximately weighs 20 kN. Extension tubes include water pipes, hydraulic hoses and electric cables. Number of extension tubes is determined by the depth of reinforcement. Vibrator and the extension tubes can be suspended by a crane or a similar machine.

In the vibro-compaction process, vibrator is suspended from crane and it sinks under its own weight and also with the aid of water or air. Granular soil is momentarily liquefied with the penetration of vibrator to the design depth. Water aid is shut off and real compaction starts (Baumann & Bauer, 1974).

In the vibro-replacement process, vibrator displaces soil radially and downwards to form a cylindrical compacted zone. Cylindrical cavity is usually kept without a material. If not, aid of air or water can be used to support the cavity. Usually, 1m depth is backfilled at a step using stones as large as 15 cm in diameter. After a step of backfill, vibrator is lowered and displaced the backfill. Process is repeated until no absorption of backfill or further penetration of vibrator is required. For cohesive soils, 10% of backfill should preferably pass from 0.5 inch (1.3 cm) sieve size which is a requirement in the cases working below water table. Collapse may occur with the increase of saturation of the soil due to suction below vibrator tip, the induced excess pore water pressure and/or high sensitivity of the soil. Vibro-replacement is applicable to clays with a sensitivity of lower than 5. Air or water pressure at the bottom may solve other 2 problems. If these precautions are inadequate, vibrator has to be lowered several times with adding additional backfill. In soft fully saturated clays with low permeability, it is obligatory to clean up the cavity with water in repetitive up and down movements (Baumann & Bauer, 1974).

Vibrator diameter ranges from 30 cm to 45 cm and with a length about 2 to 3.5 m. Total weight changes between 2 to 4 metric tons. Follower tube diameter is about 30 cm. Power development varies from 35 to 100 kW (Greenwood & Kirsch, 1984).

Vibro-compaction technique is used in granular soils and depends on whether coarse backfill is used or not. Vibro-replacement method is used in soft cohesive soil with undrained shear strength values from 15 to 50 kPa. Diameter of the columns ranges between 0.8 to 1 m, preventing gross disturbance between columns. Jet water is used in this method. Preferable backfill material is rounded or sub-angular gravels with uniform grading with size range of 25-50 mm. Vibro-displacement method is used in insensitive cohesive soil with undrained shear strengths of 30-60 kPa. Soil is displaced laterally and compressed air is generally used. Column diameter is usually 0.6 m. Backfill material is generally well graded angular type with sizes of 10 to 100 mm. Granular material is backfilled from top. A machine has been developed in Germany to feed from bottom without removal of vibrator and to construct in softer soils with undrained shear strengths of 15 – 50 kPa. In bottom feed method, size range varies between 10 to 40 mm (Greenwood & Kirsch, 1984).

Bachus and Barksdale (1989) stated that, settlement reduction ratios of 50% are achieved in the case of stone column reinforced foundations. Backfill material particle diameter generally changes between 10-89 mm. Production rates are typically 9-18 m/hr excluding the necessity of predrilling in the case of firm to stiff soils. Soils with an undrained shear strength lower than the generally accepted range of 10-50 kPa, results in large amount of deformation and excessive feeding. Stone column application is mostly economical for depths varies from 6 to 10 m. Gravel mat with a thickness of approximately 1 m is mandatory for working over compressible soils. Measured values of stress distribution ratio vary from 2.5 to 5.0, increasing marginally with time and decreasing with increasing depth.

Dry bottom feed method was generated to prevent the collapse of the perimeter of the hole. Feeding tube is included in the vibrator for bottom feed and to support the sidewalls as it is left in the hole during construction. Rounded and uniform aggregate with a maximum diameter of 38 mm to prevent clogging within the probe, is suitable for dry bottom feed method. Lifts of compaction generally varies from 600 to 1200 mm. Diameter of the constructed column varies from 760 to 1400 mm (Bachus & Barksdale, 1989).

Drilling the soil with a long (10 m) and thin (0.5 m dia.) steel tube at a vibration frequency of 50 or 60 Hertz is the first part of “vibro-flotation” technique. After that, stone with a diameter of 2 to 3 cm is backfilled with compaction at various depths as described in Hughes and Withers (1974).

According to McCabe and Egan (2010), there are 4 types of vibro-replacement methods. Dry or wet explains the usage of water, top or bottom explains where the stone is dropped. Dry top feed is commonly utilized for coarse and more competent cohesive soils in case of shallow to medium reinforcement depths. This type was seldom used in soft cohesive soils. Wet top feed is utilized for soft cohesive soils in case of medium or deep reinforcement depths below water level. Problem turned up recently due to trouble in removal of the flush arisings which was reduced the usage of this method. Dry bottom feed is frequently used and is taken the place of wet top feed. It is used in soft soils with undrained shear strengths of 15-20 kPa. Other methods can be described as bottom rammed columns which are not feasible for soft soils. McCabe and Egan (2010) recommended dry bottom feed method, because it has given more consistent results.

An interesting graph on gradation difference is shown in Figure 2.3. Stress strain characteristics were stated as comparable (Mitchell & Huber, 1985).

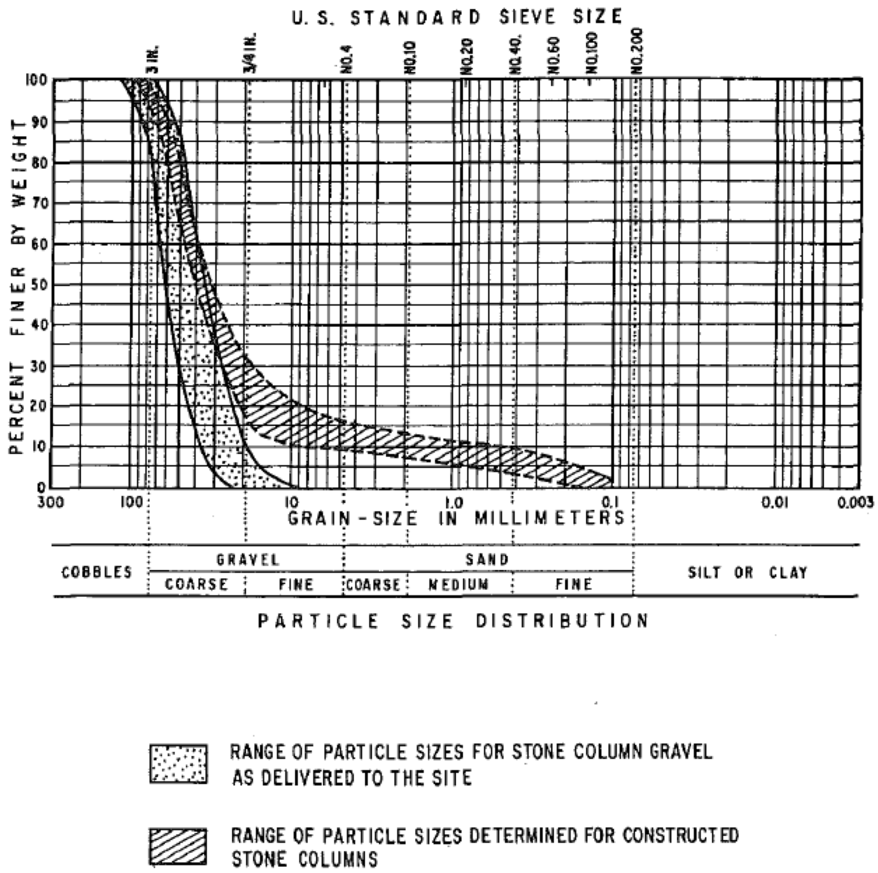

Figure 2.3 Stone Column Gravel Grain-Size Distribution (reproduced from Mitchell and Huber, 1985)

Column diameter has reached up to 200 cm (Aboshi et al., 1979). Authors also reported that undrained shear strength of the clay reduces during the installation period but recovers even exceeds the original value in one month after installation. Initial value of undrained shear strength of the clay can be used in design, because structural loading takes place usually more than one month.

Occurrence of ground heave while constructing the stone column indicates soil disturbance. Upward percolation of water in a column adjacent to another column construction indicates good construction and high permeability of the stone column (Munfakh et al.,1987).

Serridge and Sarsby (2009) indicated that the stone column construction in a typical range of 15-20 minutes generated pore pressures which were returned to pre-treatment values within 6 days. But when construction period took half an hour (lack of stone supply, monitoring delays or inexperienced operator), pre-treatment values were reached after 48 days.

Castro and Sagaseta (2012) analyzed peaks of pore pressures during installation of end bearing stone columns which were instrumented with piezometers and compared with cavity expansion theory. Undrained conditions are assumed and vertical shear stresses are neglected. In the case of first column, undrained shear strength value from cavity expansion theory to match peak excess pore pressure data was smaller than laboratory and in-situ strength tests. Possible reasons were outlined as; installation under partial undrained condition or destructuration around column. In the case of installation of subsequent columns, existence of previous columns made the analysis very hard and cavity expansion theory is not justified. Peaks of pore pressures were small at shallower depths.

Chen and Bailey (2004) presented stone column installation findings in glacial sand and silt deposits.

2.3 Field Performance

Single stone column constructed in soft clay (Canvey Island) with vibro-replacement was tested under plate loading by Hughes et al. (1976). Estimation with corrected column diameter and allowance for shear transfer to the clay (using preferably pressuremeter test data) agreed well with the observed value. Pressuremeter test data was found to be crucial for column settlement during loading.

A comparison was made at Bremerhaven field test between sand and stone columns. It was observed that the settlement reduction ratio was 0.6 for stone columns and 0.85 for sand columns after 15 months (Greenwood, 1970).

Greenwood (1991) presented 6 case histories and lessons learned from these in detail as summarized below. Stone columns interact with the soil and are not just by-passing the soil, like piles. Stiffness of the stone column is stress dependent and the value is 2-20 times stiffer than soils unlike concrete piles which are 10000 times stiffer than soil. Author mentioned that the pressuremeter test is the best way to measure principal stress ratio and also mentioned that soundings may be useful for stiffness measurement but could not give stress dependent behavior of stone columns. Small scale test may be very harmful and must be avoided which will be clearly demonstrated later in the paper. Although full scale tests are not suitable due to insufficient test site investigation and time constraints but, gave fair information on stress ratio.

i) Uskmouth: Isolated column was loaded with pressure cells monitoring at 3 different depths. Cell at 1.83m depth was read more stress than the surface readings which would be due to the stress redistribution occurred due to the stiff crust at the top. It also corroborated Hughes and Withers (1974) hypothesis in which bulging should occur at the top due to the high direct stresses and low confining stresses (Greenwood, 1991).

ii) East Brent (Somerset): Data was taken from McKenna et al. (1975). First of all, difference between silty clay and silty sand was not pointed out carefully. Central section slid after 92 days had same settlement with reinforced end in day 90. At the end of day 188, untreated end had less settlement than treated end. Linear excess pore water pressure increase in the treated depth explained the punching of the column end. Shearing displacement was occurred on the peat level at untreated end. Stone column was installed with insufficient depth causing these problems (Greenwood, 1991).

iii) St. Helens: Dummy footing on silty fill material which was unsaturated and drained was treated. Maximum Load applied was half the ultimate bearing capacity of untreated ground which results in elastic loading (Greenwood, 1991).

iv) Canvey Island: Soil under oil storage tank was treated. As loading reached the ultimate level, settlement was increased and stress concentration ratio was decreased (Greenwood, 1991).

v) Humber Bridge South Approach: Embankment on soft organic clays was treated. Chalk was used as fill material and compacted to a unit weight of much more than natural which supports that the material was turned into a plastic state. Stress measured on stone column increased progressively in second plateau of loading suggested bulging. Local direct stresses created due to the compaction of the chalk may be another logical alternative. Second evidence for this was the pore water dissipation and decrease in stress on columns after completion of the first plateau of loading. Stress ratio was unknown at the end as a result of destruction of the cells (Greenwood, 1991).

vi) Bombay, India (Misuse of loading test): LNG sphere on amorphous soft marine clay was treated. Load tests on single column and bridging 2 columns are conducted. Although results of small scale tests are satisfactory, total failure was reached at the end of test loading (Greenwood, 1991).

Attention must be paid to the determination of principal stress ratio in soil, load stress, undrained soil strength and column area. In addition, monitoring excess pore water pressure and settlement ensures a safe loading rate (Greenwood, 1991).

Baumann and Bauer (1974) presented 2 case studies in which the dormitory foundation in Konstanz was reinforced with floating stone columns. Foundation soil was varved marine clay.

Full scale field test of a reinforced earth embankment which has a reinforced foundation soil with stone column was presented by Munfakh et al. (1983). Site was instrumented with inclinometers, subsurface settlement markers, earth pressure cells and pneumatic piezometers. As the installed column spacing was reduced, pore pressure increased. Jet water is thought to be the reason for this, which was approved by the dissipation of excess pore pressures overnight. Stone column usage reduced total settlements by 40%. Settlement rate was quite high than the unimproved area. Considerable saving was attained with respect to pile option. In addition to that, cost was also reduced by the construction of the test embankment.

Mohamedzein and Al-Shibani (2011) presented a case study of an end-bearing reinforced embankment on soft soil with an undrained shear strength of min. 4 kPa.

Raju (1997a) presented case studies from Malaysia in which the undrained shear strength of the soft soil was below 15 kPa. This value is accepted as the lower bound for stone column reinforcement by most of the authorities. Soil profile for Kinrara interchange contained tin mine tailings (slimes) and Kebun Interchange contained marine clay. CPT soundings were conducted at Kebun and tip resistance values for top 11 m are between 0.1-0.3 MPa. Sand blanket was placed at the top to increase the consolidation rate and to transmit the loads to stone columns more uniformly. The embankment height at Kebun where the settlement gauge was placed was 2.6 m (including 1m surcharge which was placed to reduce consolidation time). Stone column diameter was 1.1 m with center to center spacing of 2.2 m along a depth of 12 m at Kebun. Settlement gauges were placed at the top of the stone columns and total settlement was read as 40 cm. 1 m settlement was observed for untreated ground under same circumstances. Using Taylor's square root of time, 90% of consolidation was estimated to take place in 225 days in which the construction period was 45 days.

Raju et al. (1997b) presented Kinrara and Kebun case studies previously mentioned in Raju (1997a).

Raju and Wegner (2004) presented 19 vibro replacement case histories in Asia between 1994 and 2004. In addition, wet top feed method and 3 different dry bottom feed methods were outlined.

Wiltafsky and Thurner (2009) presented a shopping center founded on weak marine deposits reinforced with stone columns in combination with vertical drains and excess preloading. During numerical simulations, improved parameters are used for the reinforced section of the marine deposits.

Instrumented field trial of a foundation reinforced with floating stone columns was undertaken by Gaeb et al. (2007). Multilevel-piezometers, multilevel-extensometers, earth pressure cells and a horizontal inclinometer were instrumented in the field. Stone columns were constructed with dry bottom feed method. Maximum excess pore pressure reading was taken at a depth equal to the bottom of the stone columns. Largest displacements were also measured at the same depth which were exceeded the limits (20 cm) of the extensometer.

A new database of settlement case histories are given by McCabe and Egan (2010). Most of the cases (except 3 small footings) were widespread loadings. Priebe's basic improvement factor with ϕ=40^{o} and ν=1/3 gave consistent results with the database.

Serridge and Sarsby (2009) conducted field trials of strip foundations on Bothkennar clay reinforced with floating stone columns constructed by dry bottom feed method. Untreated ground settlements were half the average of treated ground in a period of 44 weeks which was attributed to the dissipiation of pore pressures through stone columns. Significant stress transfer is measured underneath the columns with lengths shorter than critical length. This behavior was not seen in columns with lengths longer than critical length which supports the Hughes and Withers (1974) hypothesis.

Watts et al. (2001) investigated the performance of soft clay foundation reinforced with floating type stone columns installed by dry bottom feed technique. Length of the installed columns was greater than critical column length. Stone bulb with an approximate height of 1 m and a diameter of 1.25 m was constructed to form a firm base. In-situ measurements and stone column consumption records revealed that the column diameter was 0.75 m which is greater than the design diameter of 0.65 m. 0.4 m heave was occurred in soil between columns during installation and 0.1 m was recovered in one year period.

Van Impe et al. (1997b) introduced two widespread loading and two single footing founded on stone columns. In addition to these, a case history on rammed stone column was also introduced.

Raju et al. (1998) presented case histories from S. E. Asia improved with vibro-compaction and vibro-replacement techniques. Usage of vibro-replacement method for embankments founded on soft soils with undrained shear strength of 5 kPa was verified.

Barksdale and Goughnour (1984) presented performance of a 9m high reinforced earth wall supporting a highway approach fill founded on stone columns. Authors also compared the observed settlements with 3 widely used methods.

DeStephen et al. (1997) presented a processing center at a nuclear power station founded on hydraulic fill reinforced with floating stone columns. Dry bottom feed technique was used to construct stone columns. Authors reflected the occurrence of heave at the surface with dry bottom feed method.

Watts et al. (2000) conducted full scale load tests to investigate the performance of strip foundation resting on treated and untreated variable fill. Dry top feed method was used to construct floating type stone columns. Settlement reduction ratio was measured as 62%. Authors indicated that bulging occurred at a depth three times the column diameter. Stress measurements indicated that stress concentration ratio is overestimated by current design methods.

Bergado and Lam (1987) presented 13 full scale load tests of stone columns installed with simple bored pile machine. Bulging was observed at a depth equal to one-third to one column diameter from surface.

Cooper and Rose (1999) presented a case history, in which the roundabout embankment founded on soft alluvial deposits were reinforced with stone columns and vibrated concrete columns.

Ausilio and Conte (2007) presented a case study of a wide area reinforced with stone columns at san Michele di Serino Village in Italy. Damage is occurred during earthquake of 23 November 1980. Results of dynamic penetration tests were compared before and after the treatment. Authors implemented soil compaction effects in the Van Impe and De Beer (1983) method to calculate settlements. It was concluded that, if soil compaction was ignored, settlements would be overestimated.

Clemente and Parks (2005) investigated the performance of gas-fired power station site founded on placed fill reinforced with stone column constructed with dry bottom feed method. Large scale field load test program was conducted and settlements were monitored for 1.5 years which were showed good foundation performance.

Stuedlein and Holtz (2011) conducted full scale spread footing load tests on single and groups of stone columns. Influence of column length, gradation and compaction were analyzed statistically. Column length was important than others at small displacements. But, gradation and compaction were more important at large displacements.

Lopez and Shao (2007) presented a case study. Pre-treatment and post-treatment SPT and CPT results were used.

Ashmawy et al. (2000) presented three case histories reinforced with stone columns.

2.4 Studies Performed in the Laboratory

Hughes and Withers (1974) suggested using centrifuge force to initiate gravitational stresses. But like most of the researchers, authors assumed that the tests performed with uniform anisotropic stress field would result in similar outcomes. High straining was observed in four column diameter length from top at failure. Loading mostly affected the clay around the stone column with a diameter of 2.5 times the column diameter. As a result, authors believed that if columns constructed with spacing more than 2.5 times the column diameter, they could work individually. Consolidation was not evident at a distance 1.5 times diameter from the center of the column. Authors also indicated that when the length of the column is less than 4 times the diameter of the column, then the columns would fail in end bearing.

Wood et al. (2000) investigated load distribution between soil and column on laboratory specimens. Relative density of the sand used in the study was about 50%. Column diameter to granular average particle diameter ratio was exceeded in the prototype for the sake of simplicity in replacement and to permit shear bands up to 20 particles thick (Roscoe, 1970) to form in the columns without undue restraint. All columns installed were floating type and the footing was rigid. Loading was settlement controlled. For confining effects, columns were installed outside the loading area in accordance with the field practice. Results indicated that the mode of deformations were, bulging, diagonal shear plane formation, short column penetration or long column absorption in its own length and slender columns which acts as laterally loaded pile. Key result would be the depth at which the leading strain was taking place in a single column was primarily controlled by the footing width. It was pointed that, beyond a certain point, stress-strain behavior was not affected by increasing column length. It was also indicated that the critical length should increase as the area replacement ratio increases. It was observed that the columns at mid radius of the footing were loaded more than the others. The “unit cell” concept should consider the depth of bulging failure. Clearly, columns at the edge of the footing would fail primarily.

Shahu and Reddy (2011) presented fully drained and stress controlled laboratory tests on kaolin clay reinforced with floating columns and their numerical simulations. While short term column capacity is critical for small column groups, long term settlement is critical for large column groups. Column diameter to granular average particle diameter ratio was around 13-59 which was comparable with the field conditions such as 12 to 40. Relative density of the sand was 50% because it was hard to get a relative density of 80%. For confining effects, 10% to 20% of the columns were installed outside the loading area in accordance with the field practice. Footing load was stopped at a settlement rate of 1 mm/day. Decrease in settlement was more obvious in the case where area replacement ratio was increased from 10% to 20% than the case where area replacement ratio was increased from 20% to 30%. In one test, relative density was set to 80%. Settlement difference of two relative densities was visible at near failure stress levels. Thickness of the mat, dilation angle and the angle of shearing resistance of the sand were claimed to have least effect on settlement. On the other hand, major parameters were area ratio, depth ratio, overconsolidation ratio, relative stiffness and stress ratio M of clayey soil. Stone column and the mat were remained almost in the elastic strain range. Good agreement was obtained between simulation and observed results.

Model stone column groups installed in soft kaolin clay were investigated using radiographic techniques and miniature diaphragm pressure cells. Kaolin clay for laboratory studies should have low plasticity and faster consolidation characteristics. Before one dimensional consolidation, soil was mixed to form slurry with a water content of twice the liquid limit. This removes the effects of loading history, increases the consolidation rate and forms uniform, almost saturated specimens. Settlement of untreated case could be reduced to its half value by reinforcing stone column with an area replacement ratio of 40% in unit cell vertical load tests. Stress controlled tests allow faster rate of loading compared to the settlement controlled tests (Bachus & Barksdale, 1984).

According to Ambily and Gandhi (2007), bulging occurs at 0.5D below the surface for column area alone loading. Columns equally spaced with more than 3D affected the stiffness improvement factor (stiffness of the treated ground divided by stiffness of the untreated ground) in a negligible manner and the stiffness of the treated ground is mainly related to the angle of internal friction of stone material and area replacement ratio.

Results of large scale model stone columns constructed in kaolin were presented by Christoulas et al. (2000). Load was exerted under undrained conditions and only on the stone column. Scale of the tests is 1/3 with respect to the original dimensions used at site. Before consolidation, water content of the slurry was almost equal to the liquid limit of the kaolin. As the result of the tests, bulging was observed 2.5 to 3.0 times the column diameters from the top. Cavity expansion theory was validated. Skin friction pile concept was provided rational outcomes only for small loads, lower than the creep load. Ultimate load was observed at a settlement equal to 35% of the column diameter.

Two materials were used in the study namely: transparent material and kaolin. Samples used in the model tests were one dimensionally consolidated. Kaolin was formed as slurry with a water content of 1.35 times the liquid limit. Loading was settlement controlled (McKelvey et al., 2004). Studies proved that the columns could fail by bulging, punching, shearing or bending. Load capacity was not affected by further increase in column length more than 6 times the diameters of the column. In circular footings, increase in column length from 150 to 250 mm increased the overall performance by 5%. More increase was observed for strip footings.

Sivakumar et al. (2004) presented 2 series of consolidated undrained triaxial compression tests. Kaolin was used in the tests. Information on wet compaction placement method will be given here. Two types of loading are applied, which were entire area (uniform) and foundation type loading. In wet compaction, consolidation rate for floating columns was come out to be smaller than untreated case as opposed to expected. This phenomenon was explained by reduced permeability at the soil column interface as a result of partial blockage. For foundation loading, column length greater than 5 times the diameter of the column was not affected load carrying capacity. The ratio of the diameter of the soil to foundation is 2.5, which is less than the value (5) generally accepted to dismiss boundary effects. But Hughes and Withers (1974) observed that outer than 2.5 has little influence.

Samples were reinforced with end bearing columns only. Loading was stress controlled. Settlement reductions are considerably less than the predictions by Priebe which had zero lateral strain conditions. However, boundary condition was flexible and more realistic in this study. Minimum stress increase was observed at a depth of 5 times the diameter of the column during foundation loading (Sivakumar et al., 2011).

Black et al. (2011) one dimensionally consolidated the reinforced samples. In order to control the pore pressure under foundation loading and to obtain uniform soil stiffness/strength properties, sample was transferred to large triaxial cell and re-consolidated under isotropic stress. Kaolin Slurry was prepared at a water content of 1.5 times the liquid limit. Column installation was done by replacement although it was not representative of the field installation technique but selected for its consistency. Floating and end bearing columns were constructed in kaolin samples. Stress controlled loading was used. Authors were observed a block mechanism in the case of group of columns which was affected the settlement behavior.

Andreou et al. (2008) performed 22 triaxial compression tests on kaolin clay reinforced with sand and gravel columns. Undrained tests were performed with a deformation rate of 0.3 mm/min and drained tests were performed with 0.003 mm/min. It was concluded that, maximum load on composite foundation was extremely dependent on drainage conditions, column material and loading rate.

Al-Khafaji and Craig (2000) presented axisymmetric centrifuge (105 g) models of flexible base tank founded on clay reinforced by multiple sand columns. Serviceability limit state was investigated rather than ultimate limit state.

Najjar et al. (2010) investigated the improvement of soft clay reinforced by sand column in terms of strength and compressibility characteristics. 32 isotropically consolidated undrained triaxial tests were conducted. Triaxial test apparatus was used because; earlier studies were performed in large 1D loading chambers which was unable to control drainage. Kaolin was prepared to form slurry with a water content of 1.8 times its liquid limit. Relative density of Ottawa sand was about 44%. Critical column length was estimated as 6 times the diameter of the column. In the case of non-encased columns, 79% of the test columns were shorter than the critical column length as a result of the size limitations. Tests results revealed that; undrained shear strength of clay increased even for a_r<18%. In addition, decrease in pore pressure generation during shear and increase in Young's modulus was observed. Effective strength parameters were unaffected except for high area replacement ratios with end bearing type columns.

Ammar et al. (2009) pointed out the effect of enlarged base on the bearing capacity of stone column reinforced foundations.

Liu et al. (2009) investigated effects of additional constituents on stress concentration ratio during the column preparation.

2.5 Modeling Works

A waste water plant foundation was reinforced with stone columns in 1976 on U.S.A. 28 single column load tests were conducted. Data obtained from those tests and structural settlement readings obtained till 1982 were used for axisymmetric finite element analysis. End bearing columns were constructed in the project and gravel bed was used with varying thicknesses of 0.3 - 1 m. In analysis, stone columns surrounding central column were modeled as cylindrical rings without changing the area of the columns. FE simulations were mostly overestimated the observed single column test settlements. Two reasons were explained as: some soil encountered and defined as cohesionless soil could not drain freely under undrained test loading conditions or due to load increment intervals. Results were found to be unaffected by the modulus number K of the stone columns which was represented by the hyperbolic model (Duncan & Chang, 1970). Behavior of in-situ soils were also represented by this model. Ratio of settlement due large load compared with single column test was assumed to be 10. Settlement reduction was calculated as 30%. FE simulations were also overestimated observed structural settlements (Mitchell & Huber, 1985).

Numerical model including elastoplastic behavior was presented by Lee and Pande (1998) for stone column reinforced foundation. Homogenization technique was used for the soil column composite system by implementing discrete yield function for both materials in composite system and a sub-iteration method within an implicit backward Euler stress integration scheme based on a Taylor series expansion. Stress difference was added to the stone column. Laboratory based circular footings were simulated under axisymmetric conditions. Soil was simulated by the Cam-clay model accompanied by a tension cut-off. Stone columns were represented by Mohr Coulomb criterion accompanied by a non-associated flow rule. It was assumed that there is a pattern for the columnar inclusions and their behavior is isotropic. It was also assumed no slippage occurs between soil and the stone column. During the drained analysis, prescribed incremental settlement was applied on footing and small amount of stress was applied at the boundary of the composite system accounting for the installation of the columns. Tensile failures were obtained and higher stresses were concentrated in stone column and soil at the periphery of the rigid footing.

Gerrard et al. (1984) presented a constitutive model for stone column reinforced soft clays. Tresca yield criterion was used for soft clay and Mohr-Coulomb yield criterion was used for stone column. Stone column uniaxial strength was the sole consideration. After an area replacement ratio of 30%, decrease in settlement was gradual. Later, this work was improved by Schweiger and Pande (1986).

Schweiger and Pande (1986) presented a numerical study for stone column reinforced rigid raft foundations. Soft clay was presented by Critical State model and stone column was presented by Mohr-Coulomb criterion. Compatibility of radial stresses at the soil column interface was warranted by an additional pseudo-yield criterion. Equal strain theory was assumed. It was also assumed that the effect of stone columns is uniformly and homogeneously distributed under reinforced area. These assumptions were justified if the raft area is very large than the spacing of columns and, if the load is sustained under ultimate load. As a result, a constitutive model was presented for an “equivalent material”. Rigid footing was simulated by a 0.5 m thick gravel mat which was assumed to behave linear elastic. Plastic zone under raft was distributed to a depth equal to 65% to 85% of the diameter of the raft.

Gaeb et al. (2009) presented results of well observed (with a duration of 14 months) test embankment (10.5m high) reinforced with stone columns and simulated using different constitutive models. Due to the compaction, stiffness of the sand around stone column is increased. In addition to that, permeability of silt is also increased near stone column which is defined as smear zone. Hardening soil (HS) model is employed for the media. HS model is based on Hyperbolic model (Duncan & Chang, 1970) but, theory of plasticity, dilatancy for soil and yield cap are introduced (Plaxis Manual). In addition, silt is also simulated with HS-small (small strain stiffness effect), MCC (Modified cam Clay), S-Clay1 (considers anisotropic behavior by introducing a rotated yield surface and a rotational hardening rule). S-Clay1 also takes destructuration into account (Karstunen et al., 2005). At construction stages, all models underpredicted the surface settlement but agreed up to 300 days except HS. After day 300, actual settlement is underpredicted by models except HS. This may be caused by construction works executed which are not modeled and due to creep as reported by authors.

Guetif et al. (2007) presented information on improved soil characteristics. When improvement of the in-situ soil due to column installation and consolidation of the surrounding soil is not considered, excessive use of stone columns would lead to overdesign. Greenwood (1970) had taken the installation effects in his proposed method. Numerical simulation was done by the authors to capture the installation and consolidation effects. “Dummy material” procedure was used during analysis which consists; initially, 0.5 m diameter probe (wet top feed) was modeled as elastic material with E_{dm}=20 kPa, then the soft soil was radially displaced until the column diameter of 1.1 m was reached, at the end, stone column material was defined in this 1.1 m diameter region. Radial displacement resulted in large strains, which contradicted with the idea that, soil in the vicinity of the column remains in the elastic range adopted by Priebe (1995) and Balaam and Booker (1985). After the primary consolidation, a zone of influence which was 6 times greater than the column was estimated. In this zone, 30% increase in effective mean stress was observed. Also it was recommended to use revised Young’s modulus in this zone.

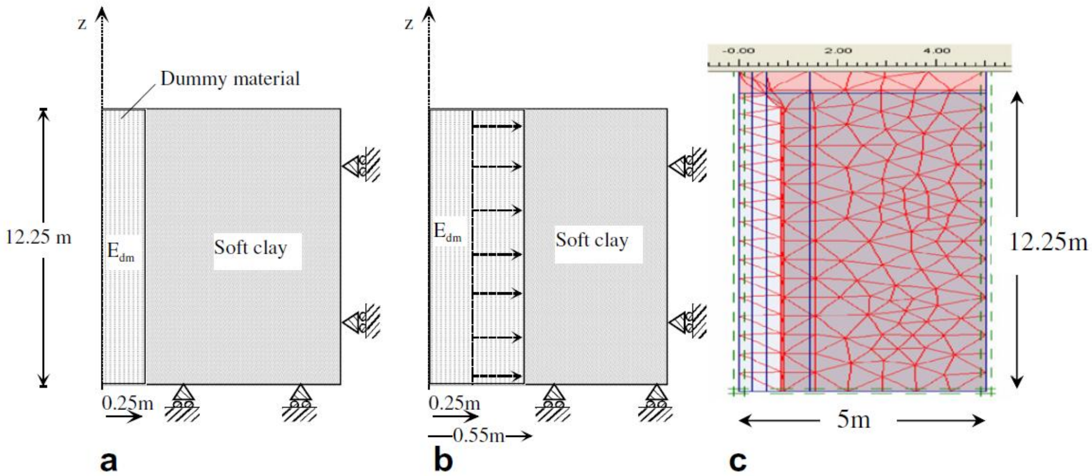

Figure 2.4 Simulation by the composite cell model of stone column expansion: (a) model of improved soil; (b) modelling column expansion; (c) discretized improved soil (Reproduced from Guetif et al., 2007)

Hassen et al. (2010) presented homogenization method for stone column reinforced foundations. Pore pressure distribution is not considered in the analysis. It was assumed that media has elastic perfectly plastic behavior. Validation of numerical procedure was made. Bearing capacity of gravitational forces included analysis yielded larger load carrying capacity for a strip footing example. Ultimate bearing capacity was relatively increased by

12% and 40% with respect to unreinforced case for gravity excluded and gravity included reinforced cases, respectively.

McCabe and Egan (2010) informed that, creep, anisotropy, destructuration and bonding are recently introduced in the new constitutive models (Karstunen et al., 2005, Leoni et al, 2008).

Castro and Karstunen (2010) simulated stone column installation in soft clay using SCLAY1 and SCLAY1S material models. Both models are Cam Clay type models. SCLAY1 also accounts for anisotropy and SCLAY1S accounts for anisotropy and destructuration. “Unit cell” model was used. Group effects were not taken into account. Under undrained conditions, prescribed displacement was applied in the radial direction of the column to account for cavity expansion during column installation as in the case of dry bottom feed method. Excess pore water pressure results of SCLAY1 and SCLAY1S were very similar except in the vicinity of the column where destructuration effects resulted in higher excess pore water pressures in SCLAY1S model. Excess pore pressure increase was observed in 13.5 times the column radius from column axis and the value is maintained at any depth. Horizontal stresses after consolidation were very different due to destructuration which limits the horizontal stresses. In contrast, lateral earth pressure after consolidation showed similar trends for both models. For design consideration assuming dissipation of excess pore pressure, authors recommended to use the value (roughly 1.4 times the initial value at rest) between 4 to 8 column radius from column axis, because plateau is observed in that range. To account for destructuration in practical stone column design, undrained shear strength value may be reduced to 80% to 85% of its initial value. Cavity expansion during installation caused development of anisotropy towards planes perpendicular to radial axis.

Shahu et al. (2000) analyzed soft ground reinforced by end bearing stone columns with granular mat on top. “Unit cell” concept is used and radial strains were not considered. Granular mat was assumed as a rigid and smooth layer. As a result of the analysis, stress concentration ratio reduces as the thickness of the granular mat increases. For low area replacement ratios (a_r<25%), sufficient thickness of granular mat improves the overall performance of the reinforced ground especially in the case of bulging at the top.

Tan et al. (2008) presented 2 conversion methods to obtain the equivalent plane strain model from axisymmetric model. In first method, soil permeability value is changed and in second method, column width is altered to trench type according to equivalent column area. Second method was more accurate as the first method lower long term settlements.

Weber et al. (2009) simulated embankment foundations reinforced with floating type stone columns with 2D and 3D analysis. Stiffness and permeability values were changed in order to simulate 2D stone trenches. Smear zone was introduced. Discrepancies between 2D and 3D analysis were due to element type and size of the element. It was concluded that 2D trench technique is not appropriate under stress states approaching failure.

Elshazly et al. (2006) investigated post-installation earth pressure coefficient (K*) in stone column reinforced soils. Field data of Mitchell and Huber (1985) was used in analysis. For the particular soil conditions, best estimate of K* is 1.5 with a lower bound of 1.1 and an upper bound of 2.5.

In addition, Elshazly et al. (2007) pointed that the settlement reduction ratio decreases (which implies further improvement) with increasing K*.

Murali Krishna et al. (2007) incorporated densification effect of stone columns by changing the deformation modulus between column and unit cell boundary. Settlement of the ground was obtained by integro-differentiation technique and finite difference method. Settlement of the ground was less when densification effect is taken into account.

Table 2.1 K* values for Vibro Installation (reproduced from Elshazly et al., 2007)

References	K^* value
Elshazly *et al.* (2006)	Between 1·1 and 2·5, with best estimate of 1·5
Elkasabgy (2005)	Between 0·7 and 2·0, with average of 1·2
Pitt *et al.* (2003)	Between 0·4 and 2·2, with average of 1·2
Watts *et al.* (2000)	Between K_o and K_p
Priebe (1995)	1·0
Goughnour (1983)	Between K_o and $1/K_o$

Deb and Dhar (2011) proposed finite difference simulation and evolutionary multi-objective optimization based method to obtain optimal parameters for a system of beams founded on stone columns. Modular ratio and the flexural rigidity of the beam were found to be the most important parameters.

Sadek and Shahrour (2008) simulated effect of eccentricity on stone column reinforced foundations.

CHAPTER 3

CASE STUDIES: NUMERICAL MODELING AND RESULTS

In this chapter case histories chosen from the literature are studied in detail to investigate the settlement behavior of soft ground reinforced with SCs. First, general information about the cases are provided including the geometry of the sites, SC installations, soil characteristics and description of constructional phases. Next, the numerical analyses of these cases are presented. Then, the results of these analyses are given together with the discussions. Later in this chapter, the parametric studies are performed to search for the effects of soil parameters used for SCs and soft ground.

3.1 Finite Element Modeling

In the analyses of geotechnical problems, exact solutions are applicable for limited conditions. An approximate solution can be obtained using numerical modeling. Finite element (FE) method is one of the numerical modeling techniques. As the name implies, FE method divides the region, body or structure into finite number of elements. Finite element codes used in this study are Plaxis 2D (version 2011.01) and Plaxis 3D (version 2011.01). 2D analyses are generally suitable for plane strain or axisymmetric conditions, whereas 3D analyses are expected to simulate the conditions in the field more accurately.

Whether the analysis is performed in 2D or 3D, the selection of element type is crucial. To obtain accurate results in a reasonable amount of time, 15-node triangular elements and 10-node tetrahedral elements are used in 2D and 3D analyses, respectively. 15-node triangular element involves 12 stress points and element interpolation function for displacement is four. On the other hand, 10-node tetrahedral element involves four stress points and element interpolation function for displacement is two.

Figure 3.1 (a) 15-node triangular element, (b) 10-node tetrahedral element

For all three cases, global mesh coarseness is set to medium and refined at least twice around SC to obtain more accurate results in 2D and 3D models. In addition, when modeling SCs, discretization angle of columns is set to 30^{o} to lessen computational effort in 3D models.

Five drainage types exist to incorporate the modeling of pore pressures in Plaxis. The first one is the (i) drained type model which can be used when generation of excess pore pressures in the body are not taken into account. The drainage models for undrained behavior are divided into three as: (ii) undrained-A (undrained effective stress analysis with effective stiffness and effective strength parameters), (iii) undrained-B (undrained effective stress analysis with effective stiffness and undrained strength parameters) and (iv) undrained-C (undrained total stress analysis with all parameters undrained). No distinction is made between pore pressures and effective stresses in undrained-C type model. The fifth one is the (v) non-porous type model in which neither initial stresses nor pore pressures are considered. In this study, undrained-A and undrained-B type models are used for soft soils to investigate the effective and undrained strength parameter effects on settlement reduction ratio. The drained type model is used for SCs, gravel mats and embankment fills because, generation of excess pore pressures are not considered for these materials.

One of the most important stages of numerical modeling is to choose the appropriate material model for modeling of SCs and soft soils. Mohr-coulomb (MC) model is used as a first approximation for the soft soils. MC requires five input parameters and these parameters must be selected in the predetermined stress range. Hardening Soil (HS) model is also introduced for soft soils in which HS requires 8 input parameters. Other materials are modeled with MC.

K_0 procedure is used throughout the analyses for the generation of initial stresses. The consolidation analysis type is used throughout analyses for proper modeling of the development and dissipation of excess pore water pressures as a function of time. Plaxis recommended using geometry line at the level of ground water for the creation of accurate pore pressure distribution.

3.2 Selection of Case Studies

In Chapter 2 of this thesis, a comprehensive literature survey on the subject of behavior of SCs was given. Table 3.1 provides the ones chosen from the literature that include the field studies where SCs were installed to improve the soft ground. Elimination among these cases is performed as if the case has one of the following properties: (i) improved soil type without clay or improved soil type with lenses of peat or no information on material characteristics, (ii) complexity of geometry or insufficient information on geometry, (iii) combination with other improvement techniques, (iv) plate load tests.

In addition to criteria defined above, elimination is performed in; (i) East Brent case (Greenwood, 1991) and (ii) Bothkennar case (Serridge & Sarsby, 2009) due to observation of untreated foundation settlement less than treated one, (iii) Bombay case (Greenwood, 1991) due to observation of failure as a result of mis-use of small scale load tests, (iv) Sueca case (Castro & Sagaseta, 2012) due to absence of loading on columns and (v) Bothkennar case (Watts et al., 2001) due to heave observation under foundation after construction of columns.

Among the candidate cases that are suitable for investigating settlement behavior of soft soils improved with SCs, three case studies were chosen for further analysis. These cases are: (i) Omdurman case, (ii) Kebun case and (iii) Canvey Island case with soft, very soft and interlayered soft clay soil properties, respectively.

Table 3.1 Selection of Case Studies

Reference and Site Location	Foundation Type	Improved Soil Type	Column Type	a_r	S_r
Ashmawy et al. (2000)					
Tampa, Florida, U.S.A.	Plate	Sand	End Bearing	-	-
Largo, Florida, U.S.A.	Plate	Fill, Sand	End Bearing	-	-
Osceola County, Florida, U.S.A.	Plate	Fill, Sand	End Bearing	-	-
Ausilio & Conte (2007)					
San Michele di Serino, Italy	Raft	Silt, Gravel	Floating	-	0.62
Barksdale & Bachus (1983a)					
Hampton, U.S.A.	Ftg.	Silt, Clay	End Bearing	0.26	-
Barksdale & Goughnour (1984)					
Iowa, U.S.A.	Emb.	Fill, Clay	End Bearing	0.42	-
New Orleans, U.S.A	Emb.	Clay, Sand	End Bearing	0.25	-
Baumann & Bauer (1974)					
Konstanz, Germany	Raft	Silt	End Bearing	0.47	0.25
Quebec City, Canada	Ftg.	Sand	End Bearing	0.59	0.25
Bergado & Lam (1987)					
Bangkok, Thailand	Plate	Clay	End Bearing	-	-
Castro & Sagaseta (2012)					
Sueca, Spain	No Load	Silt, Clay, Sand	End Bearing	0.07	-
Chen & Bailey (2004)					
Washington, U.S.A.	Emb.	Sand, Silt	End Bearing	0.26	-
Clemente et al. (2005)					
U.K.	Ftg.	Sand	End Bearing	0.33	0.29
Cooper & Rose (1999)	Emb.	Clay, Silt, Peat	End Bearing	0.08	0.54
Bristol, U.K.	Emb.	Clay, Silt, Peat	End Bearing	0.15	0.39
DeStephen et al. (1997)					
New Jersey, U.S.A.	Raft	Fill	Floating	0.39	0.50
Ellouze et al. (2010)					
Zarzis, Tunisia	Stg. Tank	Sand	End Bearing	0.32	0.50
Damietta, Egypt	Stg. Tank	Clay	End Bearing	0.15	0.50
Gaeb et al. (2007)					
Klagenfurt, Austria	Emb.	Sand, Clay	Floating	0.13	-
Goughnour & Bayuk (1979b)					
Hampton, U.S.A.	Emb.	Clay, Silt	End Bearing	0.34	0.42
Greenwood (1970)					
Bremerhaven, Germany	Emb.	Clay, Peat	End Bearing	0.25	0.61
Greenwood (1991)					
Uskmouth, U.K.	Plate	Clay	End Bearing	-	-
East Brent (Somerset), U.K.	Emb.	Clay, Peat	End Bearing	0.12	1.66
St. Helens, U.K.	Ftg.	Fill	Floating	-	-
Canvey Island, U.K.	Stg. Tank	Clay	End Bearing	0.22	0.44
Humber Bridge S. Approach, U.K.	Emb.	Clay, Peat	End Bearing	0.11	0.77
Bombay, India	Stg. Tank	Clay	End Bearing	-	-
Hughes et al. (1976)					
Canvey Island, U.K.	Plate	Clay	End Bearing	-	-

Table 3.1 Selection of Case Studies (Continued)

Reference and Site Location	Foundation Type	Improved Soil Type	Column Type	a_r	S_r
Lopez & Shao (2007) California, U.S.A.	Raft	Clay, Sand	End Bearing	0.10	-
Mitchell & Huber (1985) California, U.S.A.	Ftg.	Silt, Clay, Sand	End Bearing	0.29	0.65
Mohamedzein & Al-Shibani (2011) Omdurman, Sudan	Emb.	Clay	End Bearing	0.15	0.53
Munfakh et al. (1983) New Orleans, U.S.A.	Emb.	Clay	End Bearing	0.25	0.59
Raju (1997a) Kinrara, Malaysia	Emb.	Silt, Fill	End Bearing	0.35	0.25
Kebun, Malaysia	Emb.	Clay	End Bearing	0.20	0.40
Raju et al. (2004) Kajang, Malaysia	Emb.	Silt, Fill	End Bearing	0.24	0.38
Serridge & Sarsby (2009) Bothkennar, U.K.	Strip Ftg.	Clay	Floating	0.20	2.25
Stuedlein and Holtz (2011) Texas, U.S.A.	Plate	Clay, Sand, Silt	Floating	-	-
Van Impe et al. (1997b) Klein-Willebroek, Belgium	Ftg.	Sand, Clay	End Bearing	0.05	-
Antwerp, Belgium	Raft	Fill, Clay, Sand	End Bearing	0.20	-
Watts et al. (2000)	Strip Ftg.	Fill	End Bearing	0.21	0.68
Watts et al. (2001) Bothkennar, U.K.	Raft	Clay	Floating	-	-
Wiltafsky & Thurner (2009)	Raft	Clay, Sand, Silt	End Bearing	-	-

3.3 Case Study I: Omdurman Case

New White Nile Bridge was planned to connect the two cities (Khartoum and Omdurman) of Sudan. At the Omdurman side, soft clay exists under the approach embankment. Among other reinforcement techniques, SCs were decided as a result of time constraints. SCs were constructed and settlements were recorded during the construction of 4 m high embankment and its consolidation stage (Mohamedzein & Al-Shibani, 2011). Data of Zone IA is selected for the finite element analysis. Analysis procedure for Zone IA is outlined in this section.

3.3.1 Geometry

The height of the soft soil is 7.5 m which lies on a dense to very dense silty or clayey sand with an average thickness of 8.5 m. Groundwater level is 2.5 m below ground surface. Side slope of embankment is 2H:1V. Figure 3.2 shows the geometry of the FE analyses and the observation point for settlement. Half of the geometry under plane strain conditions is analyzed.

The length of the SCs is 8.5 m. Critical length is calculated as 5.1 m using Eq. (2.1), Eq. (2.3) and Eq. (2.4). The diameter of SCs is 0.9 m and SCs are installed on a triangular grid with a spacing of 2.25 m. The area replacement ratio is 14.5%.

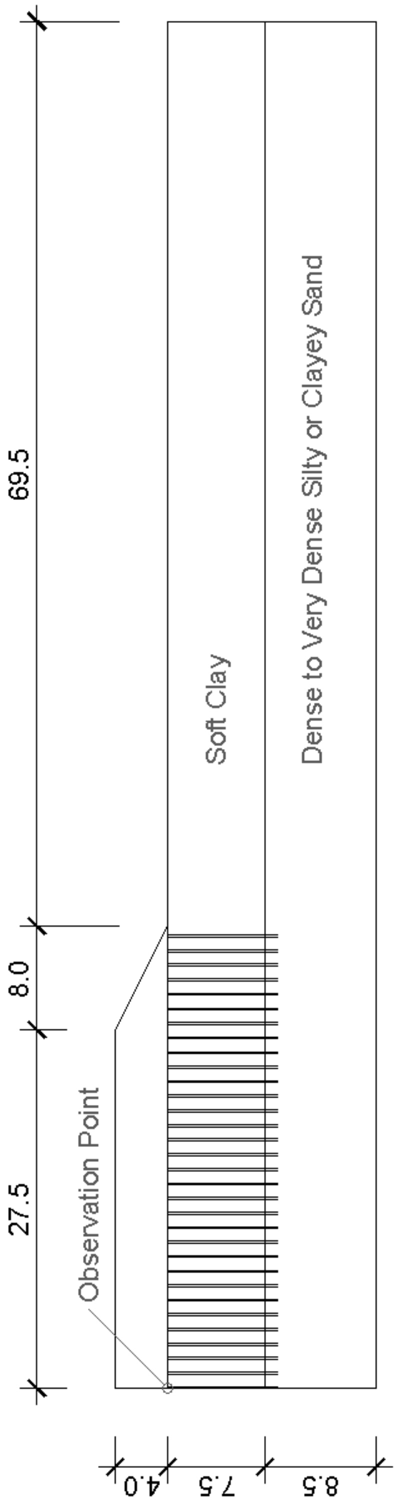

Figure 3.2 Geometry with Observation Point for Omdurman Case

Equivalent strip width (S') and new spacing (D') for 2D analysis is obtained by equating area replacement ratios of original case with converted case using Eq. (3.1) and Eq. (3.2).

$$D' = \frac{\pi * D^2}{4\sqrt{3} * S} \tag{3.1}$$

$$S' = S/2 \tag{3.2}$$

Values of D' and S' are calculated as 0.163 m and 1.125 m and they are rounded to 0.16 m and 1.12 m with a relative error of 1.8% and 0.4%, respectively.

In 2D analysis, left and right boundaries are restrained only in horizontal direction. Bottom boundary is fixed in both directions. Left and right vertical boundaries are closed to flow because left boundary is the line of symmetry and there is no free outflow at the right boundary. Bottom boundary is also closed to flow due to presence of weathered sandstone.

In 3D analysis, all side boundaries are restricted at "out of plane" direction and bottom boundary is fixed. All boundaries are closed to flow. Overview of generated mesh for the 2D and 3D analysis are shown in Figures 3.3 and 3.4, respectively.

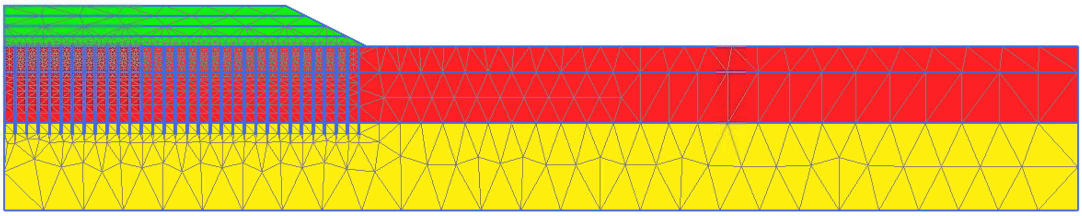

Figure 3.3 2D Mesh for Omdurman Case

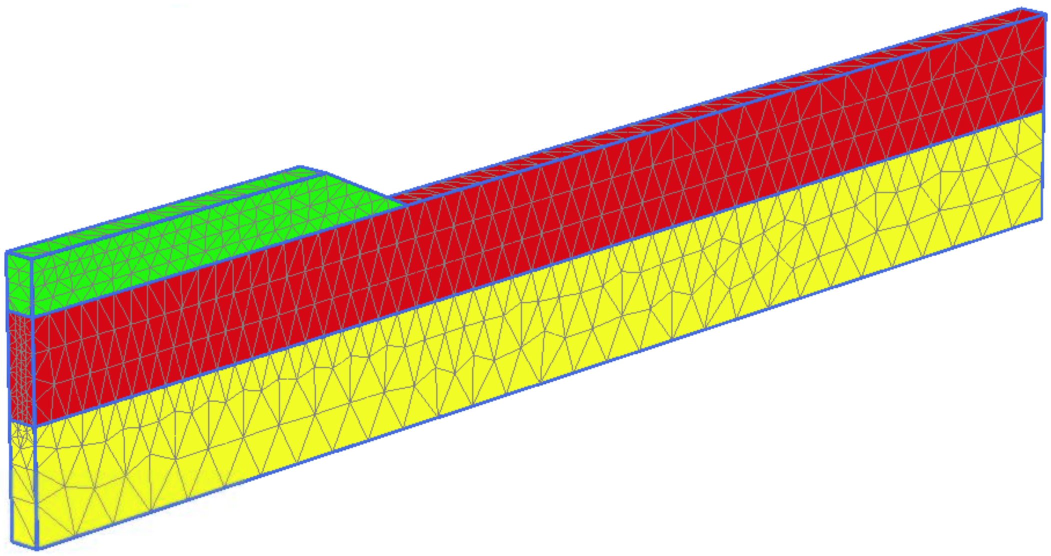

Figure 3.4 3D Mesh for Omdurman Case

Representative 3D slice is used rather than performing full 3D analysis (Gaeb et al. 2009). Domain of influence (i.e. width of the slice) for triangular spacing and square spacing can be found from Eq. (3.3) and Eq. (3.4), respectively (Balaam & Booker, 1981). For Omdurman case, Eq. (3.3) is used and d_e is found as 2.3625 m and rounded to 2.35 m with a relative error of 0.5%.

$$d_e = 1.05 * S \tag{3.3}$$

$$d_e = 1.13 * S \tag{3.4}$$

3.3.2 Material Parameters

General parameters for soft clay are given in Table 3.2. G_s is back-calculated from the Eq. (3.5), assuming fully saturated soil (S_d=100%).

$$e_0 = \frac{w_n * G_s}{S_d} \tag{3.5}$$

Unit weight of water is taken as 10 kN/m^3. γ_{dry} is calculated from the Eq. (3.6).

$$\gamma_{dry} = \frac{G_s}{(1+e)} * \gamma_w \tag{3.6}$$

Although γ_{bulk} used was 18.8 kN/m^3 for the numerical analysis performed in Mohamedzein and Al-Shibani (2011), γ_{sat} is calculated from the Eq. (3.7).

$$\gamma_{sat} = \frac{G_s + e}{(1+e)} * \gamma_w \tag{3.7}$$

c_v value given in Table 3.2 is assumed (Look, 2007). From Eq. (3.8), consolidation settlement is computed as 0.458 m.

$$s = \frac{H}{1+e_0} * \left(C_r * \log\left(\frac{\sigma'_c}{\sigma'_0}\right) + C_c * \log\left(\frac{\sigma'_0 + \Delta\sigma}{\sigma'_c}\right)\right) \tag{3.8}$$

where values of $\Delta\sigma$, σ'_0 and σ'_c are 82.38 kPa, 47.65 kPa and 67.66 kPa, respectively. C_r value is calculated from Eq. (3.9) as stated by Nagaraj and Srinivasa Murthy (1985).

$$C_r = 0.000463 * G_s * LL \tag{3.9}$$

Vertical permeability of the soft clay is calculated from the Eq. (3.10). k_h/k_v ratio is taken as 1.5 (Basett & Brodie, 1961).

$$c_v = \frac{k_v}{m_v * \gamma_w} \tag{3.10}$$

Undrained elastic modulus and undrained shear strength relationship is shown in Eq. (3.11). β coefficient is between 200 and 500 for normally consolidated sensitive clays (Bowles, 1997).

$$E_u = \beta * c_u \tag{3.11}$$

Table 3.2 General Parameters for Soft Clay (Omdurman Case)

Property	Soft Clay
PL (%)	29[a]
LL (%)	54[a]
PI (%)	26[a]
G_s	2.616
w_n (%)	64[b]
e	1.674[a]
c_u (kPa)	17.5[a]
ϕ' (deg)	29.25[a]
C_c	0.541[a]
C_r	0.065
q_c (kPa)	784[a]
OCR	1.42[a]
γ_{dry} (kN/m^3)	9.78
γ_{sat} (kN/m^3)	16.04
c_v (m^2/day)	1.55E-3
m_v (m^2/kN)	6.47E-4
$k_{vertical}$ (m/day)	1.0E-5
$k_{horizontal}$ (m/day)	1.5E-5

[a] Median values taken from Mohamedzein and Al-Shibani (2011) are shown.

[b] Upper bound value taken from Mohamedzein and Al-Shibani (2011) is shown.

Relationship between CPT tip resistance and m_v is shown in Eq. (3.12) after Mitchell and Gardner (1975).

$$m_v = \frac{1}{\alpha_m * q_c} \tag{3.12}$$

Relationship between drained and undrained modulus is shown in Eq. (3.13) which comes from equating shear modulus values of both loading cases.

$$E' = \frac{2}{3} * E_u * (1 + \vartheta') \tag{3.13}$$

Different relationship between drained and undrained modulus for soft clays is shown in Eq. (3.14) (Concrete Institute, 1999).

$$E' = 0.4 * E_u \tag{3.14}$$

From one dimensional consolidation, consolidation settlement is found from Eq. (3.15). Correction of oedometric settlement to consolidation settlement is between 1.0 and 1.1 (Skempton & Bjerrum, 1957). For this case, 1.0 value is adapted for correction from oedometric settlement.

$$s = m_v * \Delta\sigma * H \tag{3.15}$$

Relationship between drained modulus and coefficient of volume compressibility is given in Eq. (3.16).

$$E' = \frac{(1+\vartheta') * (1-2\vartheta')}{(1-\vartheta') * m_v} \tag{3.16}$$

Janbu (1963) presented Eq. (3.17) for the determination of E'. K and n values are used as 16 and 0.95, respectively (Mohamedzein and Al-Shibani, 2011). σ'_3 is calculated as 23.8 kPa for the mid-height of the soft clay to obtain an average drained modulus. P_a is taken as 100 kPa.

$$E' = K * P_a * \left(\frac{\sigma'_3}{P_a}\right)^n \tag{3.17}$$

Different drained modulus values are tabulated in Table 3.3. Drained Poisson's ratio of soft clay is taken as 0.3.

E' value is taken as 1150 kPa in the numerical analysis. Corresponding m_v value given in Table 3.2 is calculated from Eq. (3.16).

Table 3.3 Drained Modulus Values for Soft Clay (Omdurman Case)

Equations used	E' (kPa)
Eq. (3.15) and Eq. (3.16)	1002
Eq. (3.17)	410
Eq. (3.11) and Eq. (3.14)	1400
Eq. (3.11) and Eq. (3.13)	3033
Eq. (3.12) and Eq. (3.16)	1165

ϕ' value is calculated in relation with plasticity index value by using the chart given by Gibson (1953). Although K_0 is assumed as 0.5 in Mohamedzein and Al-Shibani (2011), Jaky's formula is used to obtain K_0 value (K_0=1-sinϕ). Mohr-Coulomb parameters are tabulated in Table 3.4.

Table 3.4 Mohr Coulomb Parameters for Soft Clay (Omdurman Case)

Property	Soft Clay
Type of Behavior	Undrained-A
E' (kPa)	1150
ν'	0.3
ϕ' (deg)	27
c' (kPa)	0.2
ψ (deg)	0
K_0	0.546

Dilation angle is generally accepted as zero for soft clays. Cohesion intercept is taken as 0.2 kPa to reduce numerical instabilities. Undrained-A means effective compressibility and strength characteristics are used in consolidation analysis. In addition, Hardening Soil model is also used for soft clay. Parameters are shown in Table 3.5.

Table 3.5 Hardening Soil Parameters for Soft Clay (Omdurman Case)

Property	Soft Clay
Type of Behavior	Undrained-A
E_{50}^{ref} (kPa)	2322
E_{oed}^{ref} (kPa)	1548
E_{ur}^{ref} (kPa)	6966
m	1
ν_{ur}	0.2
ϕ' (deg)	27
c' (kPa)	0.2
ψ (deg)	0

p^{ref}=50 kPa and R_f=0.9

Other material parameters are tabulated in Table 3.6. Poisson's ratios are assumed as 0.3. Jaky's formula is also obeyed for other materials. Drained modulus of stone column is calculated from Eq. (3.17). K and n values are taken as 640 and 0.43, respectively (Mohamedzein and Al-Shibani, 2011). Average σ'_3 value was used in Eq. (3.17).

Table 3.6 Mohr Coulomb Parameters for Other Materials (Omdurman Case)

Property	Dense Sand	Stone Column	Embankment Fill
Type of Behavior	Drained	Drained	Drained
PI (%)	11[a]	-	-
γ_{dry} (kN/m^3)	20[a]	22[a]	22[a]
γ_{sat} (kN/m^3)	20[a]	22[a]	22[a]
$k_{vertical}$ (m/day)	1	1	1
$k_{horizontal}$ (m/day)	1	1	1
E' (kPa)	30000	34500	40000
ν'	0.3	0.3	0.3
ϕ' (deg)	36[a]	42[a]	33[a]
c' (kPa)	0.2	0.2	14.2[a]
ψ	0	0	0
K_0	0.412	0.331	0.455

[a] Values are taken from Mohamedzein and Al-Shibani (2011).

3.3.3 Loading History

As described by Mohamedzein and Al-Shibani (2011), SCs were constructed between 26 January 1998 and 30 May 1998 (total of 124 days). After the construction of columns, settlement plates were located on top of SCs at the centerline of the embankment. Sand cushion and embankment construction took 61 days. Highest settlement (0.243 m) recorded on day 110 which counts from the end of SC consolidation period. Columns constructed in Zone I refers to 13 days by comparing the reinforced area of Zone I with other zones. Embankment was constructed in 4 lifts, assuming 1 m thickness for each lift. Sand cushion is regarded as embankment fill in this analysis.

Table 3.7 Phase Description for Omdurman Case

Phase Description	Duration (Days)
Initial Conditions (K_0 Procedure)	0
Construction of Stone Columns	13
Consolidation	111
1 m lift	16
1 m lift	16
1 m lift	16
1 m lift	13
Consolidation	49

3.3.4 2D and 3D Finite Element Model Comparison

Concern is arised from the dissipation path differences that may occur between 2D and 3D models. Representative 3D slice is used to lessen computational effort (Gaeb et al., 2009). Phase displacements of 2D, 3D FE models and observed case are shown in Figure 3.5. It should be noted that materials at the site may not be homogeneous and construction of embankment have not followed a systematic pattern. 2D models captured the observed behavior notably. In addition, agreement with observed data increased in the case of 2D HS model. For 2D models, difference with the observed data till the day 50 may due to an unclear constructional process. 3D models deviated from 2D models starting from the second lift. This deviation could not be understood for 3D models.

Mesh sensitivity analysis and comparison of 2D and 3D FE models with observed measurement are given in Table 3.8. As illustrated, generated mesh of baseline case is found to be satisfactory for both models. Relative errors of 2D models with respect to observed settlement are considered to be acceptable. Greater accuracy of 2D HS model can be also seen in this table. 2D conversion yielded comparable result with observed data. Parametric study will be carried out under 2D conditions with MC material model.

Another comparison is made between the numerical model performed by Mohamedzein and Al-Shibani (2011) with the models in this study. Settlement at ground surface in different locations measured from embankment toe is given in Figure 3.6. The amount of settlement increases from the toe toward the center of the embankment. It is reminded that the in situ settlements were higher than the numerical model of Mohamedzein and Al-Shibani (2011). Keeping that in mind, 3D MC and HS models captured the observed behavior between toe and 10 m distance. 2D HS model deviated between 4 m to 8 m but, agreement is quite good at the centerline of the embankment.

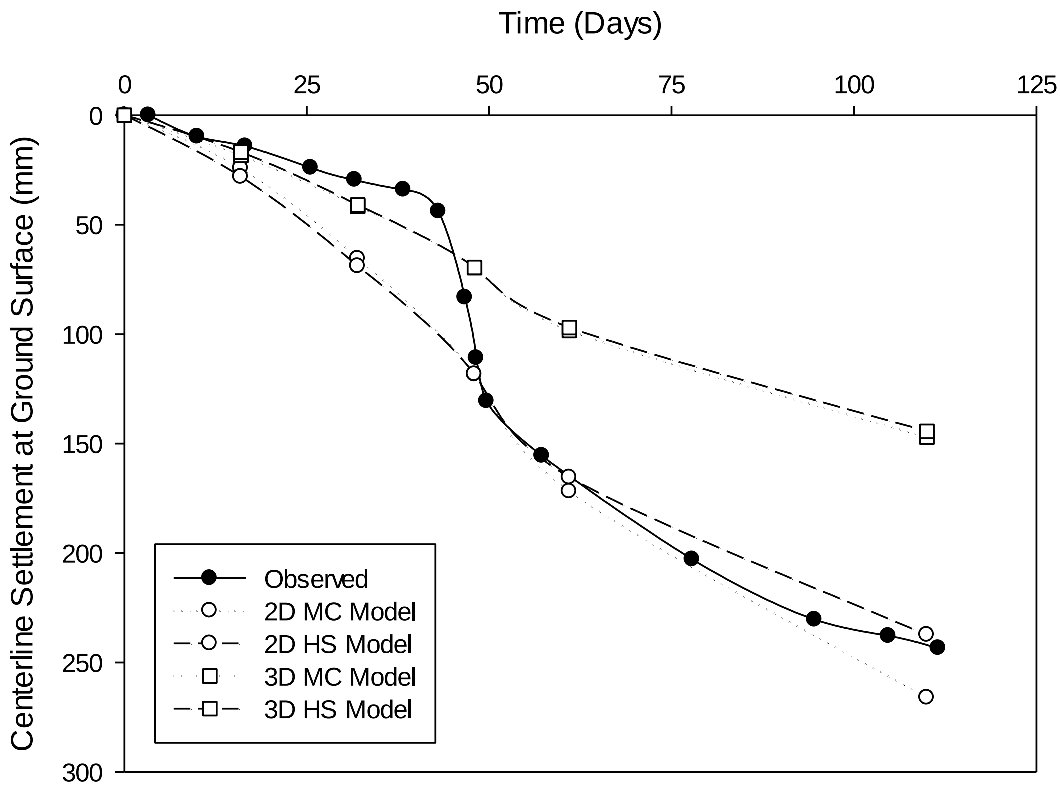

Figure 3.5 Settlement vs. Time (Omdurman Case)

Table 3.8 Settlement Comparison and Mesh Sensitivity for Omdurman Case

		2D FE Model			3D FE Model		
	Observed	MC	MC Refined Mesh	HS	MC	MC Refined Mesh	HS
Settlement (mm)	243.0	266.0	267.9	237.4	147.1	146.6	144.4
Relative Error w.r.t. Observed Value (%)		9.5	10.2	2.3	39.5	39.7	40.6
Total Number of Elements		2448	3777	2448	17006	27877	17006

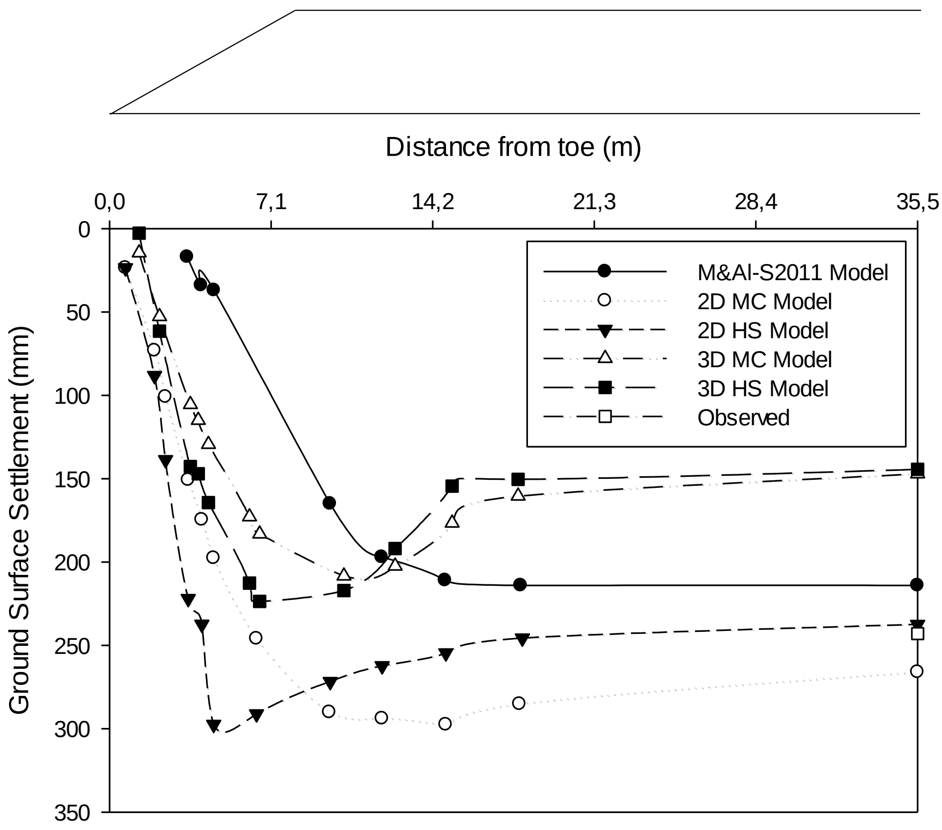

Figure 3.6 Settlement of Embankment with Different Models

3.3.5 Parametric Study

Effects of soil and column parameters on settlement reduction ratio are shown in Figures 3.7 - 3.14 and effects of parameters with depth on settlement are shown in Figures 3.15 - 3.22. MC parameters for soft clay and other materials were tabulated in Table 3.4 and Table 3.6, respectively. Although E'_{soil} also changes untreated settlement, values in Table 3.3 are investigated to show the significance of determination of true E'_{soil}. Major parameters affecting S_r are determined as; E'_{soil}, ν'_{soil}, $K_{0,soil}$ and E'_{column}. S_r decreases almost linearly with increasing value of ν_{soil} as can be seen in Figure 3.8. ϕ'_{soil} (see Figure 3.9, 3.17) and ν'_{column} (see Figure 3.12, 3.20) variation has no effect on S_r. $K_{0,soil}$ value is limited between active and passive coefficient of earth pressures. Priebe (1995) assumed the $K_{0,soil}$ value as 1.0 and Castro and Karstunen (2010) recommended to use $K_{0,soil}$ value of 1.4 in design assuming dissipation of excess pore pressures. This range was investigated in this study and $K_{0,soil}$ value equal to 1 gave better result compared to Jaky's formula as far as observed data is considered (see Figure 3.10). As can be seen from Figure 3.11, E'_{column}/E'_{soil} ratios approximately lower than 10 affected S_r remarkably. On the other hand, S_r value remained almost constant for E'_{column}/E'_{soil} ratios approximately larger than 10. Excluding the extreme cases of $\phi'_{column}=48^o$ and $\psi_{column}>\phi'_{column}-30^o$ (24 and 42 degrees in this case), stone column angle of shearing resistance and dilation angle effect on S_r is not considerable (see Figure 3.13 and 3.14). Plaxis recommended to use $\psi=\phi'-30^o$ equation to find the dilation angle.

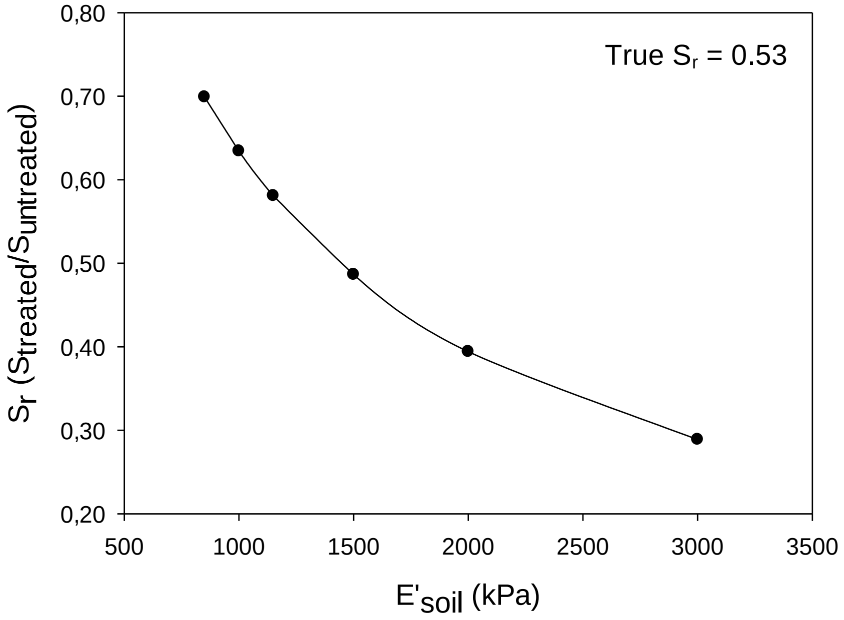

Figure 3.7 S_r versus E'_{soil} (Omdurman Case)

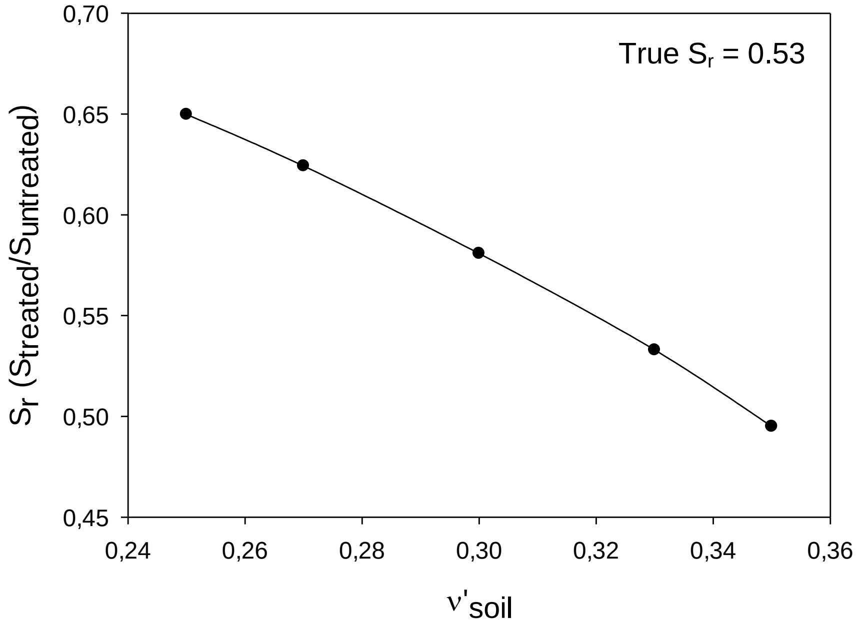

Figure 3.8 S_r versus ν'_{soil} (Omdurman Case)

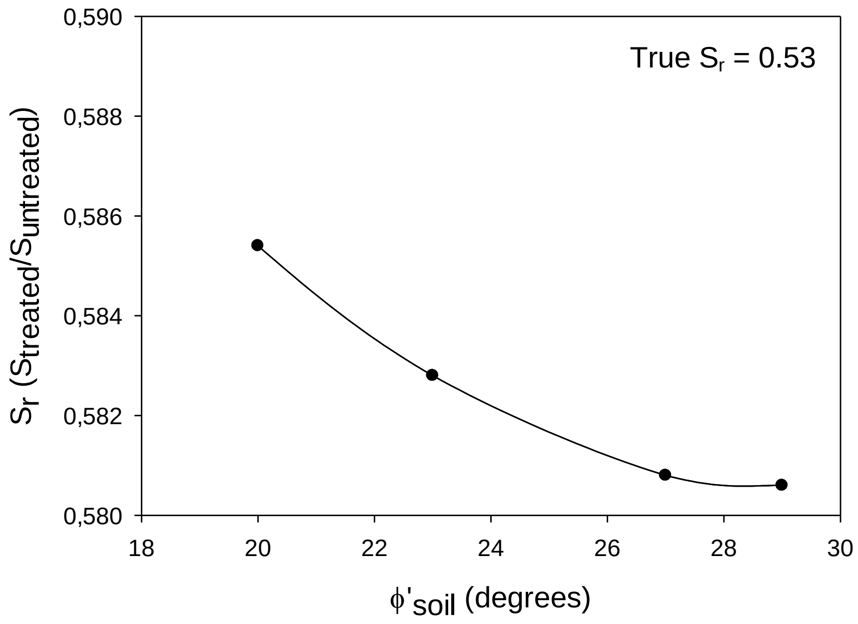

Figure 3.9 S_r versus ϕ'_{soil} (Omdurman Case)

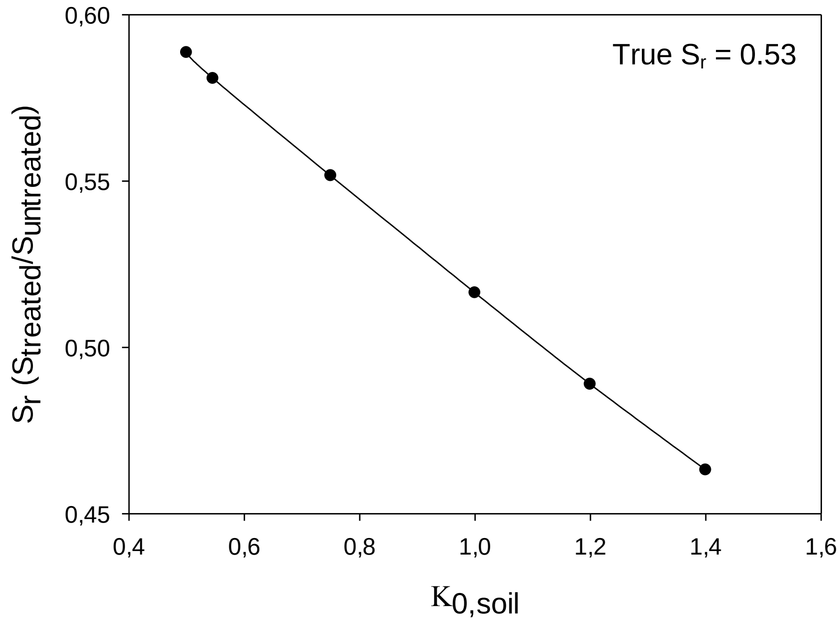

Figure 3.10 S_r versus $K_{0,soil}$ (Omdurman Case)

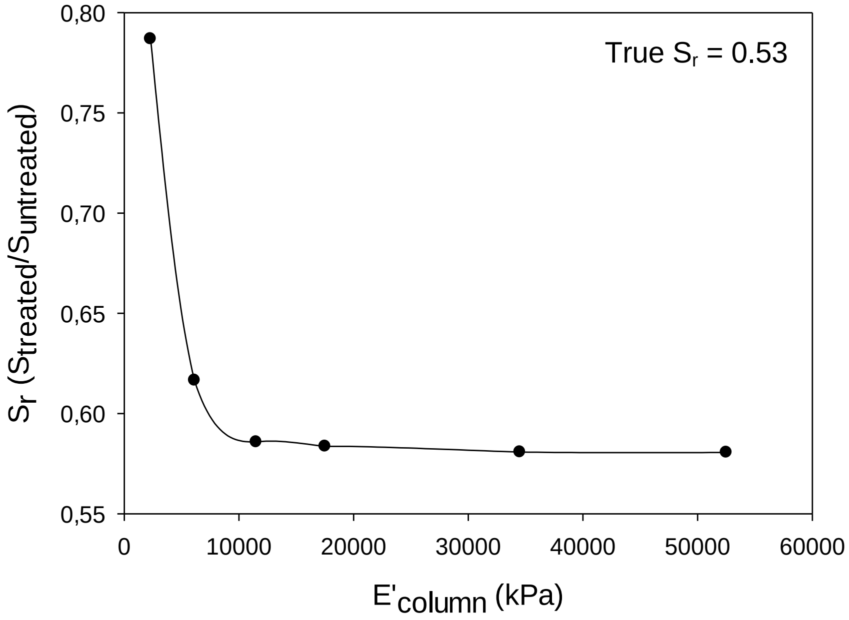

Figure 3.11 S_r versus E'_{column} (Omdurman Case)

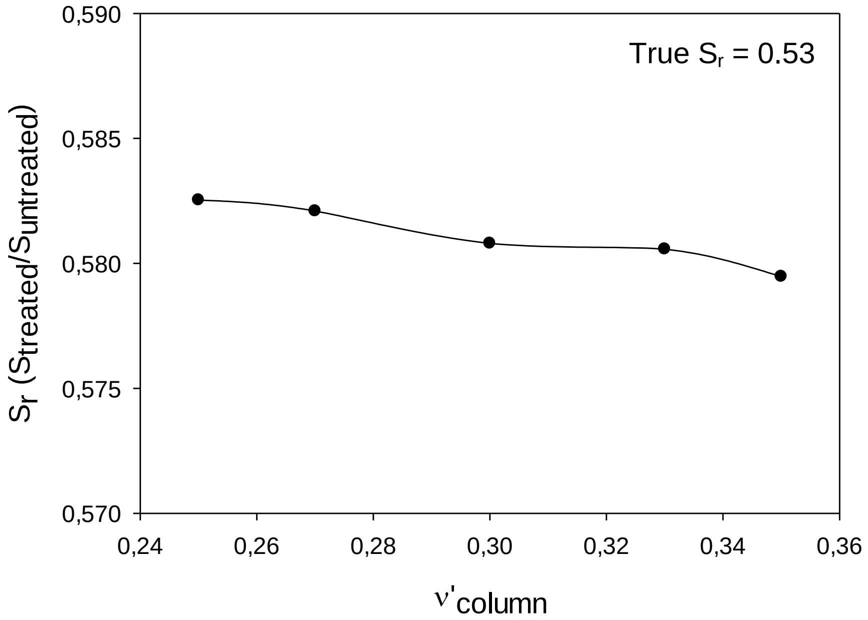

Figure 3.12 S_r versus ν'_{column} (Omdurman Case)

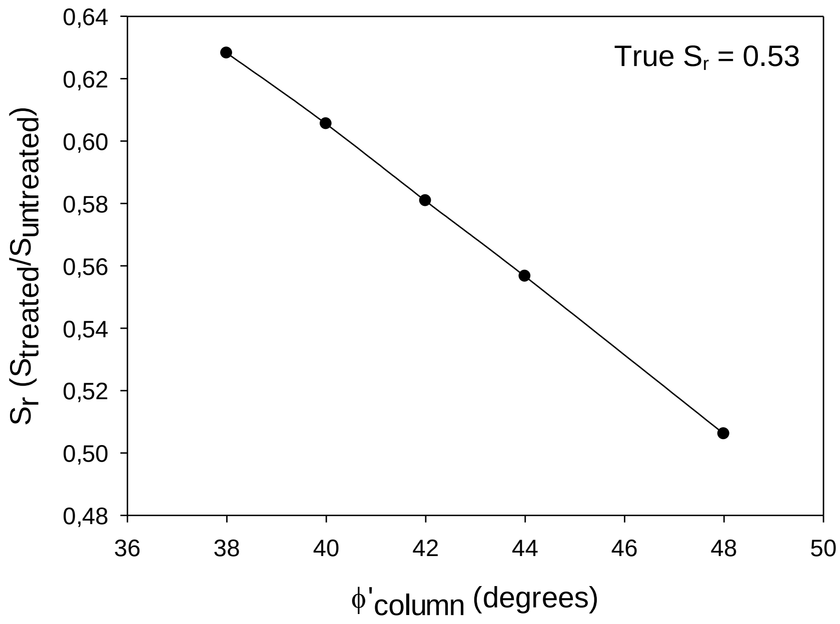

Figure 3.13 S_r versus ϕ'_{column} (Omdurman Case)

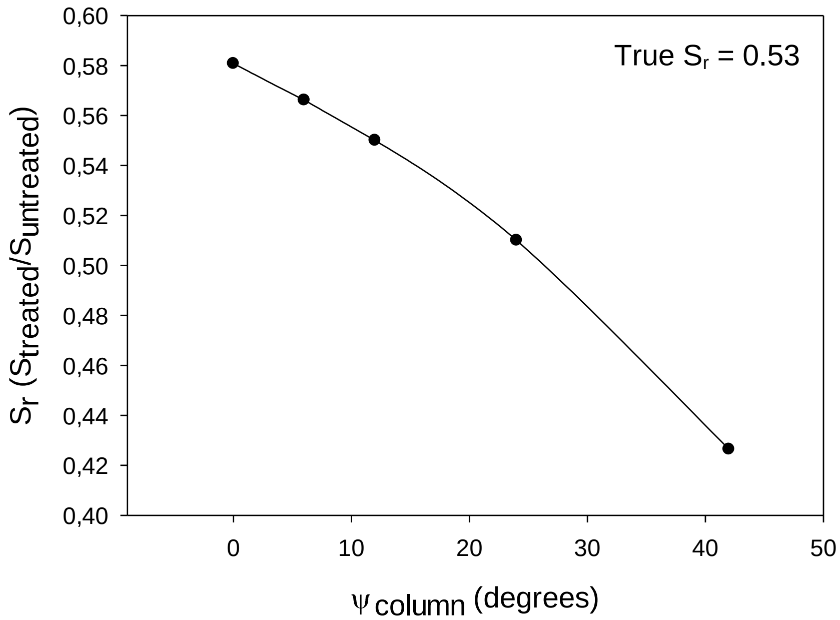

Figure 3.14 S_r versus ψ_{column} (Omdurman Case)

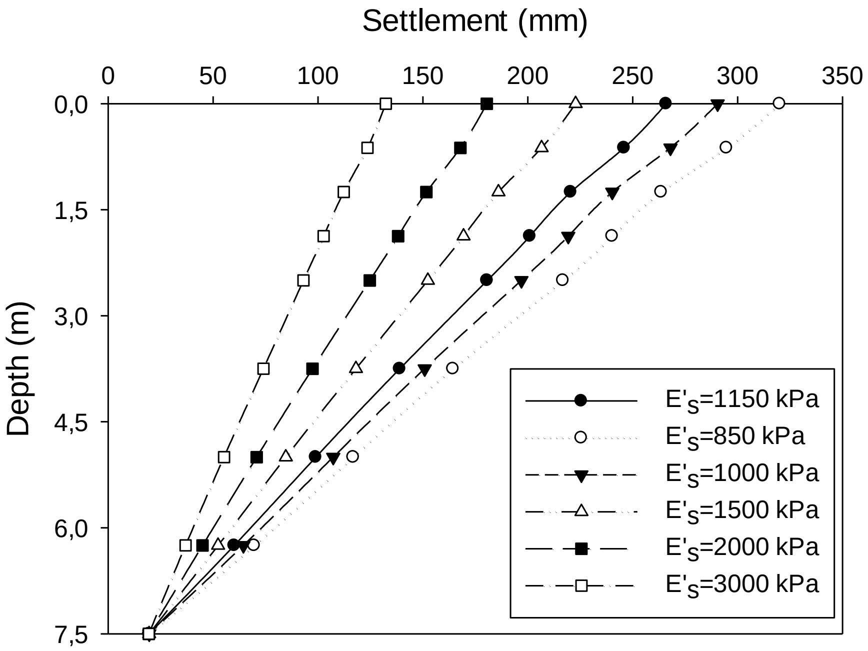

Figure 3.15 Effect of E'_{soil} with Depth (Omdurman Case)

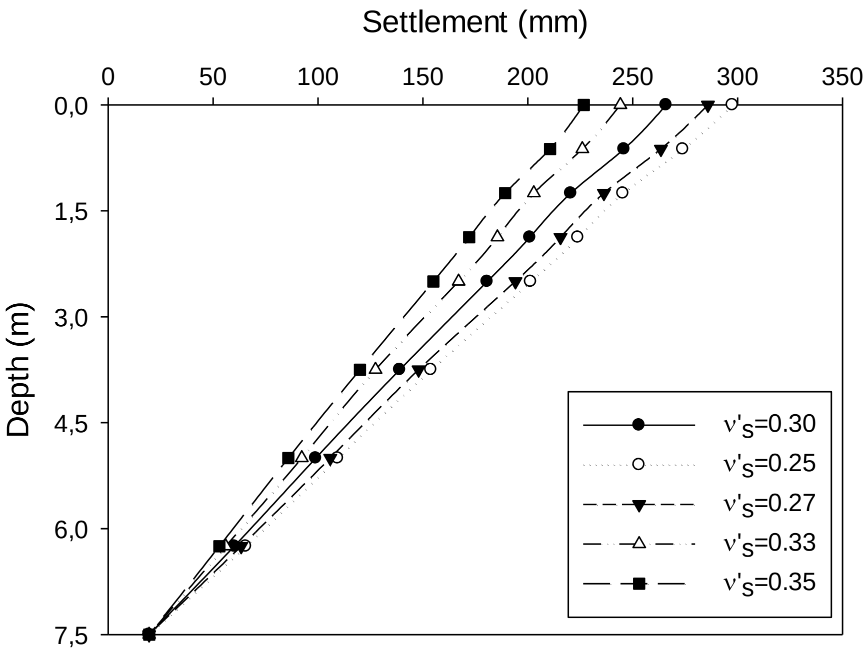

Figure 3.16 Effect of ν'_{soil} with Depth (Omdurman Case)

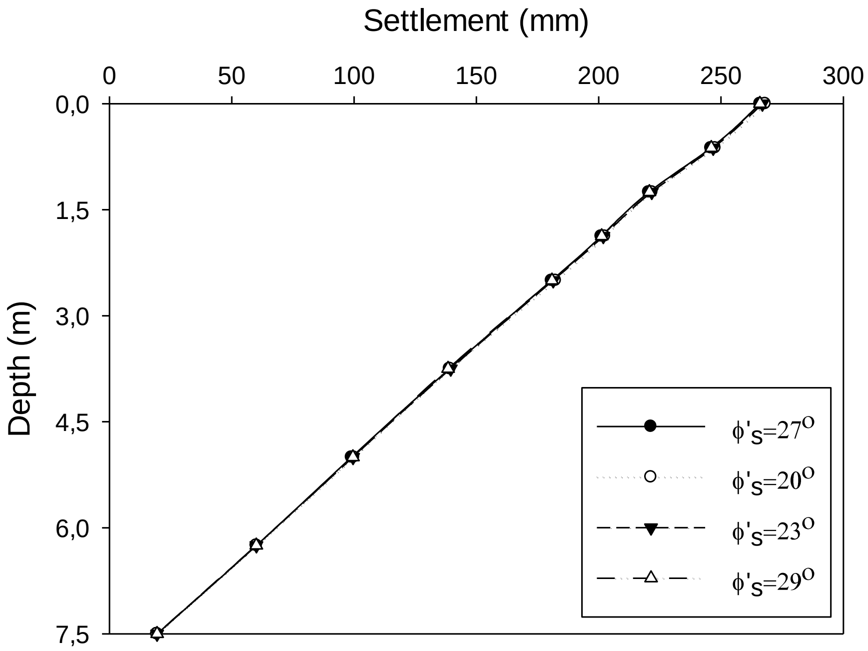

Figure 3.17 Effect of ϕ'_{soil} with Depth (Omdurman Case)

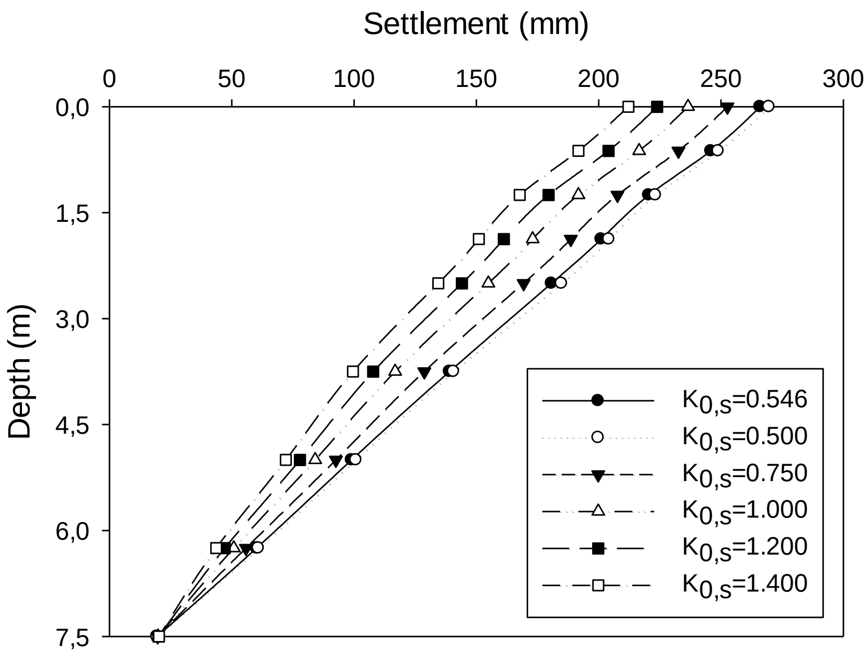

Figure 3.18 Effect of $K_{0,soil}$ with Depth (Omdurman Case)

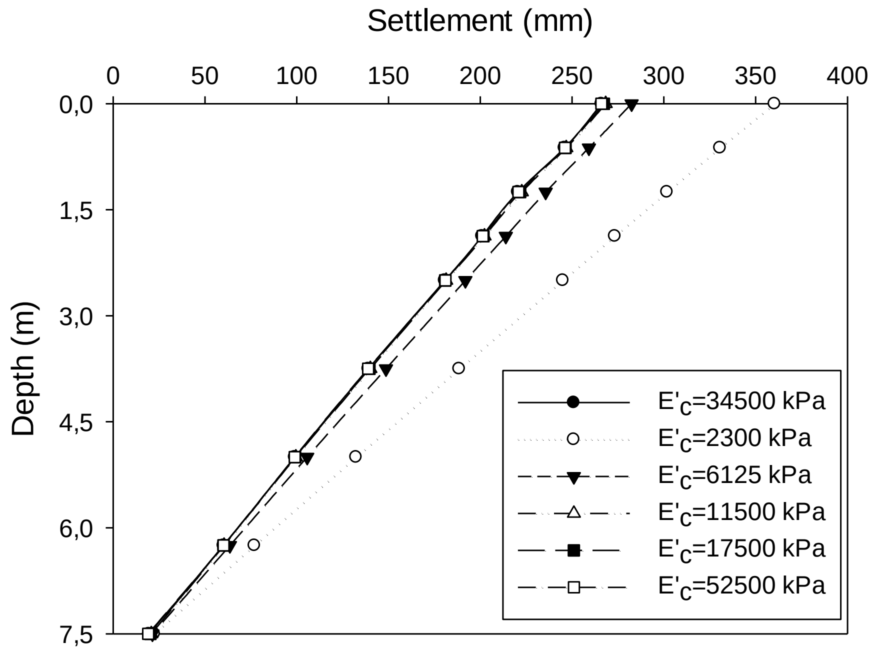

Figure 3.19 Effect of E'_{column} with Depth (Omdurman Case)

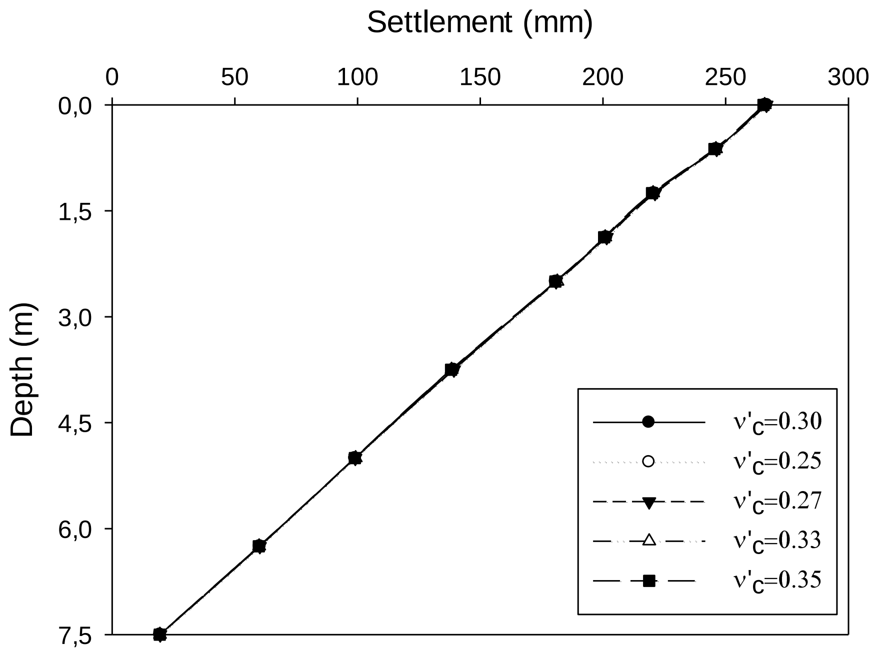

Figure 3.20 Effect of ν'_{column} with Depth (Omdurman Case)

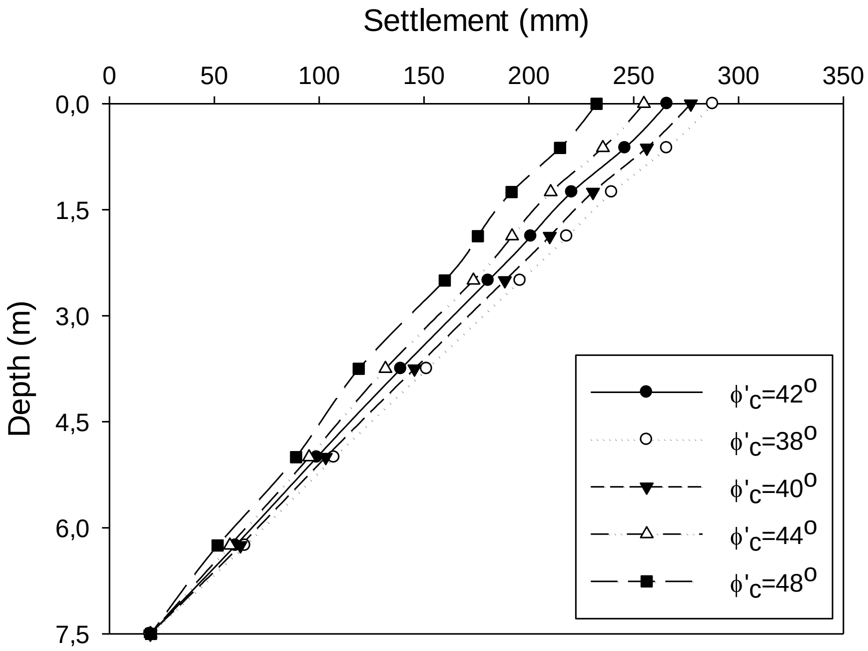

Figure 3.21 Effect of ϕ'_{column} with Depth (Omdurman Case)

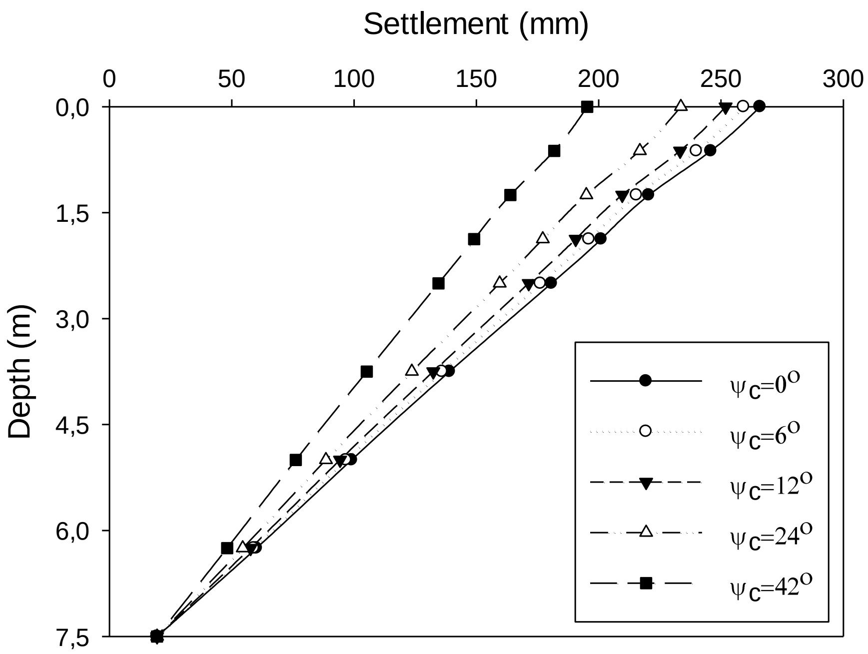

Figure 3.22 Effect of ψ_{column} with Depth (Omdurman Case)

3.4 Case Study II: Kebun Case

The new Shah Alam Expressway was intended to link two cities (Klang and Kuala Lumpur) of Malaysia. SCs were constructed with vibro replacement technique at Kebun interchange to improve soft marine clay. SCs were constructed and settlements were recorded during the construction of 1.6 m high embankment and 1 m high surcharge and its consolidation stage (Raju, 1997a, Raju et al. 1997b). Analysis procedure for Kebun case is outlined in this section.

3.4.1 Geometry

Although soft soil height from CPT data corresponds to 11 m thick soft clay in Raju (1997a), thickness is given as 10 m to 12 m in Raju et al. (1997b). It is mentioned that a ground failure observed when a 1 m sand platform was placed on soft soil.

1 m excavation is assumed in this analysis and 1 m thick sand platform is placed in the excavated area. Soft soil height is taken as 12.0 m and corresponding untreated settlement is taken as 1.0 m as stated in Raju (1997a).

SC length is 12.0 m. Critical length is calculated as 5.7 m using Eq. (2.1), Eq. (2.3) and Eq. (2.4). SC diameter is 1.1 m with a square spacing of 2.2 m. Area replacement ratio is 19.6%. Equivalent strip width (w) for 2D analysis is obtained from Eq. (3.18).

$$w = \pi * D^2/(4 * S) \tag{3.18}$$

w is calculated as 0.432 m for a spacing of 2.2 m. To lessen computational effort, value of w used in this analysis is rounded to 0.44 m with a relative error of 1.9%.

Soft clay is underlain by stiff clay up to 30 m depth. Stiff clay layer is omitted in this analysis. Groundwater level is assumed 1 m below ground surface. Side slope is assumed as 2H:1V. Sand platform is assumed to end 5 m away from the embankment toe.

Geometry and settlement observation point is shown in Figure 3.23. Geometry is analyzed under plane strain conditions in 2D.

In 2D analysis, left and right boundaries are restrained only in horizontal direction. Bottom boundary is fixed in both directions. Left and right vertical boundaries are closed to flow. Bottom boundary is opened to flow due to presence of stiff clay deposits.

In 3D analysis, all side boundaries are restricted at “out of plane” direction and bottom boundary is fixed. All boundaries are closed to flow except bottom boundary.

Representative 3D slice is used as in the previous case (Gaeb et al. 2009). Domain of influence (or width of the slice) for square spacing is found as 2.4860 m from Eq. (3.4) and rounded to 2.50 m with a relative error of 0.6%. Overview of generated mesh for the 2D and 3D analysis are shown in Figures 3.24 and 3.25, respectively.

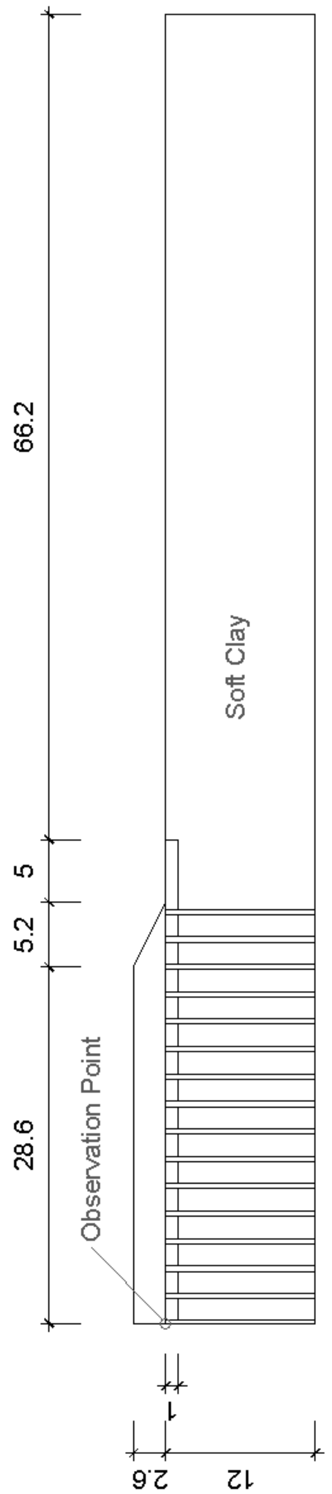

Figure 3.23 Geometry with Observation Point for Kebun Case

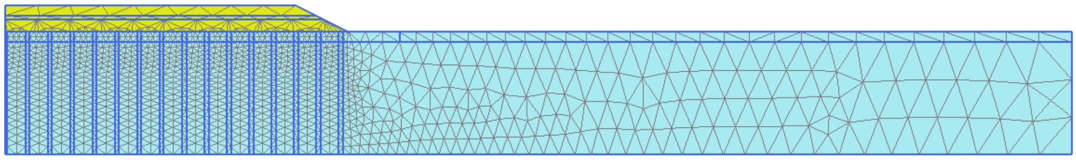

Figure 3.24 2D Mesh for Kebun Case

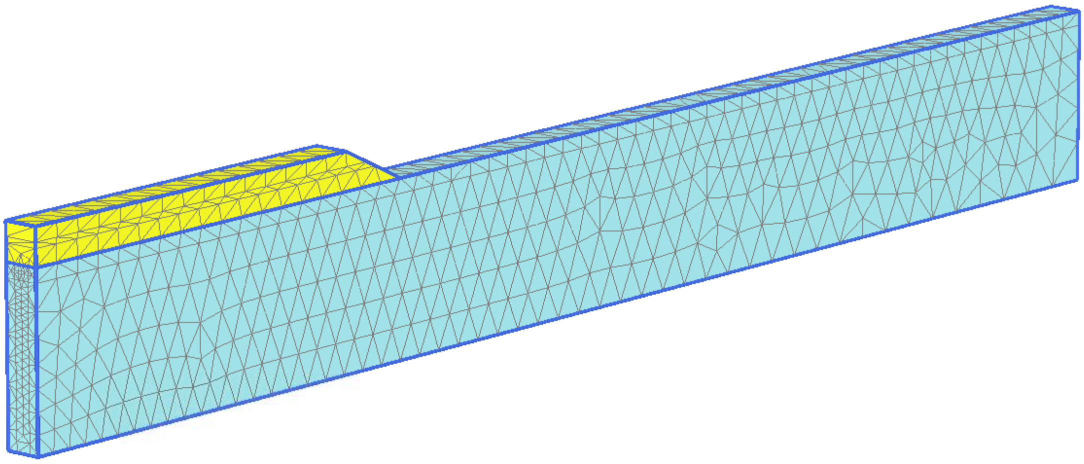

Figure 3.25 3D Mesh for Kebun Case

3.4.2 Material Parameters

General parameters for soft clay are given in Table 3.9. G_s is assumed as 2.65 and e is calculated using Eq. (3.5) assuming fully saturated soil (S_d=100%). γ_{dry} is calculated from Eq. (3.6) and γ_{sat} is calculated from the Eq. (3.7).

Eq. (3.15) is used to compute coefficient of volume compressibility, taking settlement as 1.0 m, $\Delta\sigma$ as 59.41 kPa (at mid-height of soft clay) and thickness as 11 m.

Vertical permeability of the soft clay is calculated from Eq. (3.10). k_h/k_v ratio is assumed as 1.5 (Basett & Brodie, 1961).

Table 3.9 General Parameters for Soft Clay (Kebun Case)

Property	Soft Clay
PL (%)	40[a]
LL (%)	100[a]
PI (%)	60[a]
G_s	2.65
w_n (%)	100[a]
e	2.65
S_t	4 – 5[a]
c_α (%)	1[a]
γ_{dry} (kN/m^3)	7.26
γ_{sat} (kN/m^3)	14.52
c_v (m^2/day)	2.74E-3[a]
m_v (m^2/kN)	1.49E-3
$k_{vertical}$ (m/day)	4.07E-5
$k_{horizontal}$ (m/day)	6.11E-5

[a] Values are taken from Raju (1997a) and Raju et al. (1997b).

Different drained modulus values are tabulated in Table 3.10. Drained Poisson's ratio of soft clay is taken as 0.3. Correction from oedometric settlement to actual settlement is taken as 1.1 in this case (Skempton & Bjerrum, 1957).

E' value is taken as 500 kPa at ground surface and 1000 kPa at 12 m depth. Corresponding m_v value given in Table 3.9 is calculated from Eq. (3.16) using E' value of 500 kPa.

Table 3.10 Drained Modulus Values for Soft Clay (Kebun Case)

Equations used	E' (kPa)
Eq. (3.15) and Eq. (3.16)	526
Eq. (3.11) and Eq. (3.14)	960
Eq. (3.11) and Eq. (3.13)	2080
Eq. (3.12) and Eq. (3.16)	446

ϕ' value is calculated as 20^o from Gibson (1953). Jaky's formula is used to obtain K_0 value (K_0=1-sinϕ). Mohr-Coulomb parameters for soft clay are tabulated in Table 3.11.

Undrained-B accounts for effective compressibility and undrained strength characteristics. Incremental value of E' and c_u with increasing depth are used in this analysis.

Table 3.11 Mohr Coulomb Parameters for Soft Clay (Kebun Case)

Property	Soft Clay
Type of Behavior	Undrained-B
E’ (kPa)	500[a]
ν’	0.3
c_u (kPa)	9[b]
K_0	0.658

[a] E’ is 500 kPa at ground surface and 1000 kPa at 12 m depth (Raju et al., 1997b).

[b] c_u is 9 kPa at ground surface and 15 kPa at 12 m depth (Raju et al., 1997b).

In addition, Hardening Soil model is used for soft clay as in the previous case. When modeling with Hardening Soil, stress dependency of soil stiffness could not be captured if undrained-B type drainage is used. Parameters are shown in Table 3.12.

Table 3.12 Hardening Soil Parameters for Soft Clay (Kebun Case)

Property	Soft Clay
Type of Behavior	Undrained-A
E_{50}^{ref} (kPa)	1275
E_{oed}^{ref} (kPa)	850
E_{ur}^{ref} (kPa)	3825
m	1
ν_{ur}	0.2
ϕ’ (deg)	20
c’ (kPa)	0.2
ψ (deg)	0

p^{ref}=40 kPa and R_f=0.9

Other material parameters are tabulated in Table 3.13. Embankment fill parameters are assumed in the range of engineering applications.

Permeabilities are set according to the maximum difference of 1E-5 allowed by Plaxis. Poissons ratios are assumed as 0.3.

Drained modulus of stone column is calculated from Eq. (3.17). K and n values are taken as 640 and 0.43, respectively (Mohamedzein and Al-Shibani, 2011). σ'_3 value is 18.6 kPa at the midheight of the soft clay to obtain an average modulus value.

Table 3.13 Mohr Coulomb Parameters for Other Materials (Kebun Case)

Property	Stone Column	Embankment Fill
Type of Behavior	Drained	Drained
γ_{dry} (kN/m^3)	20	22
γ_{sat} (kN/m^3)	20	22
$k_{vertical}$ (m/day)	4.07	4.07
$k_{horizontal}$ (m/day)	4.07	4.07
E' (kPa)	31000	40000
ν'	0.3	0.3
ϕ' (deg)	40[a]	38
c' (kPa)	0.2	5
ψ	0	0
K_0	0.357	0.426

[a] Value is taken from McCabe et al. (2010).

3.4.3 Loading History

SC and mat construction is assumed to finish in 20 days. After the construction of columns, settlement plates were located on top of SCs at the centerline of the embankment. Embankment was constructed in 3 lifts. It consists of 1.2 m fill lift, 0.4 m fill lift and 1 m surcharge. Settlement recordings were measured the highest settlement (0.4 m) on day 300 which commenced to count from the end of SC and mat construction process. Construction timeline is adopted from Raju et al. (1997b).

Table 3.14 Phase Description for Kebun Case

Phase Description	Duration (days)
Initial Conditions (K_0 Procedure)	0
Construction of Mat and Stone Columns	20
Consolidation	19
1.2 m Embankment Fill	14
Consolidation	12
Additional 0.4 m Fill	3
Consolidation	13
1 m Preloading	13
Consolidation	226

3.4.4 2D and 3D Finite Element Model Comparison

Representative 3D slice is used as in the previous case (Gaeb et al., 2009). Settlement versus time plot for Kebun case is shown in Figure 3.26.

2D and 3D FE model results gave remarkable agreement with in situ measurement. During the 1.2 m fill construction and its consolidation stage, models are shifted from observed case. This is attributed to the unclear constructional process at that stage.

Agreement of 3D models with the in situ measurement than the corresponding 2D models is more evident in this case. In addition, 3D HS model captured in situ measurement better than all other models as expected.

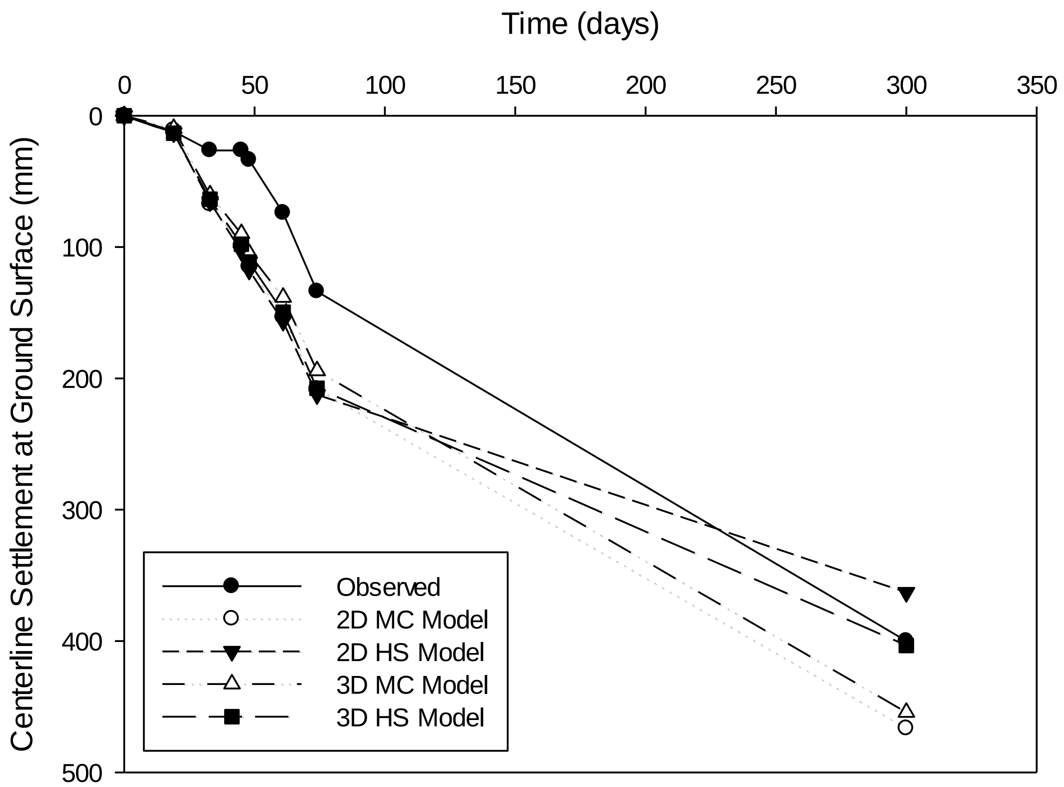

Figure 3.26 Settlement vs. Time (Kebun Case)

Mesh sensitivity analysis and comparison of settlements are given in Table 3.15. As can be seen, generated meshes of cases are found to be sufficient for 2D and 3D models.

HS models yielded better agreement with in situ measurement than MC models. 2D conversion yielded comparable result with representative 3D slice. Parametric study will be carried out under 2D conditions with MC material model as in the previous case.

Table 3.15 Settlement Comparison and Mesh Sensitivity for Kebun Case

		2D FE Model			3D FE Model		
	Observed	MC	MC Refined Mesh	HS	MC	MC Refined Mesh	HS
Settlement (mm)	400.0	466.5	483.7	363.0	454.3	459.4	403.3
Relative Error w.r.t. Observed Value (%)		16.6	20.9	9.3	13.6	14.9	0.8
Total Number of Elements		1787	2833	1787	17498	31000	17498

3.4.5 Parametric Study

Effects of soil and column parameters on settlement reduction ratio are shown in Figures 3.27 - 3.33 and effects of parameters with depth on settlement are shown in Figures 3.34 - 3.40. MC parameters for soft clay and other materials were tabulated in Table 3.11 and Table 3.13, respectively.

Results are similar with the Omdurman case. Although E'_{soil} also changes untreated settlement, values in Table 3.10 are investigated to show the significance of determination of true E'_{soil}. Major parameters affecting S_r are determined as; E'_{soil}, ν'_{soil}, $K_{0,soil}$ and E'_{column}.

S_r decreases almost linearly with increasing value of ν'_{soil} as shown in Figure 3.28.

ν'_{column} variation gave inconsistent results and omitted in this case.

$K_{0,soil}$ value equal to 1 also gave better result compared to Jaky's formula as far as observed data is considered (see Figure 3.30).

As illustrated in Figure 3.31, E'_{column}/E'_{soil} ratios approximately lower than 10 affected S_r notably. In contrast, S_r value remained almost constant for E'_{column}/E'_{soil} ratios approximately larger than 10.

Excluding the extreme cases of $\phi'_{column}=48^o$ and $\psi_{column}>\phi'_{column}-30^o$ (20 and 40 degrees in this case), stone column angle of shearing resistance (Figure 3.32 and 3.39) and angle of dilation (Figure 3.33 and 3.40) effect on S_r are not considerable, respectively.

Undrained-B drainage type is used to investigate the effect of $c_{u,soil}$ on S_r which was expected to be similar to E'_{column} variation. $c_{u,soil}$ could not be varied as desired. S_r value decreases with increasing $c_{u,soil}$ is the only observation obtained from Figure 3.29.

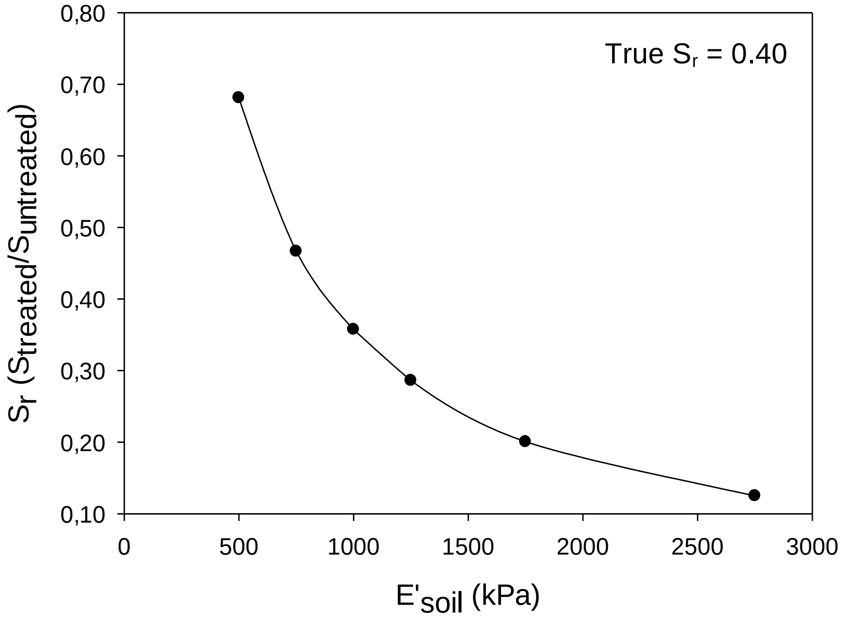

Figure 3.27 S_r versus E'_{soil} (Kebun Case)

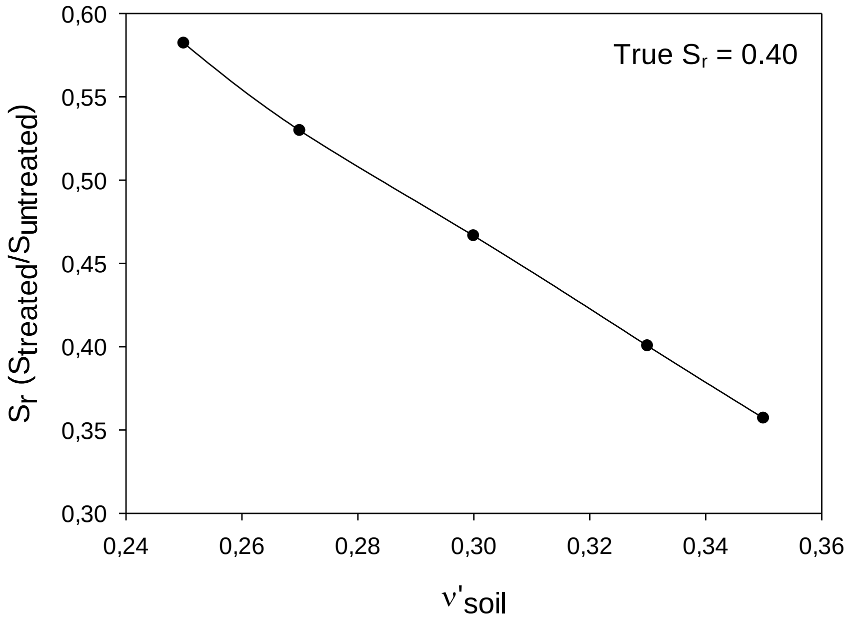

Figure 3.28 S_r versus ν'_{soil} (Kebun Case)

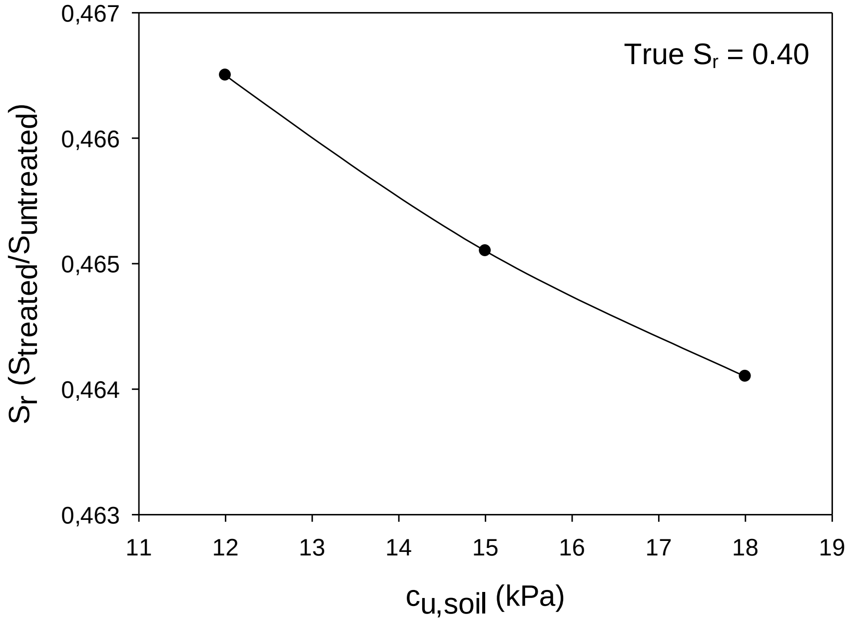

Figure 3.29 S_r versus $c_{u,soil}$ (Kebun Case)

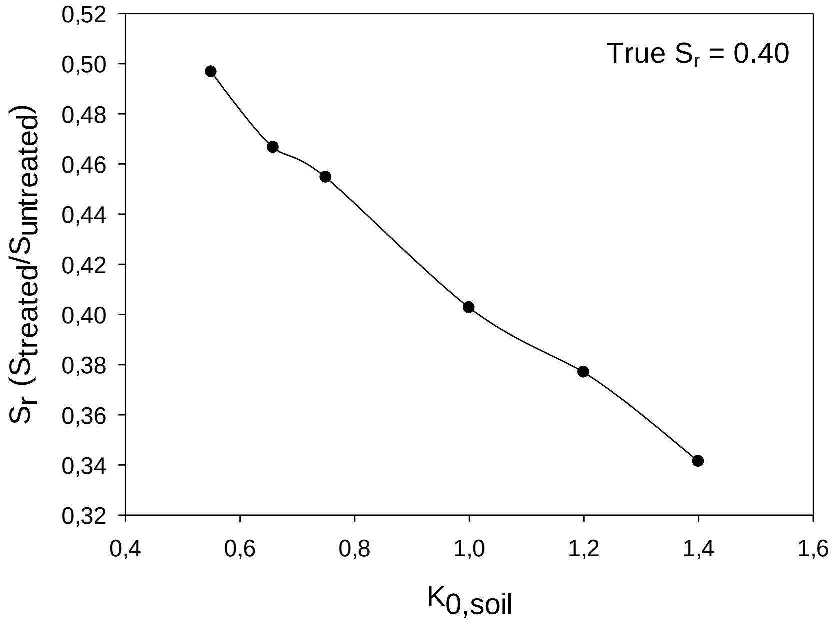

Figure 3.30 S_r versus $K_{0,soil}$ (Kebun Case)

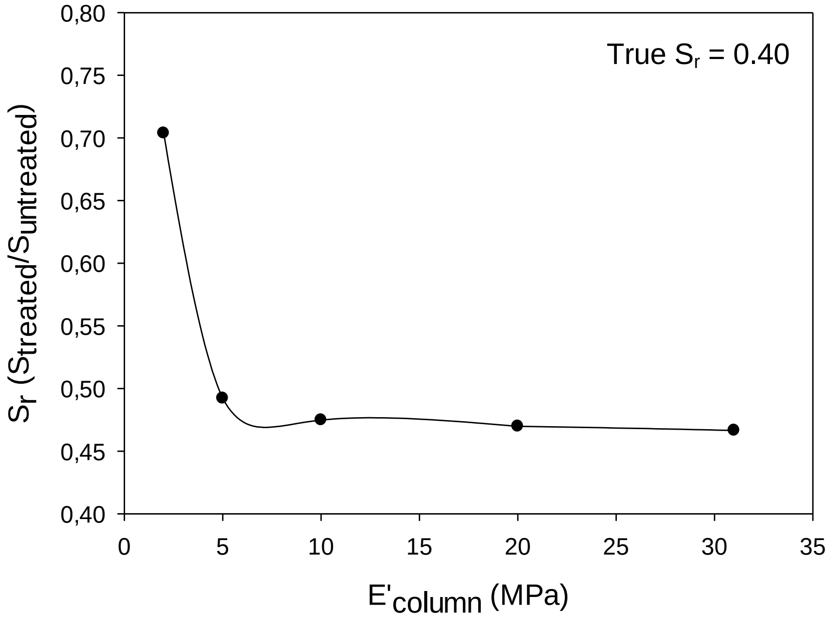

Figure 3.31 S_r versus E'_{column} (Kebun Case)

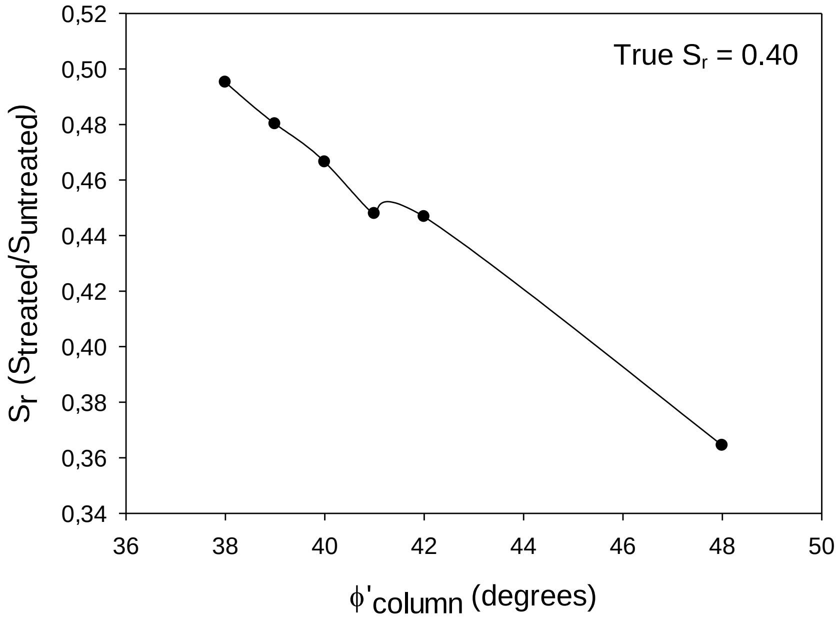

Figure 3.32 S_r versus ϕ'_{column} (Kebun Case)

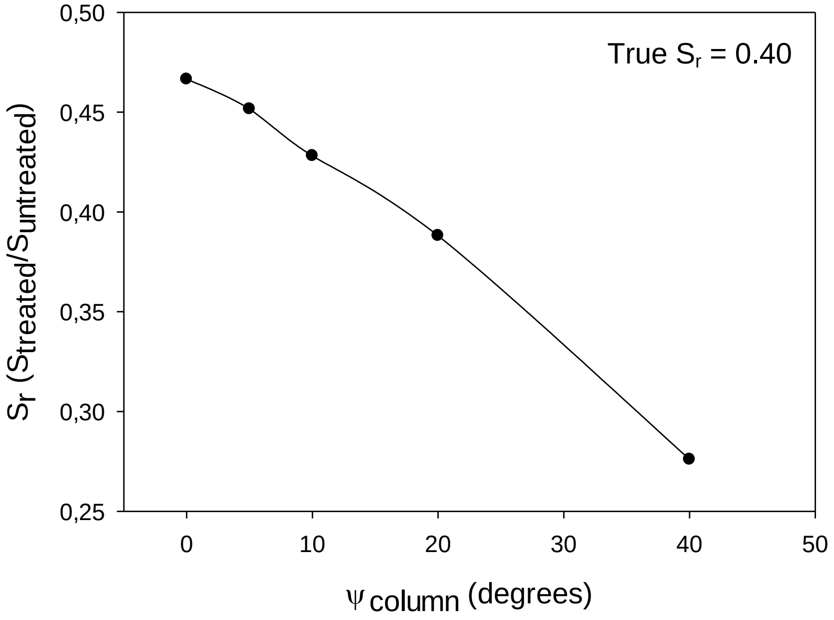

Figure 3.33 S_r versus ψ_{column} (Kebun Case)

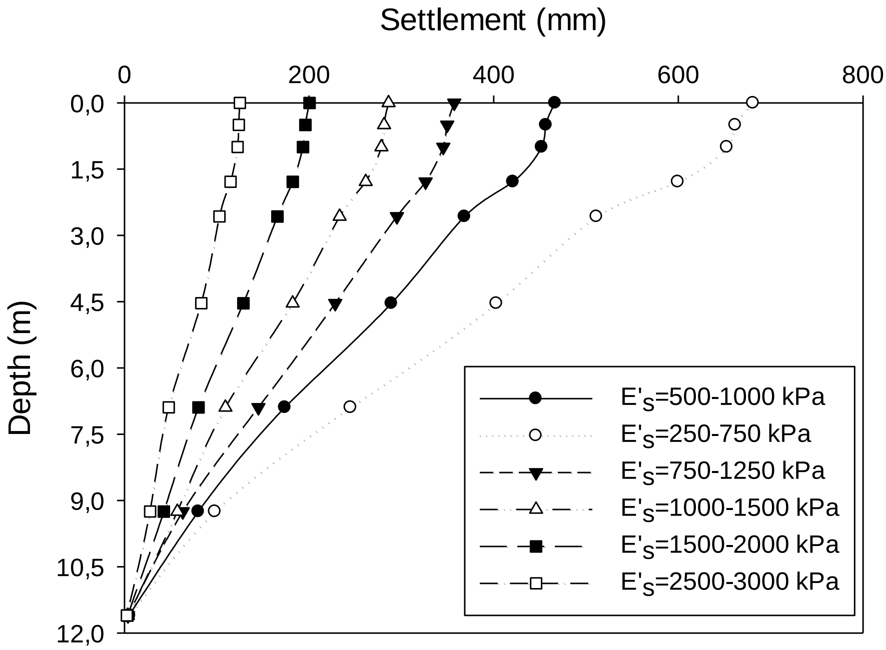

Figure 3.34 Effect of E'_{soil} with Depth (Kebun Case)

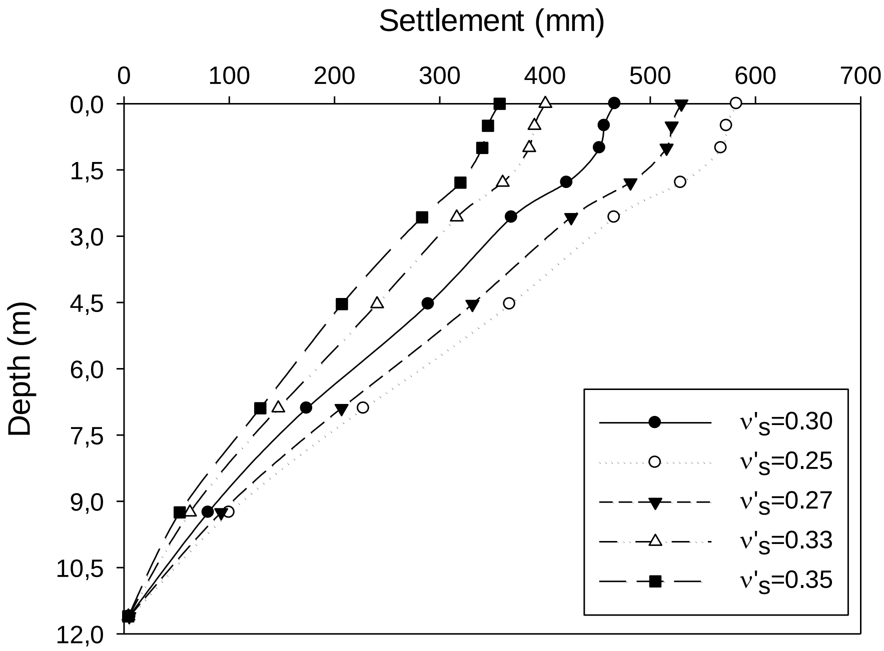

Figure 3.35 Effect of ν'_{soil} with Depth (Kebun Case)

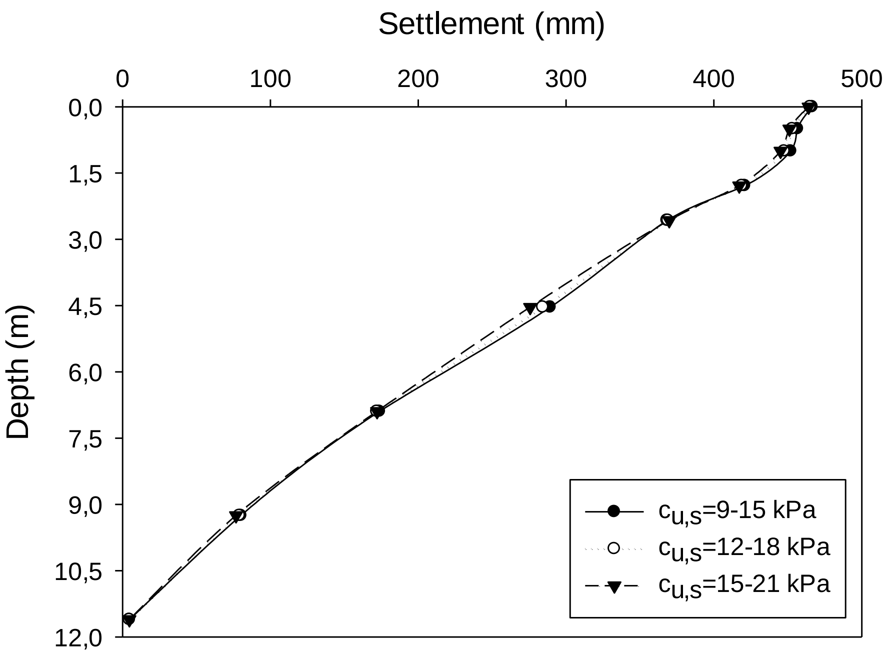

Figure 3.36 Effect of $c_{u,soil}$ with Depth (Kebun Case)

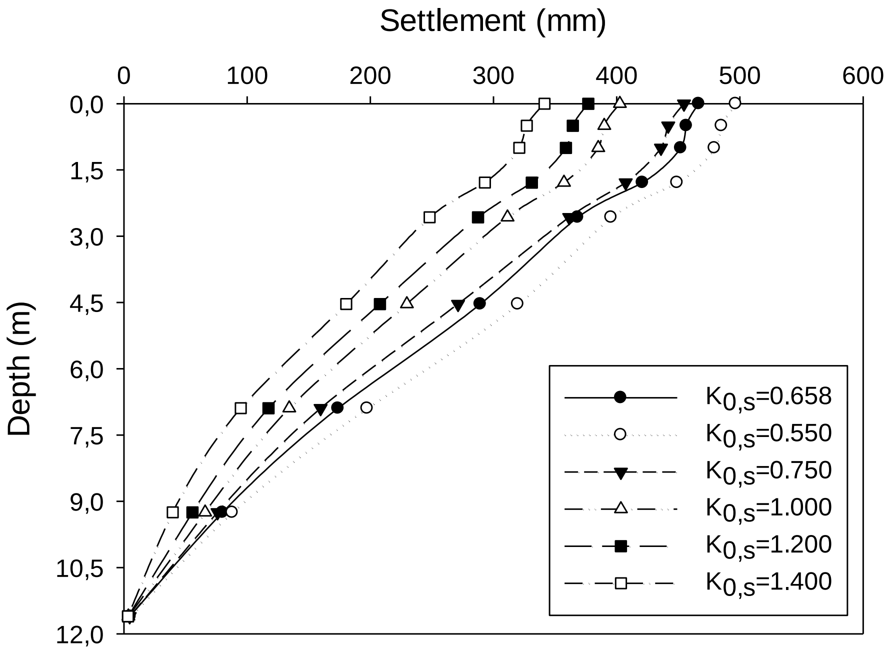

Figure 3.37 Effect of $K_{0,soil}$ with Depth (Kebun Case)

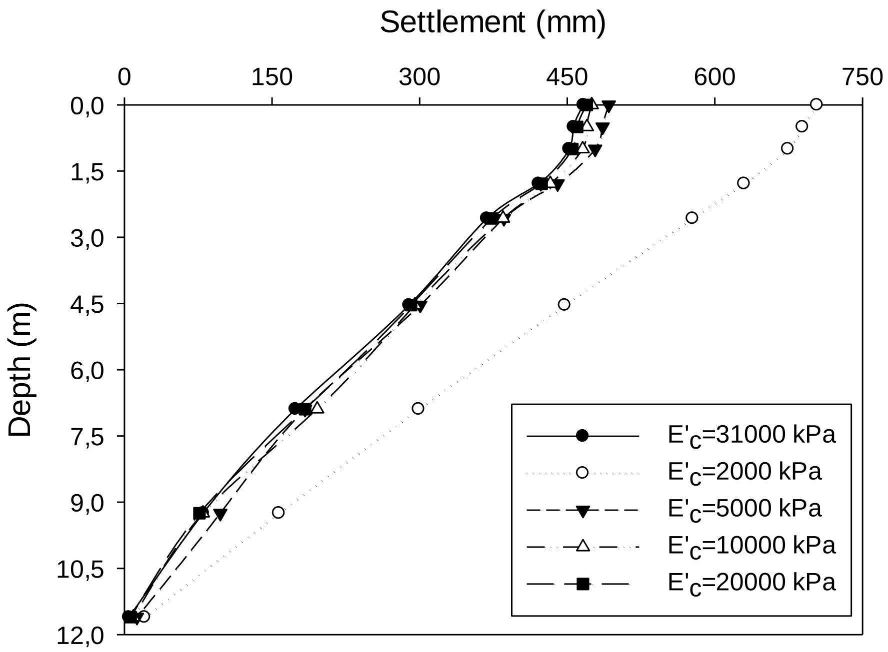

Figure 3.38 Effect of E'_{column} with Depth (Kebun Case)

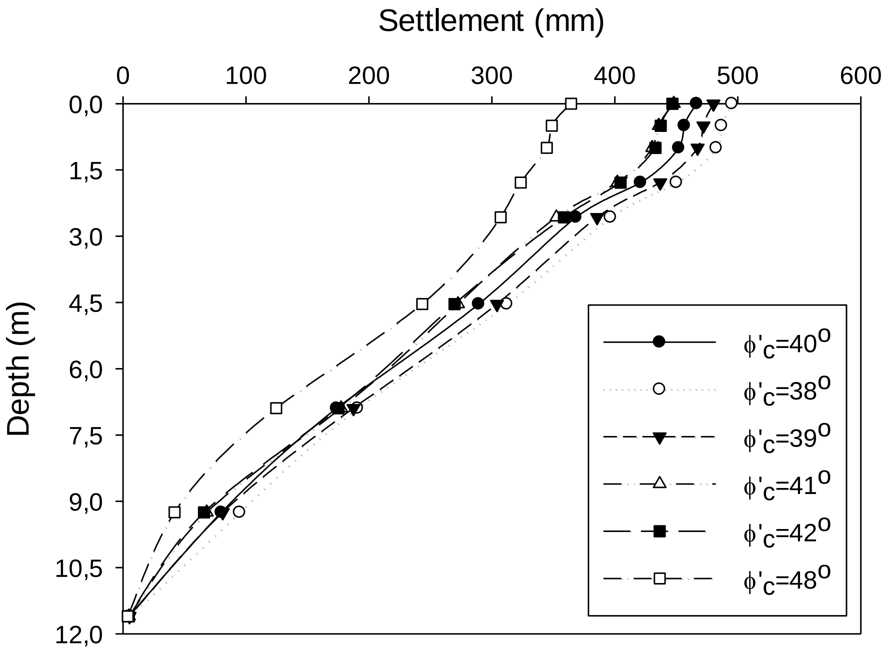

Figure 3.39 Effect of ϕ'_{column} with Depth (Kebun Case)

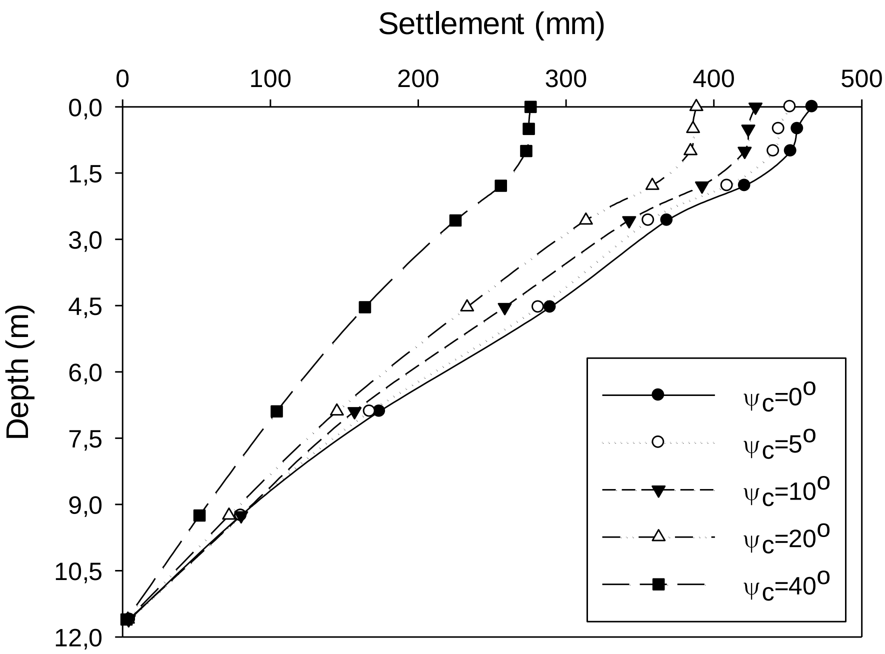

Figure 3.40 Effect of ψ_{column} with Depth (Kebun Case)

3.5 Case Study III: Canvey Island Case

An oil storage tank founded on SC reinforced ground is constructed at Canvey Island, United Kingdom. Diameter of the tank is 36 m and tank base is flexible. SCs are constructed within a radius of 24 m (an annulus of 6 m) from the center of the tank. After that, free draining rolled gravel, asphalt topped pad with a thickness of 1 m is constructed and settlements are recorded during water and oil test loading (Greenwood, 1991). This loading data is used for finite element modeling. Analysis procedure is outlined in this section.

3.5.1 Geometry

Soft soil height used in this analysis is 9 m including 4 different materials. Top soil with a thickness of 0.4 m is underlain by firm to stiff becoming soft silty clay with a thickness of 1.2 m. These materials are underlain by very soft organic silty clay with small pockets of peat with a thickness of 6.6 m. This material is underlain by clayey silt with a thickness of 0.8 m. Medium dense silty fine sand is encountered below soft soils.

SC length is 10 m but, 9 m length is used in this analysis as the medium dense silty fine sand is omitted in this analysis. Critical length is calculated as 3.5 m using Eq. (2.1), Eq. (2.3) and Eq. (2.4). SC diameter is 0.75 m with a triangular spacing of 1.52 m. Area replacement ratio is 22.1%.

Unloading between water load and oil load is ignored and base plate is omitted in this analysis. Total of 931 columns are assumed to be constructed under the tank plus annulus. Geometry is analyzed under axisymmetric conditions for 2D modeling.

Only 2D analysis geometry will be introduced here because, 3D analysis is not done due to meshing problems. It is thought that Plaxis 3D (version 2011.01) could not able to generate mesh due to closer spacing (2 times diameter of the column) and/or excessive number of columns. Symmetry can be captured at 60 degrees slice which yields approximately 150 columns. Geometry and settlement observation point is shown in Figure 3.41.

Center column diameter is assumed as 0.76 m with a relative error of 1.3%. Spacing of the rings is assumed as 1.3 m and corresponding ring thicknesses are calculated which would yield the same amount of SC area. Inner 16 ring thicknesses are calculated as 0.324 m and used value is 0.32 m with a relative error of 1.2%. 17^{th} ring thickness is calculated as 0.23 and used value is 0.24 with a relative error of 4.3%. 18^{th} ring thickness (which is approximately at the perimeter of the annulus) is calculated as 0.126 m and used value is 0.12 m with a relative error of 4.8%. Original SC area was 411.3 m^2 and the value used in this analysis is 406.9 m^2 with a relative error of 1.1%.

Groundwater level is 1.6 m below the ground surface. At the annulus, pad is assumed to be constructed with a thickness of 1 m for 4 m width and lowered at the next 2 meters. Side slope at the annulus is assumed as 2H:1V. Left and right boundaries are free to move in vertical direction and restrained in horizontal direction. Bottom boundary is fixed in both directions. Left and right vertical boundaries are closed to flow. Bottom boundary is opened to flow due to presence of medium dense silty fine sand. Overview of generated mesh for the 2D is shown in Figures 3.42.

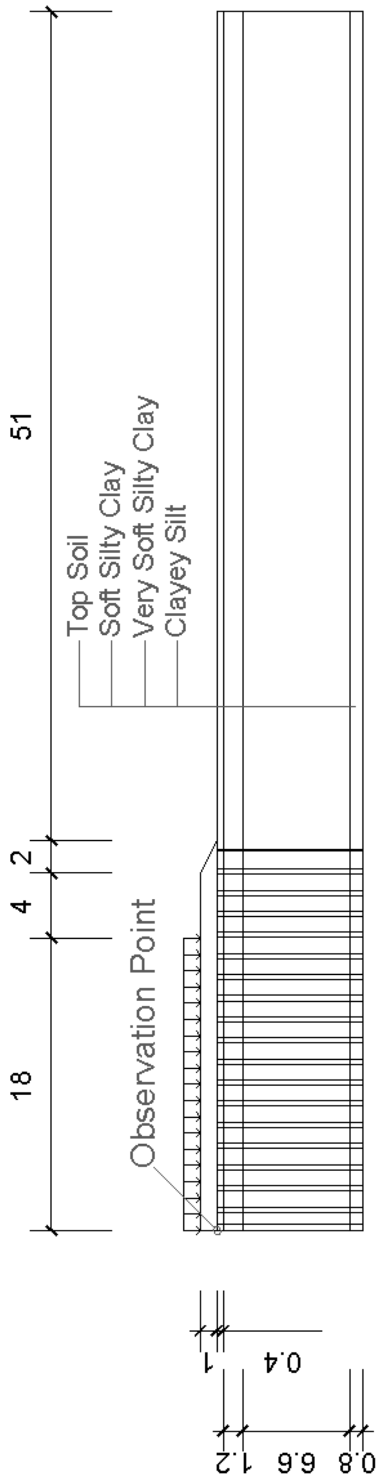

Figure 3.41 Geometry with Observation Point for Canvey Island Case

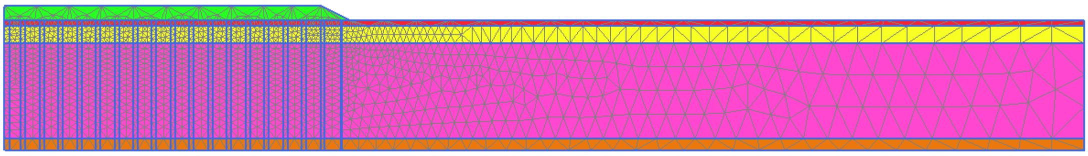

Figure 3.42 2D Mesh for Canvey Island Case

3.5.2 Material Parameters

c_u, m_v and c_v values were given in Greenwood (1991) for soft soils, except top soil. Average values are used for given parameters. General parameters for soft soils are given in Table 3.16.

Table 3.16 General Parameters for Soft Soils (Canvey Island Case)

Property	Top Soil	Soft Silty Clay	Very Soft Silty Clay	Clayey Silt
Thickness (m)	0.4	1.2	6.6	0.8
c_v (m^2/day)	1.10E-3	1.10E-3[a]	6.85E-4[a]	1.58E-2[a]
m_v (m^2/kN)	5.0E-4	6.5E-4[a]	8.5E-4[a]	1.8E-4[a]
$k_{vertical}$ (m/day)	5.48E-6	7.12E-6	5.82E-6	2.84E-5
$k_{horizontal}$ (m/day)	8.22E-6	1.07E-5	8.73E-6	4.25E-5

[a] Values are taken from Greenwood (1991).

Total consolidation settlement is calculated as 914 mm by using Eq. (3.15) with the average values of m_v. Result is shown in Table 3.17. Calculated settlement is comparable with the untreated settlement result by Priebe (1995).

Table 3.17 Consolidation Settlement (Canvey Island Case)

Layer	$\Delta\sigma$ (kPa)	H	$m_{v.ave}$ (m^2/kN)	s_c (mm)
Top Soil	151	0.4	5.0E-04	30
Soft Clay	148	1.2	6.5E-04	115
Very Soft Clay	134	6.6	8.5E-04	751
Clayey silt	123	0.8	1.8E-04	18

Plasticity index is assumed as 18% for all soft soils. G_s is assumed as 2.6 and water content is assumed as 61.5% for all soft soils. Corresponding e value is found as 1.6 from Eq. (3.5) assuming fully saturated soil (S_d=100%). γ_{dry} is calculated from the Eq. (3.6) as 10.00 kN/m^3 and γ_{sat} is calculated from Eq. (3.7) as 16.16 kN/m^3 for all soft soils. Vertical permeability is calculated from Eq. (3.10). k_h/k_v ratio is assumed as 1.5 (Basett & Brodie, 1961). Mohr-Coulomb parameters are tabulated in Table 3.18.

Table 3.18 Mohr Coulomb Parameters for Soft Soils (Canvey Island Case)

Property	Top Soil	Soft Silty Clay	Very Soft Silty Clay	Clayey Silt
Type of Behavior	Undrained-B	Undrained-B	Undrained-B	Undrained-B
E' (kPa)	1486	1143	874	4127
ν'	0.3	0.3	0.3	0.3
c_u (kPa)	30	26[a]	23[a]	30[a]
K_0	0.6	0.6	0.6	0.6

[a] Values are taken from Greenwood (1991).

Drained modulus of elasticity of soft soils are found from Eq. (3.16) assuming ν=0.3 for all materials. ϕ' value is calculated as 23.6^o from Gibson (1953) for all soft soils. Jaky's formula is used to obtain K_0 value (K_0=1-sinϕ). Undrained-B accounts for effective compressibility and undrained strength characteristics.

In addition, Hardening Soil model is also used for very soft silty clay only. Because confining pressure effect on modulus is considered to be negligible for other layers as the thickness of other layers are very thin. Parameters are shown in Table 3.19.

Table 3.19 Hardening Soil Parameters for Very Soft Silty Clay (Canvey Island Case)

Property	Soft Clay
Type of Behavior	Undrained-A
E_{50}^{ref} (kPa)	1275
E_{oed}^{ref} (kPa)	850
E_{ur}^{ref} (kPa)	3825
m	1
ν_{ur}	0.2
ϕ' (deg)	23.55
c' (kPa)	0.2
ψ (deg)	0

p^{ref}=50 kPa and R_f=0.9

Other material parameters are tabulated in Table 3.20. SC and pad parameters are assumed in the range of engineering applications. SC drained modulus is found by using Eq. (3.17). K and n values are taken as 640 and 0.43, respectively. Permeability of other materials are set according to the maximum difference of 1E-5 allowed by Plaxis.

Table 3.20 Mohr Coulomb Parameters for Other Materials (Canvey Island Case)

Property	Stone Column	Pad
Type of Behavior	Drained	Drained
γ_{dry} (kN/m^3)	20	22
γ_{sat} (kN/m^3)	20	22
$k_{vertical}$ (m/day)	0.548	0.548
$k_{horizontal}$ (m/day)	0.548	0.548
E' (kPa)	33250	40000
ν'	0.3	0.3
ϕ' (deg)	40[a]	38
c' (kPa)	0.2	5
ψ	0	0
K_0	0.357	0.384

[a] Value is taken from McCabe et al. (2010).

3.5.3 Loading History

As mentioned earlier, unloading between water and oil test loading is omitted in this analysis. SC construction is assumed to finish in 19 days (assuming 30 minutes for construction of a single column out of 931 columns). Settlement plates were placed on SCs before the pad construction.

1 m pad construction is assumed to finish in 15 days. Consolidation period of 16 days is assumed for pad to dissipate pore pressures.

To simulate incremental loading (maximum load of 130 kPa after 150 days), 20 kPa load is assumed to be placed in 5 days with a consolidation period of 12 days.

Settlement recordings were measured the highest settlement on day 150 which commenced to count from the end of SC construction process.

Table 3.21 Phase Description for Canvey Island Case

Phase	Phase Description	Duration (days)
0	Initial Conditions (K_0 Procedure)	0
1	Construction of Stone Columns	19
2	1 m. Pad Construction	15
3	Consolidation	16
4	20 kPa load	5
5	Consolidation	12
6	40 kPa load	5
7	Consolidation	12
8	60 kPa load	5
9	Consolidation	12
10	80 kPa load	5
11	Consolidation	12
12	100 kPa load	5
13	Consolidation	12
14	120 kPa load	5
15	Consolidation	12
16	130 kPa load	5
17	Consolidation	12

3.5.4 2D Finite Element Model

As mentioned before, 3D analysis is not done due to meshing problems. Reason for this problem could be closer spacing (2 times diameter of the column) and/or excessive number of columns. Phase displacements of 2D FE model and in situ measurement are shown in Figure 3.43. Overall trend is captured reasonably by 2D models.

Mesh sensitivity analysis and comparison of 2D FE model with in situ measurement are given in Table 3.22. At first sight, difference with observed settlement is attained to the assumed load lift duration (5days) and its consolidation stage (12 days). Analyses with different durations for load lifts (total duration stayed constant as 150 days) are performed but relative error value had not been lower than 14% for 2D MC model. As a result, parametric study will be carried out with 2D MC model without changing lift durations.

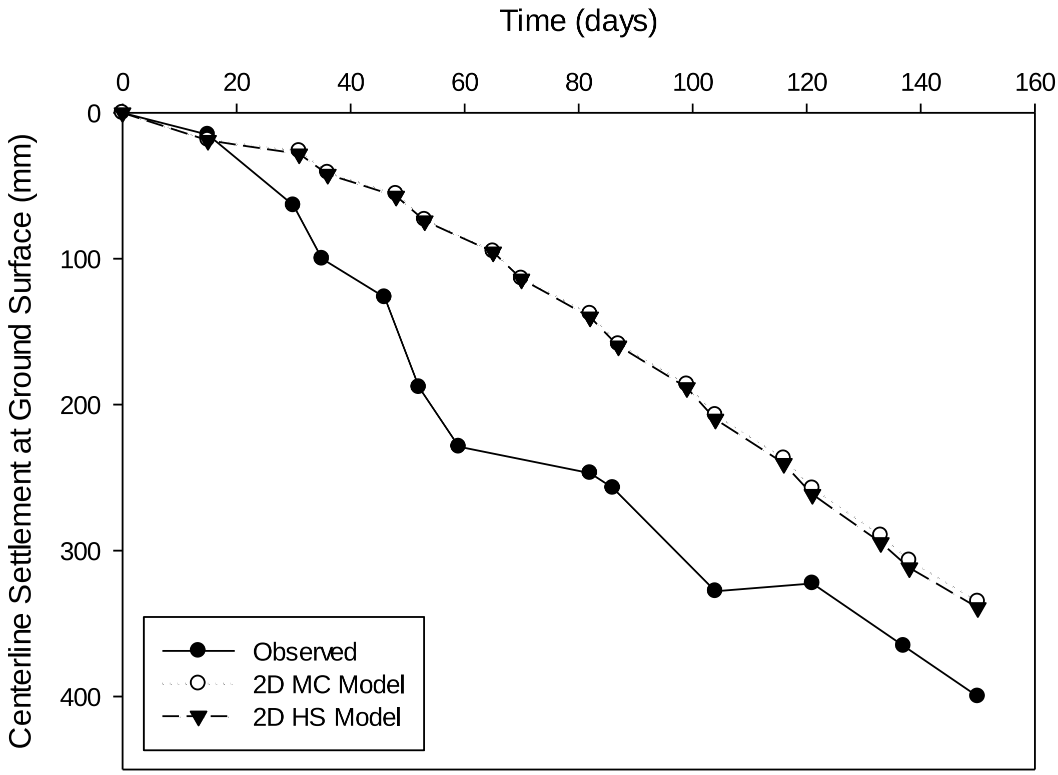

Figure 3.43 Settlement vs. Time (Canvey Island Case)

Table 3.22 Settlement Comparison and Mesh Sensitivity for Canvey Island Case

		2D FE Model		
	Observed	MC	MC Refined Mesh	HS
Settlement (mm)	400.0	335.1	339.4	339.2
Relative Error w.r.t. Observed Value (%)		16.2	15.2	15.2
Total Number of Elements		2397	3582	2397

3.5.5 Parametric Study

Effects of soil and column parameters on settlement reduction ratio are shown in Figures 3.44 - 3.49 and effects of parameters with depth on settlement are shown in Figures 3.50 - 3.55. MC parameters for soft clay and other materials were tabulated in Table 3.18 and Table 3.20, respectively. Very soft clay parameters are varied only in terms of soft soil, because, thickness of very soft clay is the thickest one. Major parameters affecting S_r are determined as; E'_{soil}, $K_{0,soil}$ and E'_{column}. ν_{soil} effect on S_r was not significant as opposed to the previous cases (see Figure 3.45). Other soft clay layers Poisson's ratios are remained constant in this parametric study. This would be a reason for less change of S_r with varying ν_{soil}. ν_{column} and $c_{u,soil}$ variation gave inconsistent results and omitted in this case. $K_{0,soil}$ value equal to 1 did not give better result compared to Jaky's formula as far as observed data is considered (see Figure 3.46). As can be seen from Figure 3.47, E'_{column}/E'_{soil} ratios approximately lower than 10 affected S_r remarkably. On the other hand, S_r value remained almost constant for E'_{column}/E'_{soil} ratios approximately larger than 10. Excluding the extreme cases of $\phi'_{column}=48^o$ and $\psi_{column}>\phi'_{column}-30^o$ (20 and 40 degrees in this case), stone column angle of shearing resistance (see Figure 3.48 and 3.54) and angle of dilation (see Figure 3.49 and 3.55) effect on S_r are not considerable, respectively.

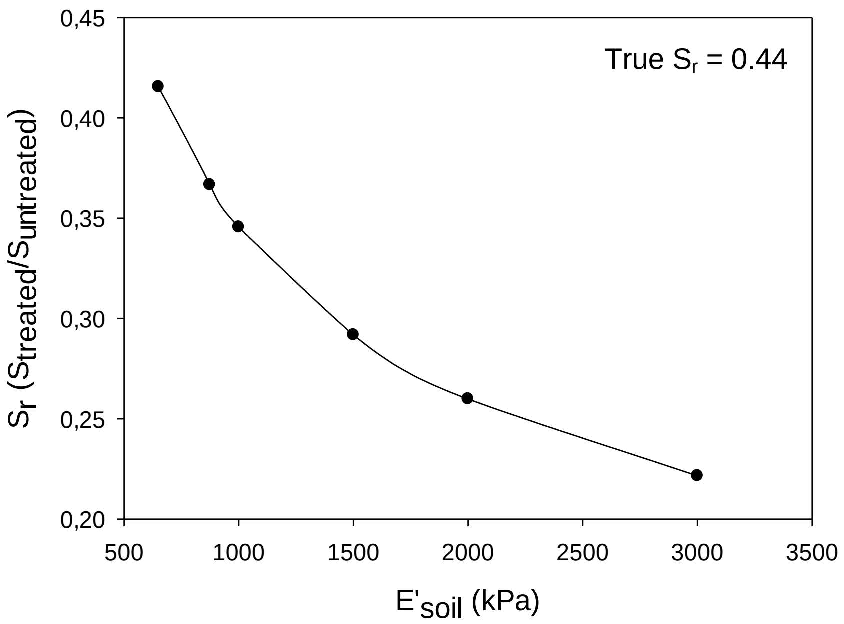

Figure 3.44 S_r versus E'_{soil} (Canvey Island Case)

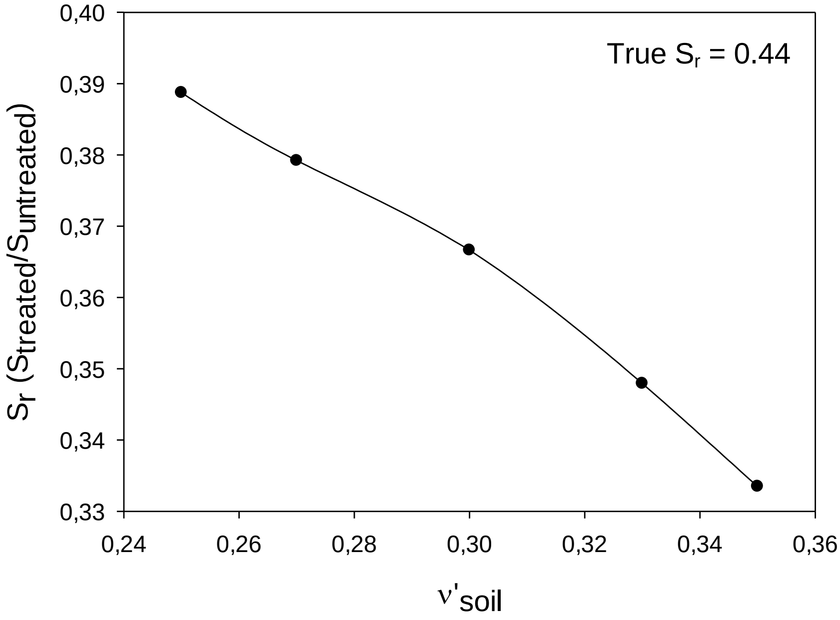

Figure 3.45 S_r versus ν'_{soil} (Canvey Island Case)

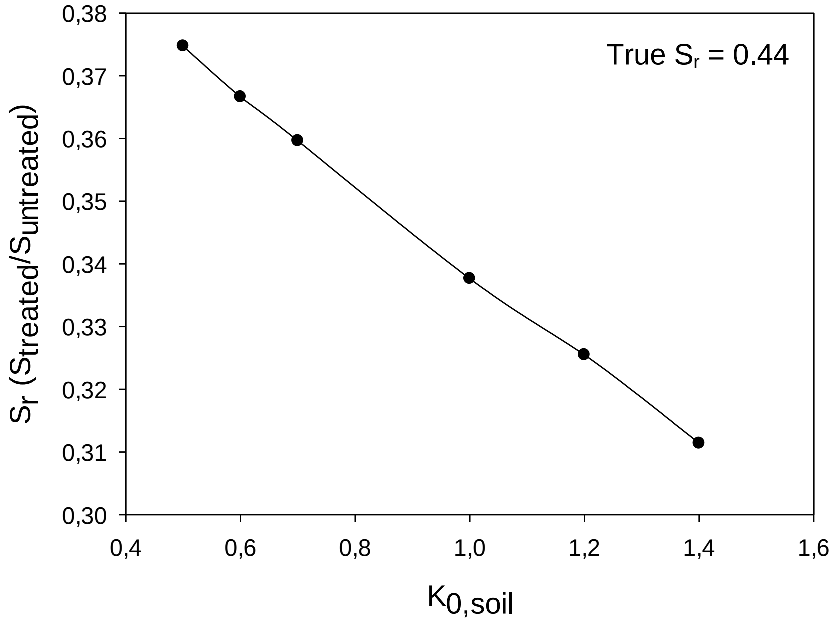

Figure 3.46 S_r versus $K_{0,soil}$ (Canvey Island Case)

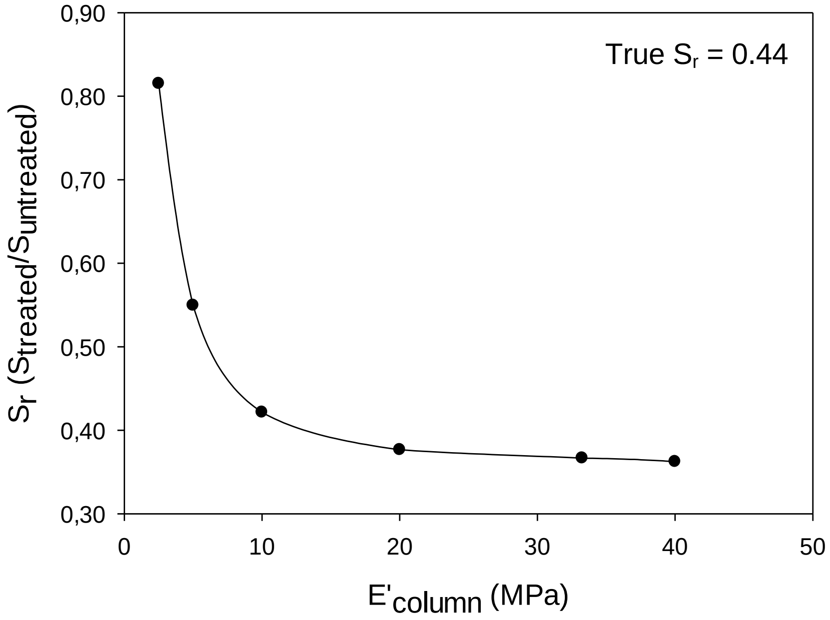

Figure 3.47 S_r versus E'_{column} (Canvey Island Case)

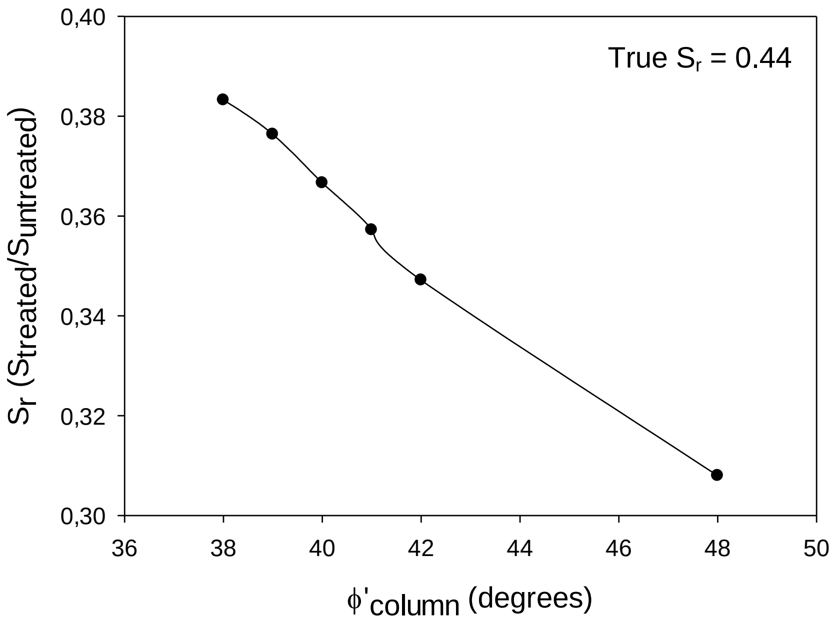

Figure 3.48 S_r versus ϕ'_{column} (Canvey Island Case)

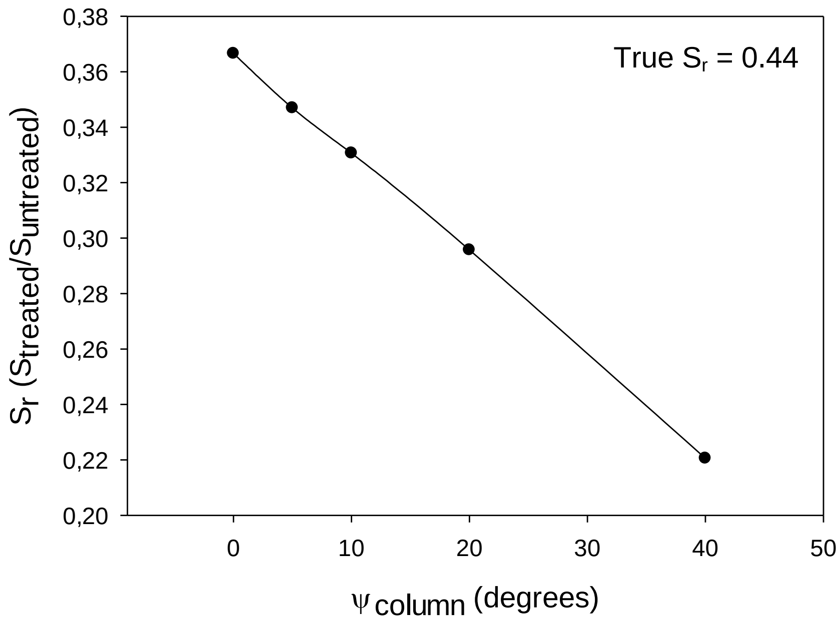

Figure 3.49 S_r versus ψ_{column} (Canvey Island Case)

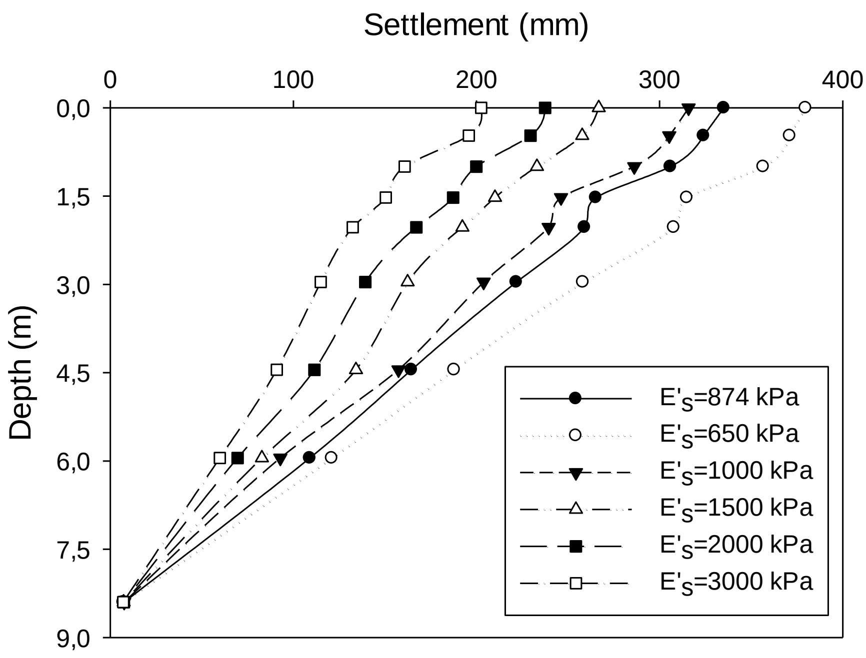

Figure 3.50 Effect of E'_{soil} with Depth (Canvey Island Case)

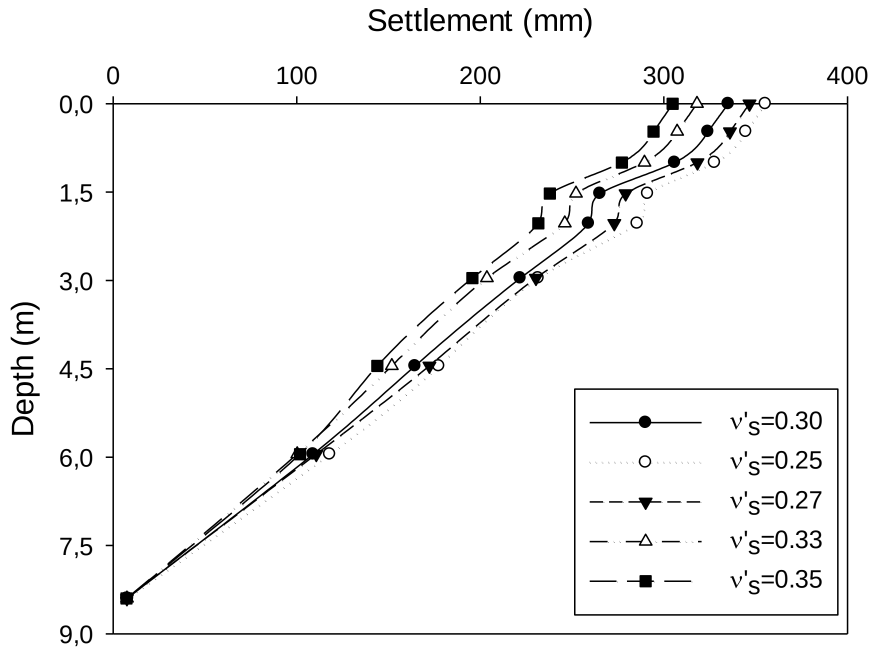

Figure 3.51 Effect of ν'_{soil} with Depth (Canvey Island Case)

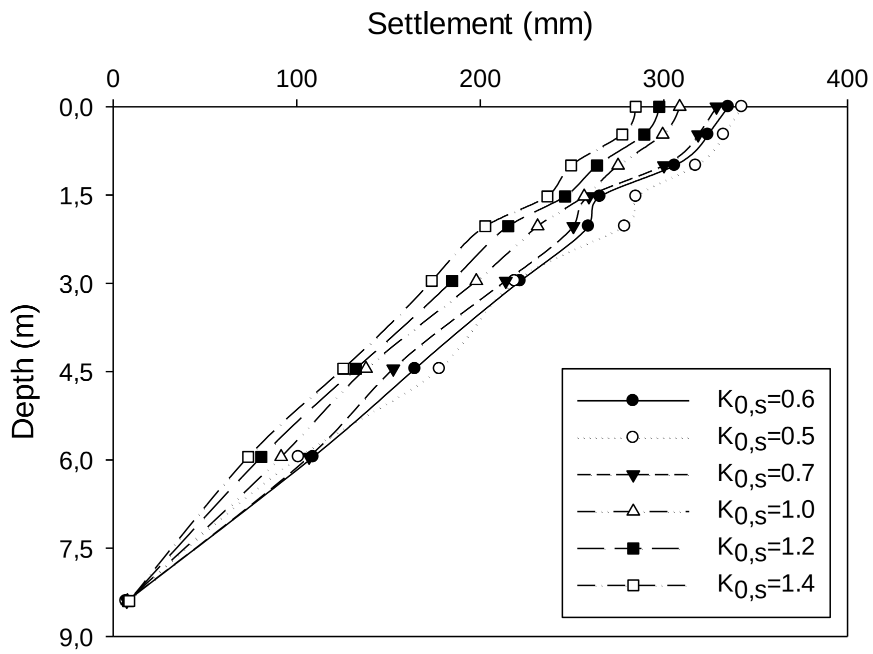

Figure 3.52 Effect of $K_{0,soil}$ with Depth (Canvey Island Case)

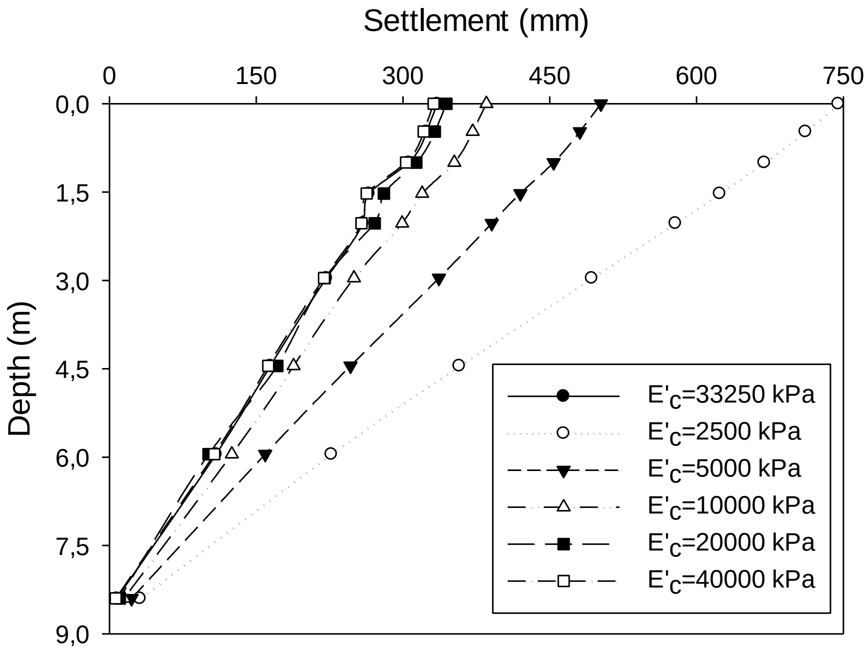

Figure 3.53 Effect of E'_{column} with Depth (Canvey Island Case)

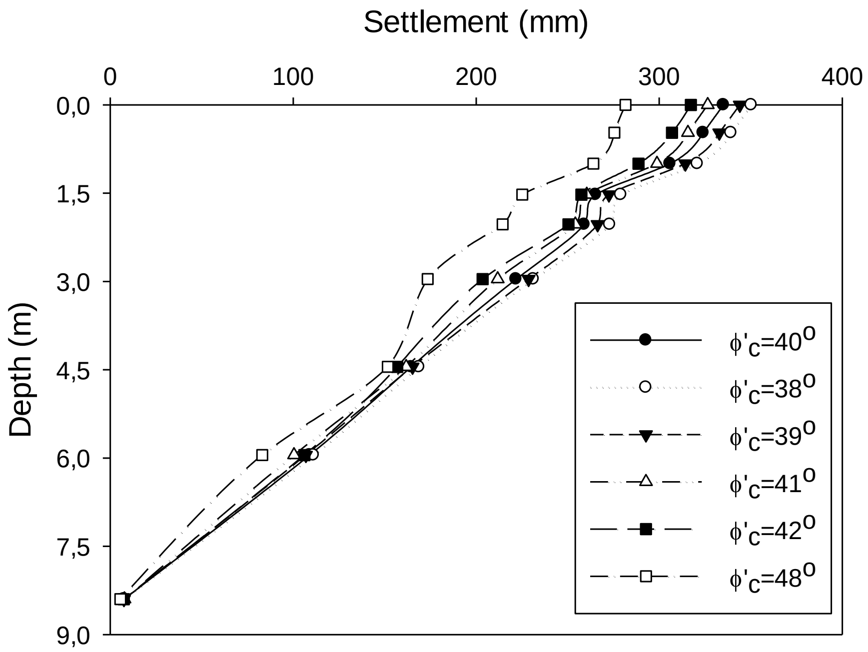

Figure 3.54 Effect of ϕ'_{column} with Depth (Canvey Island Case)

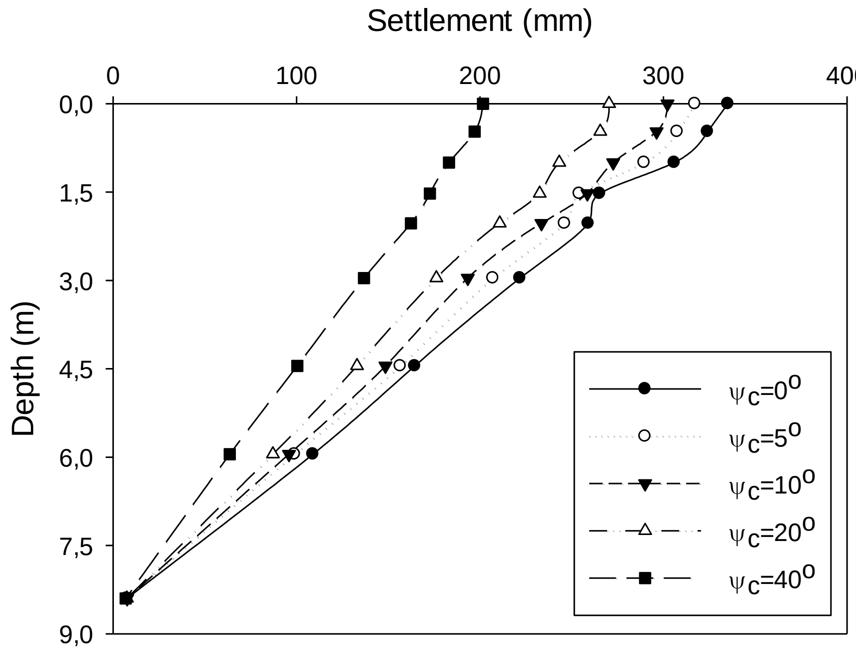

Figure 3.55 Effect of ψ_{column} with Depth (Canvey Island Case)

3.6 Composition of Parametric Studies

Composition of parametric studies is made and illustrated in Figures 3.56 – 3.61. As can be seen from Figure 3.56, variation of S_r with varying E'_{soil} is similar for Omdurman and Kebun cases. Less variation is observed for Canvey Island case, but overall trend is similar in all three cases. When E'_{column}/E'_{soil} ratios are approximately lower than 10, E'_{column} effect on S_r is remarkable as shown in Figure 3.59 for all three cases. S_r decreases almost linearly with increasing ν'_{soil} (see Figure 3.57). Variation in S_r is remarkable in Omdurman and Kebun cases. Linear trend is also observed for $K_{0,soil}$ variation including small deviations in Kebun case as illustrated in Figure 3.58. ϕ'_{column} and ψ_{column} effect on S_r can be seen in Figure 3.60 and 3.61, respectively. In overall, parallel results are obtained from the parametric studies of three cases. In addition, relative errors with respect to in situ measurements of all three case studies were around 10% to 15% for 2D models except 2D HS model of Omdurman case. This difference may decrease by using advanced material models like S-CLAY1 or SCLAY1S for soft soil (Castro & Karstunen, 2010).

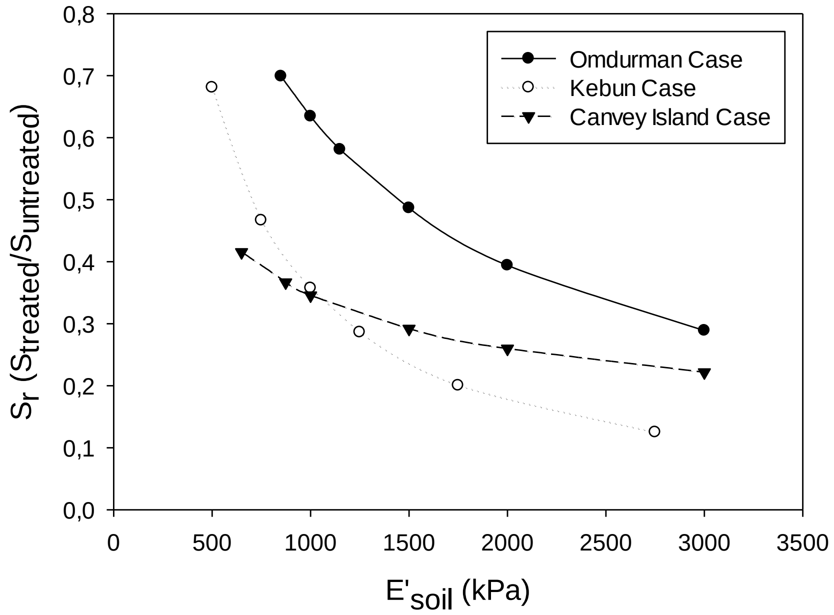

Figure 3.56 S_r versus E'_{soil}

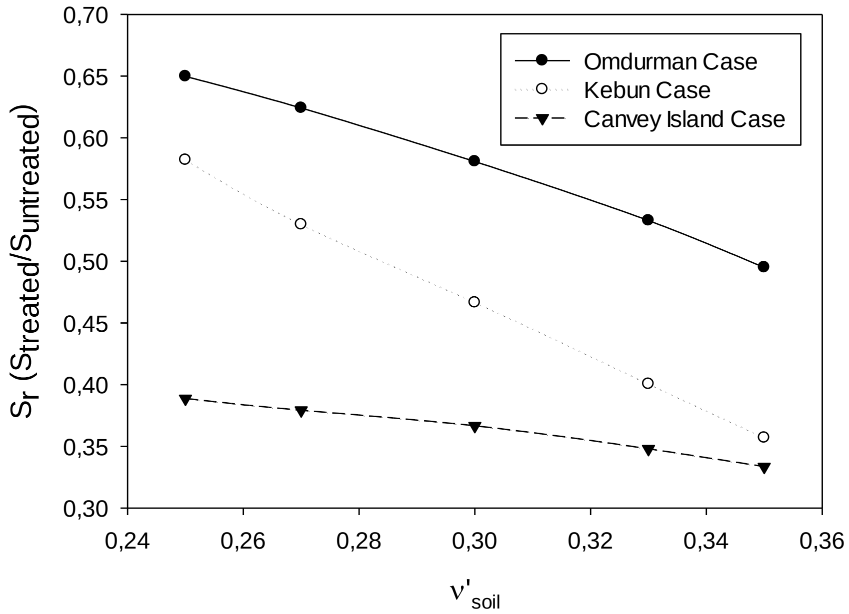

Figure 3.57 S_r versus ν'_{soil}

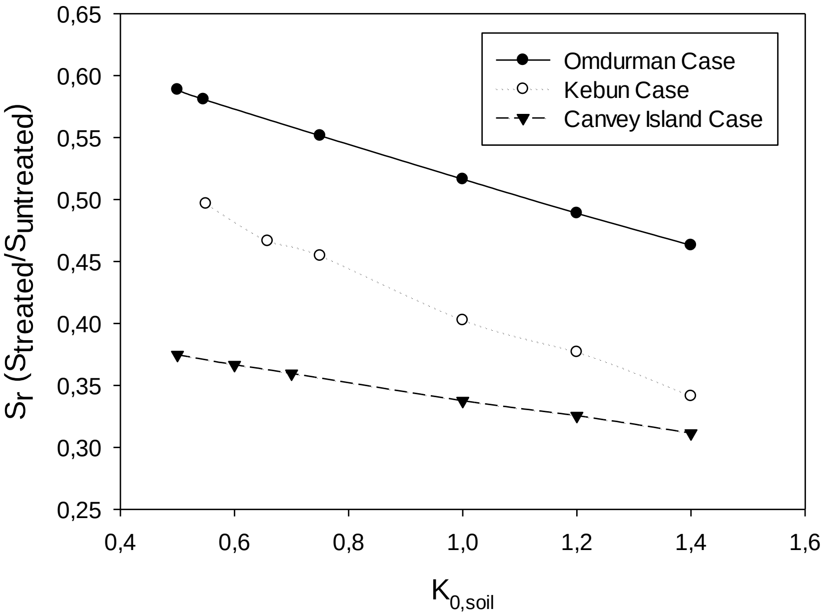

Figure 3.58 S_r versus $K_{0,soil}$

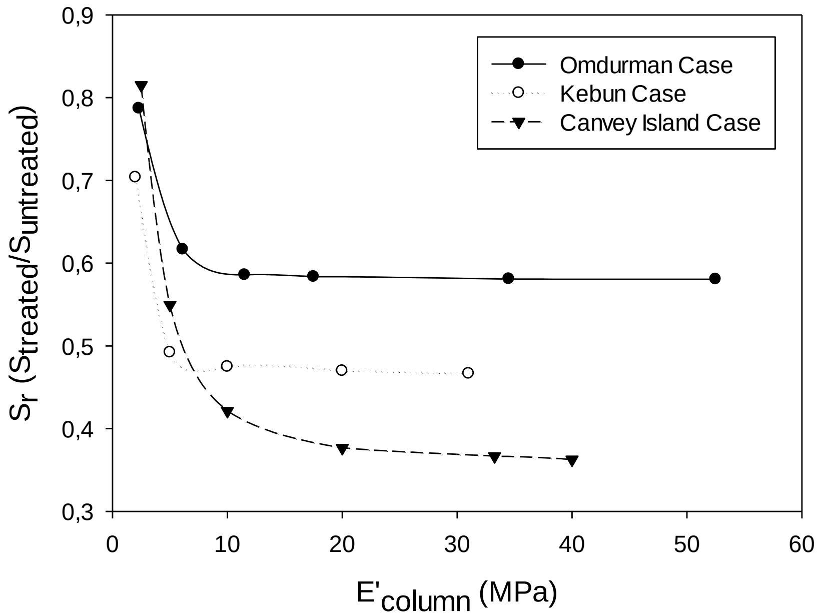

Figure 3.59 S_r versus E'_{column}

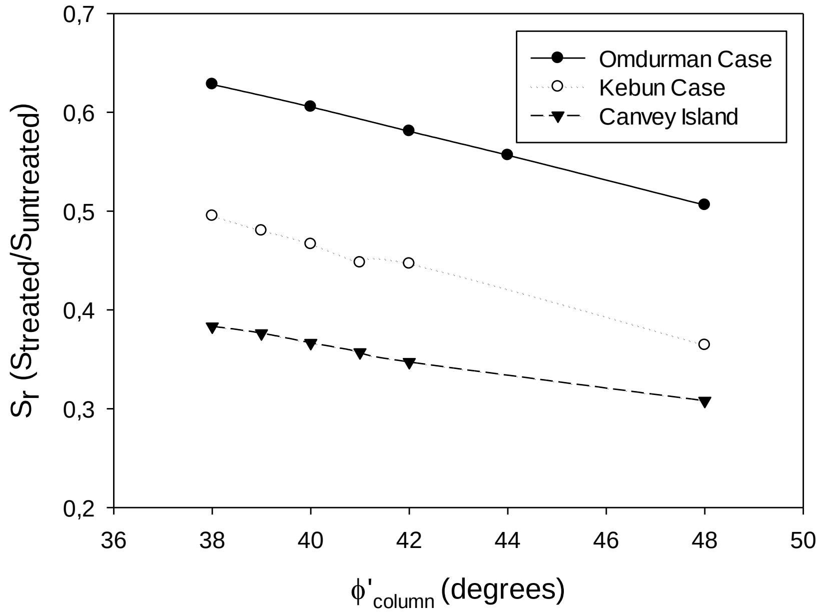

Figure 3.60 S_r versus ϕ'_{column}

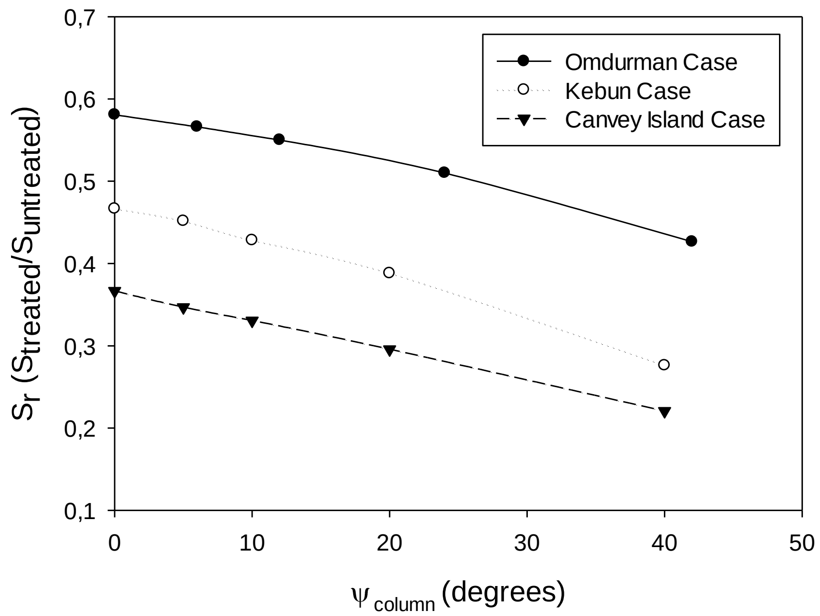

Figure 3.61 S_r versus ψ_{column}

CHAPTER 4

SUMMARY AND CONCLUSIONS

4.1 Summary

This study initially concentrated on comprehensive review of the literature about stone column reinforced soils (especially soft clays). It is believed that a proper coverage was established about the information on state of the art papers.

At the second stage, emphasis was given to comparison of three dimensional representative slice model with the two dimensional one for end-bearing stone column reinforced soft clay foundation. Mohr Coulomb and Hardening Soil models were used in the comparison studies. In addition, comparison was also made between these two material models.

And finally, parametric study was undertaken to investigate the most influencing parameters among various parameters on settlement reduction ratio. In addition, parameter effects on settlement with depth were also investigated. Mohr Coulomb model was solely used in the parametric studies.

To achieve parametric and comparison studies, three individual case studies were chosen. General information, geometrical properties, material characteristics and loading histories are introduced extensively for these case studies.

4.2 Conclusions

Comparison studies on model conversion did not reveal results as expected in terms of 3D representative slice models. Two dimensional conversion of individual stone columns into equivalent strips gave reasonable agreement with the in situ measurements. In contrast, 3D representative slice models of Omdurman case deviated from in situ measurements with a relative error of approximately 40%. Moreover, Canvey Island case could not be modeled under 3D conditions due to closer spacing (2 times diameter of the column) and/or excessive number of columns. But, 3D representative slice models of Kebun case revealed better agreement with in situ measurements than 2D models.

Comparison studies on material models revealed that the Hardening Soil model represented soft clay behavior better than Mohr Coulomb model.

Parametric studies on settlement reduction ratio (S_r) revealed similar results under stress levels considered for end-bearing SC reinforced soft clay foundation (Omdurman Case), very soft clay foundation (Kebun Case) and interlayered soft clay foundation (Canvey Island Case). Major findings of this study can be summarized as follows:

- Correct estimation of E'_{soil} is essential as found from all three cases.
- Major parameters affecting S_r are found as; E'_{soil}, E'_{column}, ν_{soil} and $K_{0,soil}$ for Omdurman and Kebun cases and E'_{soil}, E'_{column} and $K_{0,soil}$ for Canvey Island case.

- E'_{column}/E'_{soil} ratios approximately lower than 10 affected S_r notably. In contrast, S_r value remained almost constant for E'_c/E'_s ratios approximately larger than 10.

- ϕ'_{soil} and ν'_{column} has no effect on S_r as determined from Omdurman case.

- $K_{0,soil}$ value equal to 1 gave better results compared to $K_0=1-\sin\phi'$ as far as the observed data are considered in Omdurman and Kebun cases. S_r decreases linearly for increasing $K_{0,soil}$ as found from all cases.

- Stone column angle of shearing resistance and angle of dilation effect on S_r are not significant. Relationship of these two parameters with S_r is almost linear.

4.3 Future Research

More parametric studies may be performed on other case histories to strengthen the findings of this study. Especially, effect of ν_{soil} on S_r may be investigated.

Advanced soil models can be used to simulate soft soil and stone column behavior, in the presence of soil data for advanced soil model parameters.

A laboratory study can be conducted to investigate the relation between drained and undrained modulus of soft clays.

REFERENCES

Aboshi, H., Ichimoto, E., Enoki, M., & Harada, K. (1979). The Compozer - a method to improve characteristics of soft clays by inclusion of large diameter sand columns. *Proc. Int. Conf. on Soil Reinforcement: Reinforced Earth and Other Techniques, 1*, 211-216.

Al-Khafaji, Z. A., & Craig, W. H. (2000). Drainage and reinforcement of soft clay tank foundation by sand columns. *Geotechnique, 50*(6), 709-713.

Alamgir, M., Miura, N., Poorooshasb, H. B., & Madhav, M. R. (1996). Deformation analysis of soft ground reinforced by columnar inclusions. *Computers & Geotechnics, 18*(4), 267-290.

Ambily, A. P., & Gandhi, S. R. (2007). Behavior of stone columns based on experimental and FEM analysis. *Journal of Geotechnical and Geoenvironmental Engineering, 133*(4), 405-415.

Ammar, A. M. S., Liu, X., Lin, H., & Ren, J. (2009). Enlarged base stone columns to improve soft clay soil. *Int. Conf. on Transportation Eng.*, 4240-4246.

Andreou, P., Frikha, W., Frank, R., Canou, J., Papadopoulos, V., & Dupla, J.-C. (2008). Experimental study on sand and gravel columns in clay. *Ground Improvement, 161*(GI4), 189-198.

Ashmawy, A. K., Rokicki, R., & Plaskett, M. E. (2000). Predicted and actual settlement of soils improved by vibro replacement. *Advances in Grouting and Ground Modification*, 281-295.

Ausilio, E., & Conte, E. (2007). Soil compaction by vibro-replacement: a case study. *Ground Improvement, 11*(3), 117-126.

Bachus, R. C., & Barksdale, R. D. (1984). Vertical and lateral behavior of model stone columns. *Proc. of the Conf. on In Situ Soil and Rock Reinforcement, Paris, 99-104*.

Bachus, R. C., & Barksdale, R. D. (1989). Design methodology for foundations on stone columns *Foundation Engineering: Current Principles and Practices* (pp. 244-257): ASCE GSP No. 22.

Baez, J. I., & Martin, G. R. (1992). Quantitative evaluation of stone column techniques for earthquake liquefaction mitigation. Proc. X World Conf. Earthquake Engrg., Madrid, Vol.3, pp.1477-1483.

Balaam, N. P., & Booker, J. R. (1981). Analysis of rigid rafts supported by granular piles. *International Journal of Numerical and Analytical Methods in Geomechanics, 5*(4), 379-403.

Balaam, N. P., & Booker, J. R. (1985). Effect of stone column yield on settlement of rigid foundations in stabilized clay. *International Journal of Numerical and Analytical Methods in Geomechanics, 9*(4), 331-351.

Balaam, N. P., & Poulos, H. G. (1983). The behavior of foundations supported by clay stabilized by stone columns. Proc. 8th European Conf. on Soil Mechanics and Foundation Engineering, Helsinki, Vol. 1, pp.199-204.

Barksdale, R. D., & Goughnour, R. R. (1984). Settlement performance of stone columns in the US. *Proc. of the Conf. on In Situ Soil and Rock Reinforcement, Paris, 105-110*.

Basett, D. J., & Brodie, A. F. (1961). A Study of Matabitchual varved clay. *Ont. Hydro Res. News, 13*(4), 1-6.

Baumann, V., & Bauer, G. E. A. (1974). The performance of foundations on various soils stabilized by the vibro-compaction method. *Canadian Geotechnical Journal, 11*(4), 509-530.

Bergado, D. T., & Lam, F. L. (1987). Full scale load test of granular piles with different densities and different proportions of gravel and sand on soft bangkok clay. *Soils and Foundations, 27*(1), 86-93.

Black, J. A., Sivakumar, V., & Bell, A. (2011). The settlement performance of stone column foundations. *Geotechnique, 61*(11), 909-922.

Borges, J. L., Domingues, T. S., & Cardoso, A. S. (2009). Embankments on soft soil reinforced with stone columns - numerical analysis and proposal of a new design method. *Geotechnical and Geological Engineering, 27*(6), 667-679.

Bouassida, M., de Buhan, P., & Dormieux, L. (1995). Bearing capacity of a foundation resting on a soil reinforced by a group of columns. *Geotechnique, 45*(1), 25-34.

Bouassida, M., Jellali, B., & Porbaha, A. (2009). Limit analysis of rigid foundations on floating columns. *International Journal of Geomechanics, 9*(3), 89-101.

Bowles, J. E. (1997). *Foundation analysis and design, 5th. Ed.* New York: McGraw-Hill.

Brauns, J. (1978). Die anfangstraglast von schottersäulen im bindigen untergrund. *Die Bautechnik, 55*(8), 263-271.

Brinkgreve, R. B. J., Swolfs, W. M., & Engin, E. (2011a). Plaxis 2D Version 2011 Manual.

Brinkgreve, R. B. J., Swolfs, W. M., & Engin, E. (2011b). Plaxis 3D Version 2011 Manual.

Castro, J., & Karstunen, M. (2010). Numerical simulations of stone column installation. *Canadian Geotechnical Journal, 47*(10), 1127-1138.

Castro, J., & Sagaseta, C. (2009). Consolidation around stone columns. Influence of column deformation. *International Journal for Numerical and Analytical Methods in Geomechanics, 33*(7), 851-877.

Castro, J., & Sagaseta, C. (2012). Pore pressure during stone column installation. *Ground Improvement, 165*(GI2), 97-109.

Chen, B. S., & Bailey, M. J. (2004). Lessons learned from a stone column test program in glacial deposits. *GeoSupport 2004: Drilled Shafts, Micropiling, Deep Mixing, Remedial Methods, and Specialty Foundation Systems*, 508-519.

Christoulas, S. T., Bouckovalas, G., & Giannaros, C. H. (2000). An experimental study on model stone columns. *Soils and Foundations, 40*(6), 11-22.

Clemente, J. L. M., & Parks, C. D. (2005). Stone Columns for Control of Power Station Foundation Settlements. *GSP 136 Innovations in Grouting and Soil Improvement*, 1-10.

Concrete Institute. (1999). Industrial Floors and Pavements Guidelines.

Cooper, M. R., & Rose, A. N. (1999). Stone column support for an embankment on deep alluvial soils. Proc. Instn. Civ. Engrs. Geotech. Engng, 137, 15-25.

Datye, K. R. (1982). Settlement and bearing capacity of foundation system with stone columns. *Proc. Symp. on Soil and Rock Improvement Techniques*. Asian Institute of Technology, Bangkok, Thailand.

Deb, K., & Dhar, A. (2011). Parameter estimation for a system of beam resting on stone column-reinforced soft soil. *International Journal of Geomechanics*.

DeStephen, R. A., Kozera, D. W., & Swekosky, F. J. (1997). Design of floating stone columns in hydraulic fill. In R. H. borden, Holtz, R. D., and Juran, I. (Ed.), *Grouting, Soil Improvement, and Geosynthetics, GSP No. 30*. ASCE, New York.

Duncan, J. M., & Chang, C-Y. (1970). Nonlinear analysis of stress and strain in soils. *Journal of the Soil Mechanics and foundations Division, ASCE, 96*(SM5).

Ellouze, S., Bouassida, M., Hazzar, L., & Mroueh, H. (2010). On settlement of stone column foundation by Priebe’s method. *Ground Improvement, 163*(GI2), 101-107.

Elshazly, H., Hafez, D., & Mossaad, M. (2006). Back-calculating vibro-installation stresses in stone-column-reinforced soils. *Ground Improvement, 10*(2), 47-53.

Elshazly, H., Hafez, D., & Mossaad, M. (2007). Settlement of circular foundations on stone-column-reinforced grounds. *Ground Improvement, 11*(3), 163-170.

Engelhardt, K., & Golding, H. C. (1975). Field testing to evaluate stone column performance in a seismic area. *Geotechnique, 25*(1).

Frikha, W., Bouassida, M., & Canou, J. (2008). Calibration of an elastoplastic model for the prediction of stone column ultimate bearing capacity. *GeoCongress 2008: Geosustainability and Geohazard Mitigation*, 604-611.

Gaeb, M., Schweiger, H. F., Kamrat-Pietraszewska, D., & Karstunen, M. (2009). Numerical analysis of a floating stone column foundation using different constitutive models. *Geotechnics of Soft Soils - Focus on Ground Improvement*, 137-142.

Gaeb, M., Schweiger, H. F., Thurner, R., & Adam, D. (2007). Field trial to investigate the performance of a floating stone column foundation. *European Conference on Soil Mechanics and Geotechnical Engineering*, 1311-1316.

Gerrard, C. M., Pande, G. N., & Schweiger, H. F. (1984). Modelling behaviour of soft clays reinforced with stone columns. *Proc. of the Conf. on In Situ Soil and Rock Reinforcement, Paris, 145-150*.

Gibson, R. E. (1953). Experimental determination of the true cohesion and true angle of internal friction in clays. Proc. of 3rd Int. Conf. on Soil Mech. and Foundation Eng., Zurich, 126-130.

Gibson, R. E., & Anderson, W. F. (1961). In situ measurements of soil properties with the pressuremeter. *Civil Eng. and Pub. Works Rev., Vol. 56, No 658*.

Goughnour, R. R. (1983). Settlement of vertically loaded stone columns in soft ground. Proc. 8th European Conf. on Soil Mechanics and Foundation Engineering, Helsinki, Vol. 1, pp.235-240.

Goughnour, R. R., & Bayuk, A. A. (1979a). Analysis of stone column - Soil matrix interaction under vertical load. C. R. Coll. Int. Renforcement des Sols, Paris, pp. 271-277.

Goughnour, R. R., & Bayuk, A. A. (1979b). A field study of long term settlements of loads supported by stone columns in soft ground. C. R. Coll. Int. Renforcement des Sols, Paris, pp. 279-285.

Greenwood, D. A. (1970). Mechanical improvement of soils below ground surface. *Proc. Conf. Ground Eng.*, 11-22.

Greenwood, D. A. (1991). Load tests on stone columns *Deep Foundations and Improvements, Design, Construction and Testing* (pp. 148-171): ASTM 1089.

Greenwood, D. A., & Kirsch, K. (1984). Specialist ground treatment by vibratory and dynamic methods - State of Art. *Proc. Int. Conf. on Piling and Ground Treatment*, 17-45.

Guetif, Z., Bouassida, M., & Debats, J. M. (2007). Improved soft clay characteristics due to stone column installation. *Computers & Geotechnics, 34*(2), 104-111.

Hassen, G., de Buhan, P., & Abdelkrim, M. (2010). Finite element implementation of a homogenized constitutive law for stone column-reinforced foundation soils, with application to the design of structures. *Computers & Geotechnics, 37*, 40-49.

Hughes, J. M. O., & Withers, N. J. (1974). Reinforcing of soft cohesive soils with stone columns. *Ground Engineering, 7*(3), 42-49.

Hughes, J. M. O., Withers, N. J., & Greenwood, D. A. (1976). A field trial of the reinforcing effect of a stone column in soil. *Proc., Ground Treatment by Deep Compaction, Institution of Civil Engineers*, 32-44.

Janbu, N. (1963). Soil compressibility as determined by oedometer and triaxial tests. *Proc. Eur. Conf. Soil Mech. and Found. Eng., 1*, 259-263.

Juillie, Y., & Sherwood, D. E. (1983). Improvement of Sabkha soil of the Arabian Gulf Coast. Proc. 8th European Conf. on Soil Mechanics and Foundation Engineering, Helsinki, Vol. 2, pp.781-788.

Karstunen, M., Krenn, H., Wheeler, S. J., Koskinen, M., & Zentar, R. (2005). Effect of anisotropy and destructuration on the behaviour of Murro test embankment. *International Journal of Geomechanics, 5*(2), 87-97.

Kurka, J., & Zavoral, J. (2009). New approach to calculation of stresses and strains in compressible ground improved with vibrated gravel-sand columns and model verification. *Proc. 17th Int. Conf. on Soil Mech. and Geotech. Eng.*, 2288-2291.

Lee, J. S., & Pande, G. N. (1998). Analysis of stone-column reinforced foundations. *International Journal for Numerical and Analytical Methods in Geomechanics, 22*(12), 1001-1020.

Leoni, M., Karstunen, M., & Vermeer, P. A. (2008). Anisotropic creep model for soft soils. *Geotechnique, 58*(3), 215-226.

Liu, X., Ammar, A. M. S., Lin, H., & Ren, J. (2009). The stress concentration ratio of stone columns under confined condition. *Int. Conf. on Transportation Eng.*, 4247-4255.

Look, B. (2007). *Handbook of Geotechnical Investigation and Design Tables*: Taylor and Francis, London.

Lopez, R. A., & Shao, L. (2007). Use of static and seismic deformation criteria for vibro replacement stone columns - a case history. *GSP 172 Soil Improvement*.

Madhav, M. R., & Miura, N. (1994). Stone columns. *XIII Int. Conf. on Soil Mech. and Foundation Eng., New Delhi, India*, 163-164.

Madhav, M. R., & Van Impe, W. F. (1994). Load transfer through a gravel bed on stone column reinforced soil. *Geotechnical Engineering, J. of the Southeast Asian Geotechnical Society*, 47-62.

Madhav, M. R., & Vitkar, P. P. (1978). Strip footing on weak clay stabilized with a granular trench or pile. *Canadian Geotechnical Journal, 15*(4), 605-609.

McCabe, B. A., & Egan, D. (2010). A review of the settlement of stone columns in compressible soils. *GeoShanghai 2010 International Conference*, 197-204.

McCabe, B. A., Mcneill, J. A., & Black, J. A. (2007). Ground Improvement using the Vibro Stone Column Technique. *The Institution of Engineers of Ireland*, 1-12.

McKelvey, D., Sivakumar, V., Bell, A., & Graham, J. (2004). Modelling vibrated stone columns in soft clay. *Proc. Instn. Civ. Engrs. Geotech. Engng, 157, 137-149*

McKenna, J. M., Eyre, W. A., & Wolstenholme, D. R. (1975). Performance of an embankment supported by stone columns in soft ground. *Geotechnique, 25*(1), 51-59.

Mitchell, J. K., & Gardner, W. S. (1975). In situ measurement of volume change characteristics. *Proc. ASCE Specialty Conf. on In-Situ Measurement of Soil Properties, 2*, 279-345.

Mitchell, J. K., & Huber, T. R. (1985). Performance of a stone column foundation. *ASCE, Journal of Geotechnical Engineering, 3*(2), 205-223.

Mohamedzein, Y. E.-A., & Al-Shibani, I. H. (2011). Performance of an embankment supported on soft soil reinforced by stone columns. *Ground Improvement, 164*(GI4), 213-224.

Munfakh, G. A., Abramson, L. W., Barksdale, R. D., & Juran, I. (1987). "In-Situ Ground Reinforcement", Soil Improvement - A Ten Year Update. In J. P. Welsh (Ed.), *Geotechnical Special Publication No. 12, ASCE, 1-17*.

Munfakh, G. A., Sarkar, S. K., & Castelli, R. P. (1983). Performance of a test embankment founded on stone columns. Proc. Int. Conf. on Advances in Piling and Ground treatment for Foundations, London, pp. 259-265.

Murali Krishna, A., Madhav, M. R., & Madhavi Latha, G. (2007). Densification effect of granular piles on settlement response of treated ground. *Ground Improvement, 11*(3), 127-136.

Nagaraj, T. S., & Srinivasa Murthy, B. R. (1985). Prediction of the preconsolidation pressure and recompression index of soils. *Geotechnical Testing Journal, GTJODJ, 8*(4), 192-202.

Najjar, S. S., Sadek, S., & Maaaroun, T. (2010). Effect of sand columns on the undrained load response of soft clays. *Journal of Geotechnical and Geoenvironmental Engineering, 136*(9), 1263-1277.

Poorooshasb, H. B., & Madhav, M. R. (1985). Application of rigid plastic dilatancy model for prediction of granular pile settlement. *Proc. 5th ICONMIG, Nagoya, Japan*.

Poorooshasb, H. B., & Meyerhof, G. G. (1997). Analysis of behavior of stone columns and lime columns. *Computers & Geotechnics, 20*(1), 47-70.

Priebe, H. J. (1995). The design of vibro replacement. *Ground Engineering, 28*(12), 31-37.

Priebe, H. J. (2005). The application of Priebe's method to extremely soft soils, floating foundations and proof against slope or embankment failure. *Ground Engineering*.

Raju, V. R. (1997a). The Behaviour of Very Soft Soils Improved by Vibro Replacement. *Ground Improvement Conference, London*.

Raju, V. R., Alam, M., & Ha, P. (1997b). Vibro Replacement - a technique for extensive ground improvement works in very soft cohesive soils at the Shah Alam Expressway. *4. Geotechnique Colloquium, Darmstadt*.

Raju, V. R., & Wegner, R. (2004). Ground improvement using vibro replacement in Asia 1994 to 2004 - a 10 year review. *5th Int. Conf. on Ground Improvement Techniques, Kuala Lumpur*.

Raju, V. R., Wegner, R., & Godenzie, D. (1998). Ground Improvement using Vibro Techniques. *Ground Improvement Conference, Singapore*.

Roscoe, K. H. (1970). The influence of strains in soil mechanics: 10th Rankine Lecture. *Geotechnique, 20*(2), 129-170.

Sadek, M., & Shahrour, I. (2008). Eccentricity effect on a footing supported by a stone column. *Ground Improvement, 161*(GI2), 65-70.

Saha, A., & De, P. K. (1994). Field and analytical study of stone columns by non-linear strain. *XIII Int. Conf. on Soil Mech. and Foundation Eng., New Delhi, India*, 1211-1214.

Schweiger, H. F., & Pande, G. N. (1986). Numerical analysis of stone column supported foundations. *Computers & Geotechnics, 2*(6), 347-372.

Serridge, C. J., & Sarsby, R. W. (2009). A review of field trials investigating the performance of partial depth vibro stone columns in a deep soft clay deposit. *Geotechnics of Soft Soils - Focus on Ground Improvement*, 293-298.

Shahu, J. T., Madhav, M. R., & Hayashi, S. (2000). Analysis of soft ground-granular pile-granular mat system. *Computers & Geotechnics, 27*(1), 45-62.

Shahu, J. T., & Reddy, Y. R. (2011). Clayey Soil Reinforced with Stone Column Group: Model Tests and Analyses. *Journal of Geotechnical and Geoenvironmental Engineering, 137*(12), 1265-1274.

Sivakumar, V., Jeludine, D. K. N. M., Bell, A., Glynn, D. T., & Mackinnon, P. (2011). The pressure distribution along stone columns in soft clay under consolidation and foundation loading. *Geotechnique, 61*(7), 613-620.

Sivakumar, V., McKelvey, D., Graham, J., & Hughes, D. (2004). Triaxial tests on model sand columns in clay. *Canadian Geotechnical Journal, 41*(2), 299-312.

Skempton, A. W., & Bjerrum, L. (1957). A contribution to the settlement analysis of foundations on clay. *Geotechnique, 7*(4), 168-178.

Stuedlein, A. W., & Holtz, R. D. (2011). Analysis of footing load tests on aggregate pier reinforced clay. *Journal of Geotechnical and Geoenvironmental Engineering, 138*(9), 1091-1103.

Tan, S. A., Tjahyono, S., & Oo, K. K. (2008). Simplified plane-strain modeling of stone-column reinforced ground *Journal of Geotechnical and Geoenvironmental Engineering, 134*(2), 185-194.

Van Impe, W. F., & De Beer, E. (1983). Improvement of settlement behavior of soft layers by means of stone columns. Proc. 8th European Conf. on Soil Mechanics and Foundation Engineering, Helsinki, Vol. 1, pp.309-312.

Van Impe, W. F., De Cock, F., Van Der Cruyssen, J. P., & Maertens, J. (1997b). Soil improvement experiences in Belgium: Part III. Case Histories. *Ground Improvement, 1*, 179-191.

Van Impe, W.F., Madhav, M.R., & Vandercruyssen, J.P. (1997). Considerations in Stone Column Design. In M.C.R. Davies and F. Schlosser (Ed.), *Ground Improvement Geosystems- Densification and Reinforcement* (pp. 190-196).

Watts, K. S., Chown, R. C., Serridge, C. J., & Crilly, M. S. (2001). Vibro stone columns in soft clay soil - a trial to study the influence of column installation on foundation performance. *Proc. 15th Int. Conf. on Soil Mech. and Ground Eng., Istanbul, 3*, 1867-1870.

Watts, K. S., Johnson, D., Wood, L. A., & Saadi, A. (2000). An instrumented trial of vibro ground treatment supporting strip foundations in a variable fill. *Geotechnique, 50*(6), 699-708.

Weber, T. M., Springman, S. M., Gaeb, M., Racansky, V., & Schweiger, H. F. (2009). Numerical modelling of stone columns in soft clay under an embankment. *Geotechnics of Soft Soils - Focus on Ground Improvement*, 305-311.

Wiltafsky, C., & Thurner, R. (2009). Soil improvement by vibro replacement and preloading for the foundation of a shopping centre on weak marine deposits. *Geotechnics of Soft Soils - Focus on Ground Improvement*, 429-434.

Wood, D. M., Hu, W., & Nash, D. F. T. (2000). Group effects in stone column foundations: model tests. *Geotechnique, 50*(6), 689-698.

Xie, K.-H., Lu, M.-M., & Liu, G.-B. (2009). Equal strain consolidation for stone columns reinforced foundation. *International Journal for Numerical and Analytical Methods in Geomechanics, 33*(15), 1721-1735.

Zhang, L., Zhao, M., Shi, C., & Zhao, H. (2012). Settlement calculation of composite foundation reinforced with stone columns. *International Journal of Geomechanics*.

APPENDIX A

RESULTS OF PARAMETRIC STUDIES

Appendix A presents the results of parametric studies in table format. Values in first row are the baseline analysis parameters. Only varied parameters are shown in tables. Subscripts s and c stand for soil and column, respectively.

Table A.1 Parametric Study Result for Omdurman Case

E_s (kPa)	ν_s	ϕ_s (deg)	$K_{0.s}$	E_c (kPa)	ν_c	ϕ_c (deg)	ψ_c (deg)	S_r
1150	**0.3**	**27**	**0.546**	**34500**	**0.3**	**42**	**0**	**0.5808**
"	"	"	"	"	"	"	6	0.5662
"	"	"	"	"	"	"	12	0.5500
"	"	"	"	"	"	"	24	0.5100
"	"	"	"	"	"	"	42	0.4264
"	"	"	"	2300	"	"	"	0.7869
"	"	"	"	6125	"	"	"	0.6166
"	"	"	"	11500	"	"	"	0.5858
"	"	"	"	17500	"	"	"	0.5836
"	"	"	"	52500	"	"	"	0.5806
850	"	"	"	"	"	"	"	0.6989
1000	"	"	"	"	"	"	"	0.6343
1500	"	"	"	"	"	"	"	0.4865
2000	"	"	"	"	"	"	"	0.3941
3000	"	"	"	"	"	"	"	0.2889
"	"	"	"	"	"	38	"	0.6282
"	"	"	"	"	"	40	"	0.6055
"	"	"	"	"	"	44	"	0.5566
"	"	"	"	"	"	48	"	0.5061
"	"	20	"	"	"	"	"	0.5854
"	"	23	"	"	"	"	"	0.5828
"	"	29	"	"	"	"	"	0.5806
"	0.25	"	"	"	"	"	"	0.6498
"	0.27	"	"	"	"	"	"	0.6242
"	0.33	"	"	"	"	"	"	0.5330
"	0.35	"	"	"	"	"	"	0.4950
"	"	"	"	"	0.25	"	"	0.5825
"	"	"	"	"	0.27	"	"	0.5821
"	"	"	"	"	0.33	"	"	0.5806
"	"	"	"	"	0.35	"	"	0.5795
"	"	"	0.5	"	"	"	"	0.5886
"	"	"	0.75	"	"	"	"	0.5515
"	"	"	1	"	"	"	"	0.5164
"	"	"	1.2	"	"	"	"	0.4889
"	"	"	1.4	"	"	"	"	0.4631

Table A.2 Parametric Study Result for Kebun Case

E_s (kPa)	ν_s	$c_{u.s}$ (kPa)	$K_{0.s}$	E_c (kPa)	ν_c	ϕ_c (deg)	ψ_c (deg)	S_r
500-1000	**0.3**	**9-15**	**0.658**	**31000**	**0.3**	**40**	**0**	**0.4665**
"	"	"	"	"	"	"	5	0.4516
"	"	"	"	"	"	"	10	0.4281
"	"	"	"	"	"	"	20	0.3881
"	"	"	"	"	"	"	40	0.2760
"	"	"	"	2000	"	"	"	0.7037
"	"	"	"	5000	"	"	"	0.4922
"	"	"	"	10000	"	"	"	0.4748
"	"	"	"	20000	"	"	"	0.4698
250-750	"	"	"	"	"	"	"	0.6809
750-1250	"	"	"	"	"	"	"	0.3573
1000-1500	"	"	"	"	"	"	"	0.2861
1500-2000	"	"	"	"	"	"	"	0.2005
2500-3000	"	"	"	"	"	"	"	0.1250
"	"	"	"	"	"	38	"	0.4952
"	"	"	"	"	"	39	"	0.4802
"	"	"	"	"	"	41	"	0.4479
"	"	"	"	"	"	42	"	0.4468
"	"	"	"	"	"	48	"	0.3644
"	"	12-18	"	"	"	"	"	0.4651
"	"	15-21	"	"	"	"	"	0.4641
"	"	"	0.55	"	"	"	"	0.4966
"	"	"	0.75	"	"	"	"	0.4546
"	"	"	1.0	"	"	"	"	0.4026
"	"	"	1.2	"	"	"	"	0.3769
"	"	"	1.4	"	"	"	"	0.3413
"	0.25	"	"	"	"	"	"	0.5821
"	0.27	"	"	"	"	"	"	0.5297
"	0.33	"	"	"	"	"	"	0.4004
"	0.35	"	"	"	"	"	"	0.3570

Table A.3 Parametric Study Result for Canvey Island Case

E_s (kPa)	ν_s	$c_{u.s}$ (kPa)	$K_{0.s}$	E_c (kPa)	ν_c	ϕ_c (deg)	ψ_c (deg)	S_r
874	**0.3**	**23**	**0.6**	**33250**	**0.3**	**40**	**0**	**0.3666**
"	"	"	"	"	"	"	5	0.3469
"	"	"	"	"	"	"	10	0.3306
"	"	"	"	"	"	"	20	0.2957
"	"	"	"	"	"	"	40	0.2206
"	"	"	"	2500	"	"	"	0.8150
"	"	"	"	5000	"	"	"	0.5496
"	"	"	"	10000	"	"	"	0.4214
"	"	"	"	20000	"	"	"	0.3767
"	"	"	"	40000	"	"	"	0.3625
650	"	"	"	"	"	"	"	0.4154
1000	"	"	"	"	"	"	"	0.3455
1500	"	"	"	"	"	"	"	0.2918
2000	"	"	"	"	"	"	"	0.2598
3000	"	"	"	"	"	"	"	0.2216
"	"	"	"	"	"	38	"	0.3833
"	"	"	"	"	"	39	"	0.3764
"	"	"	"	"	"	41	"	0.3572
"	"	"	"	"	"	42	"	0.3472
"	"	"	"	"	"	48	"	0.3080
"	"	"	0.5	"	"	"	"	0.3747
"	"	"	0.7	"	"	"	"	0.3596
"	"	"	1.0	"	"	"	"	0.3376
"	"	"	1.2	"	"	"	"	0.3255
"	"	"	1.4	"	"	"	"	0.3114
"	0.25	"	"	"	"	"	"	0.3887
"	0.27	"	"	"	"	"	"	0.3792
"	0.33	"	"	"	"	"	"	0.3479
"	0.35	"	"	"	"	"	"	0.3335

APPENDIX B

TOTAL DISPLACEMENT CONTOURS

FOR CASE HISTORIES

Appendix B presents the output results of total displacements for three case histories.

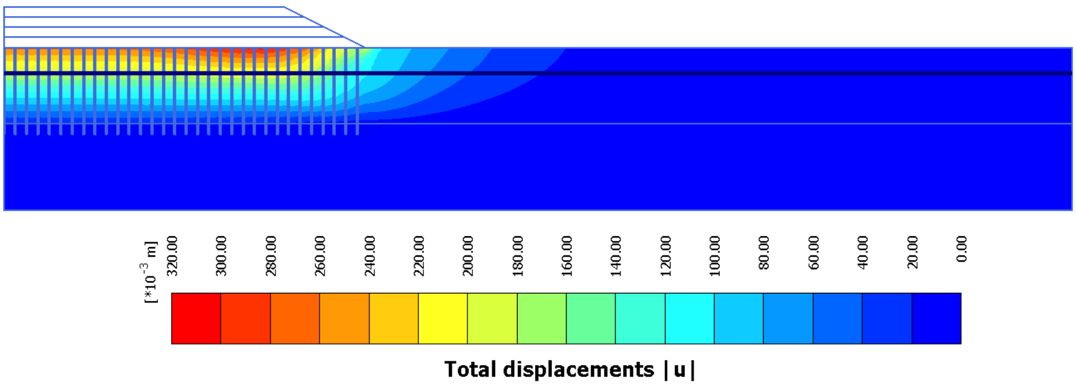

Figure B.1 Total Displacement Contours for Omdurman Case 2D MC Model

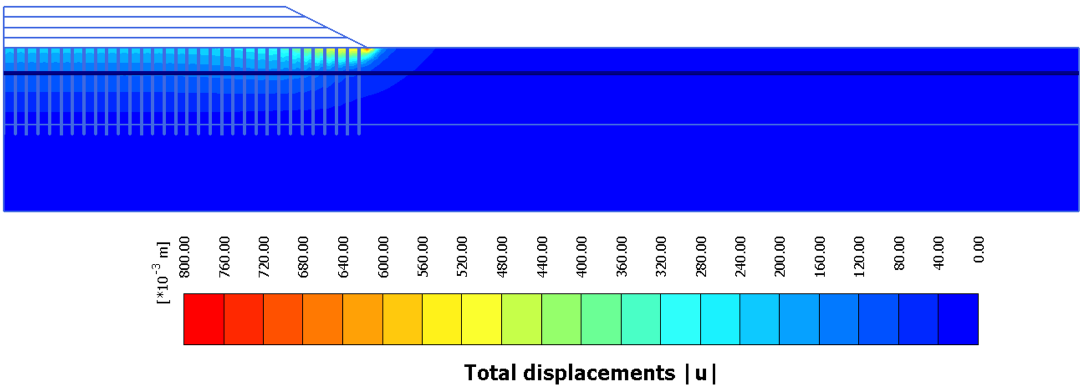

Figure B.2 Total Displacement Contours for Omdurman Case 2D HS Model

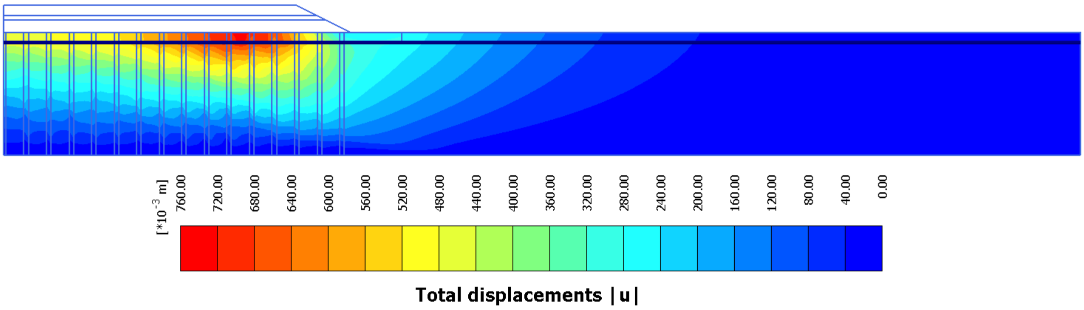

Figure B.3 Total Displacement Contours for Kebun Case 2D MC Model

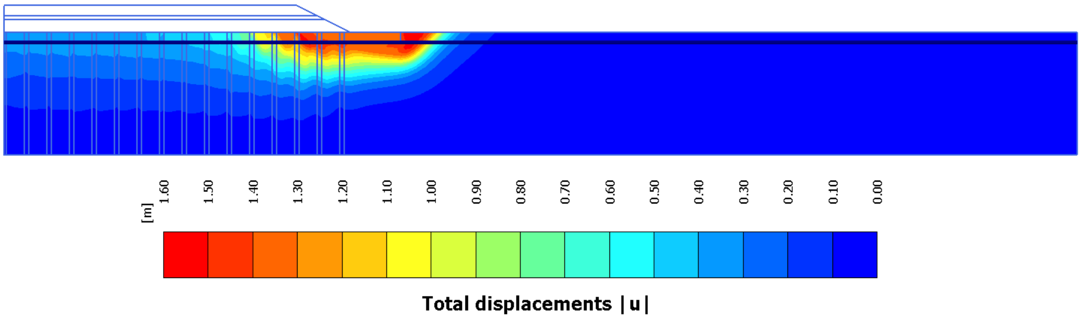

Figure B.4 Total Displacement Contours for Kebun Case 2D HS Model

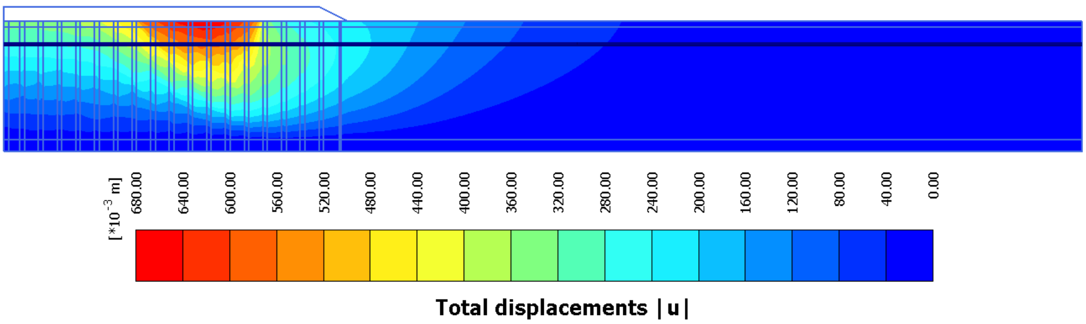

Figure B.5 Total Displacement Contours for Canvey Island Case 2D MC Model

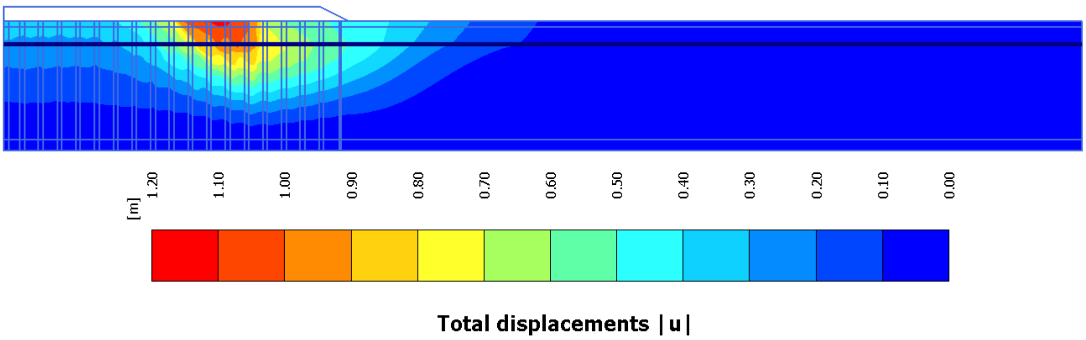

Figure B.6 Total Displacement Contours for Canvey Island Case 2D HS Model

APPENDIX C

PORE PRESSURE GENERATION FOR CASE HISTORIES

Appendix C presents the output results of excess pore water pressures generated in three case histories 2D MC models.

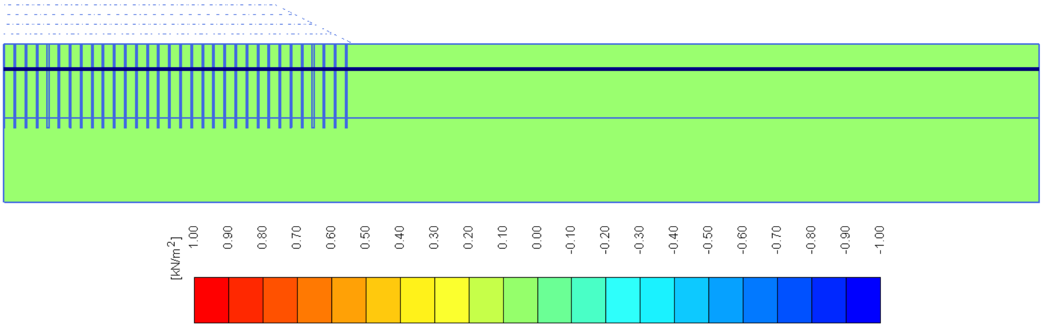

Figure C.1 Initial Phase Pore Pressure Generation for Omdurman Case

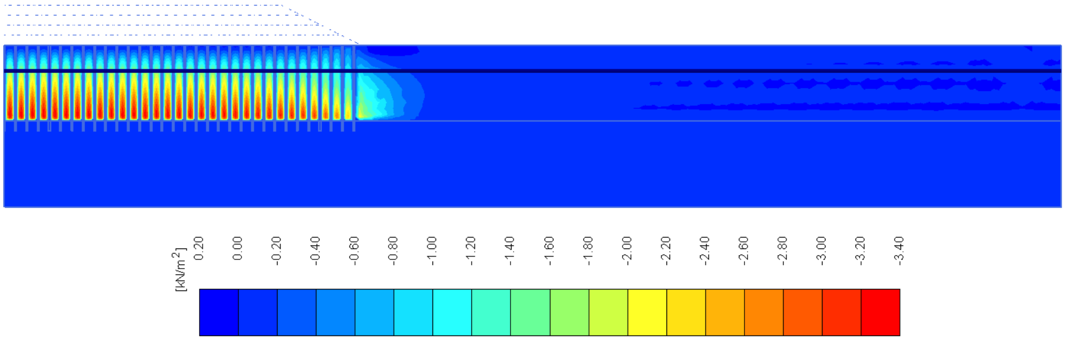

Figure C.2 Phase-1 Pore Pressure Generation for Omdurman Case

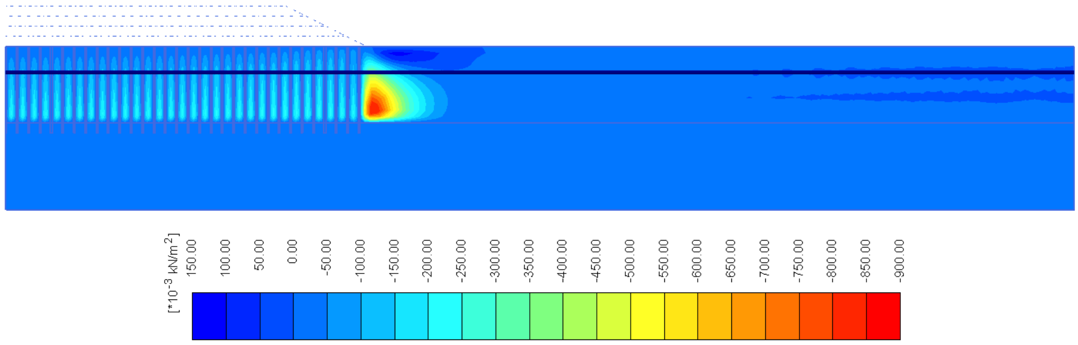

Figure C.3 Phase-2 Pore Pressure Generation for Omdurman Case

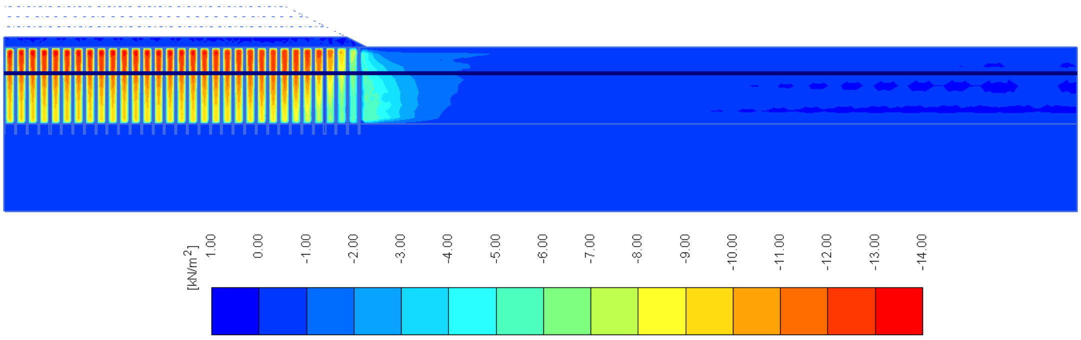

Figure C.4 Phase-3 Pore Pressure Generation for Omdurman Case

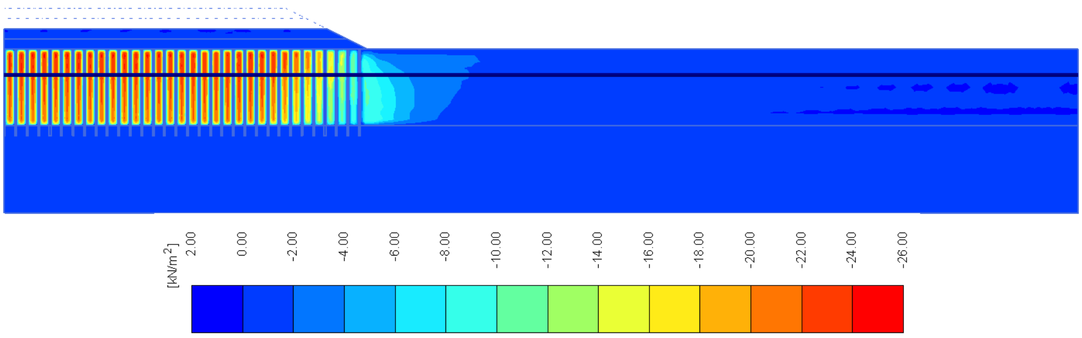

Figure C.5 Phase-4 Pore Pressure Generation for Omdurman Case

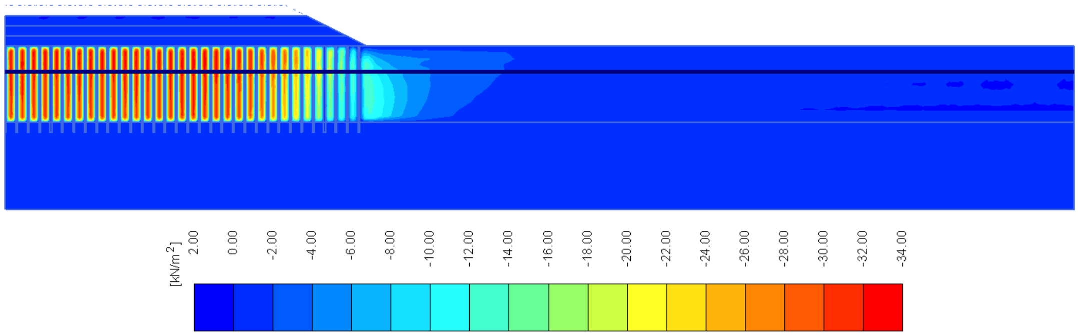

Figure C.6 Phase-5 Pore Pressure Generation for Omdurman Case

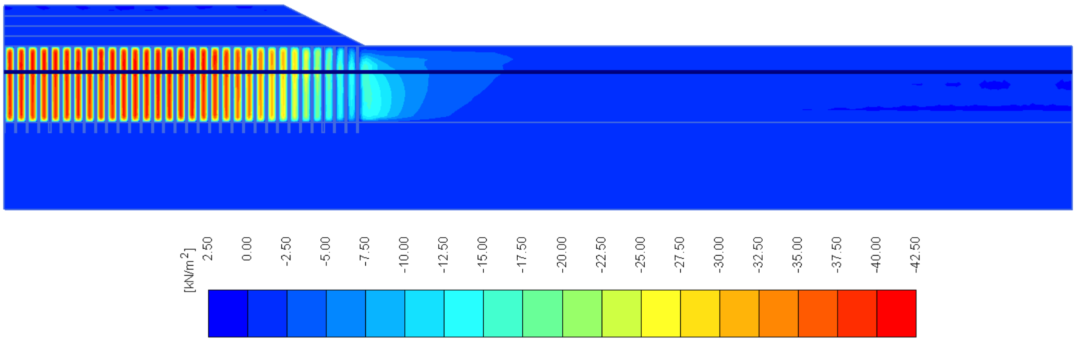

Figure C.7 Phase-6 Pore Pressure Generation for Omdurman Case

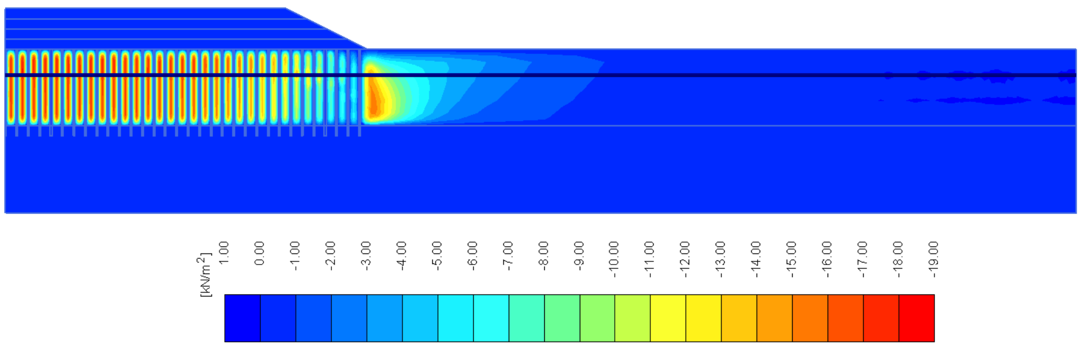

Figure C.8 Phase-7 Pore Pressure Generation for Omdurman Case

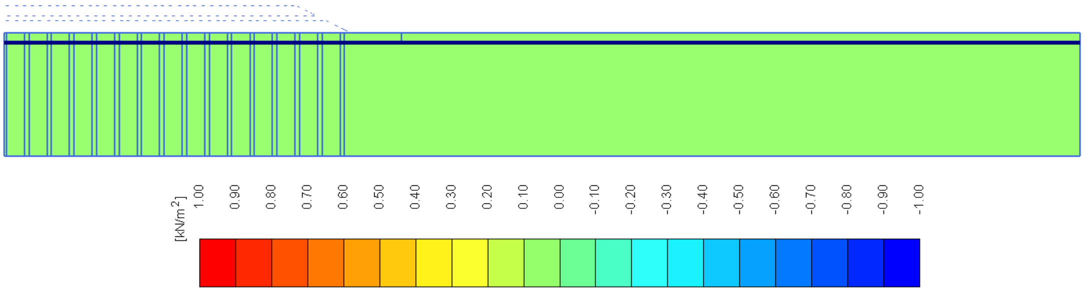

Figure C.9 Initial Phase Pore Pressure Generation for Kebun Case

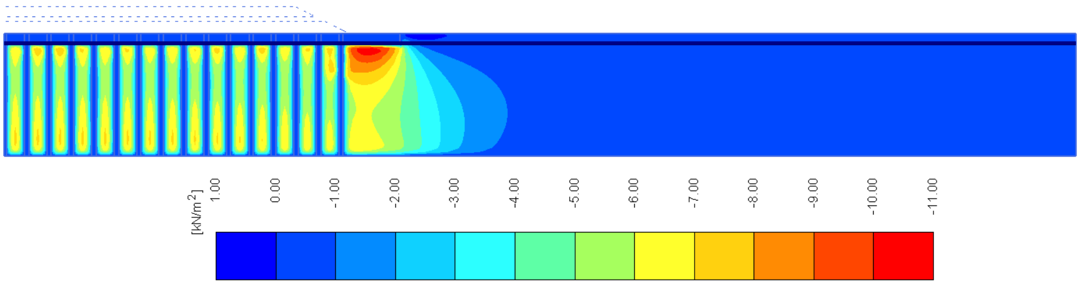

Figure C.10 Phase-1 Pore Pressure Generation for Kebun Case

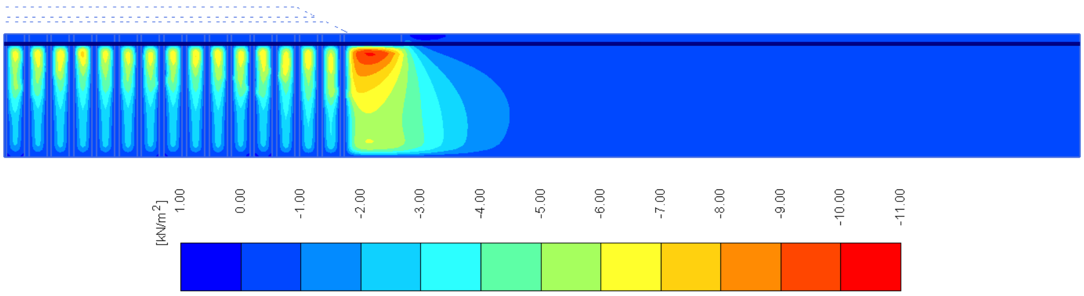

Figure C.11 Phase-2 Pore Pressure Generation for Kebun Case

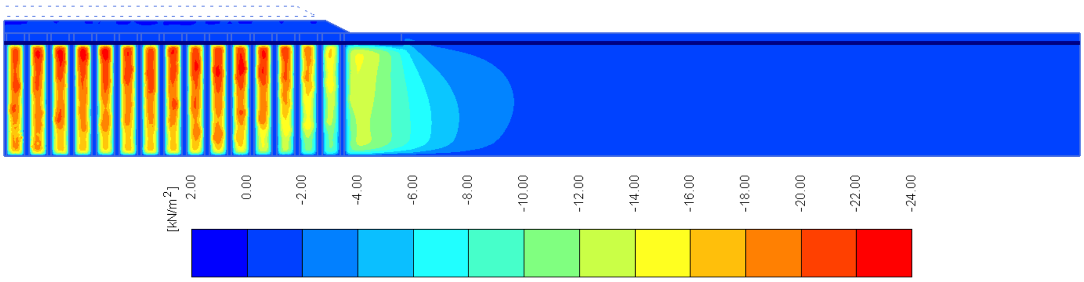

Figure C.12 Phase-3 Pore Pressure Generation for Kebun Case

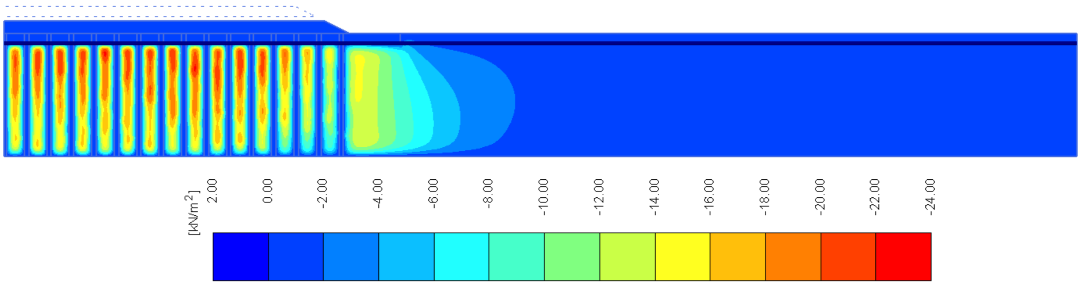

Figure C.13 Phase-4 Pore Pressure Generation for Kebun Case

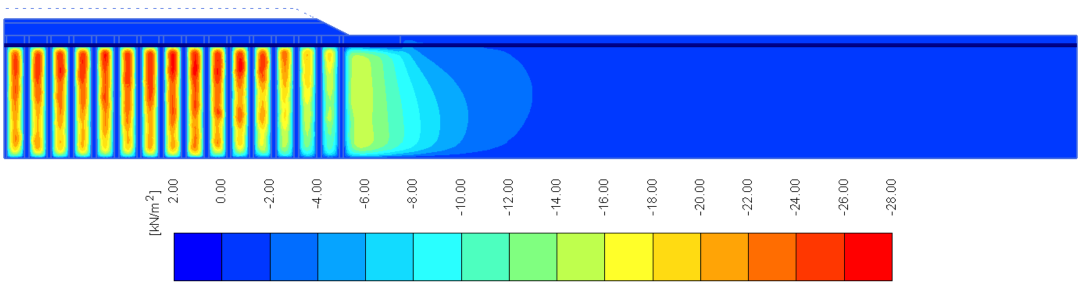

Figure C.14 Phase-5 Pore Pressure Generation for Kebun Case

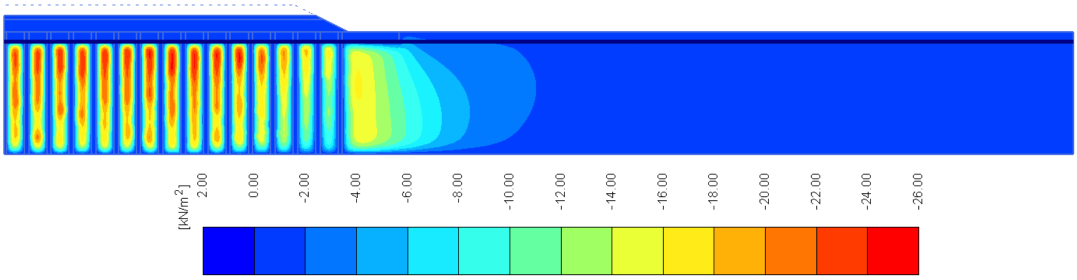

Figure C.15 Phase-6 Pore Pressure Generation for Kebun Case

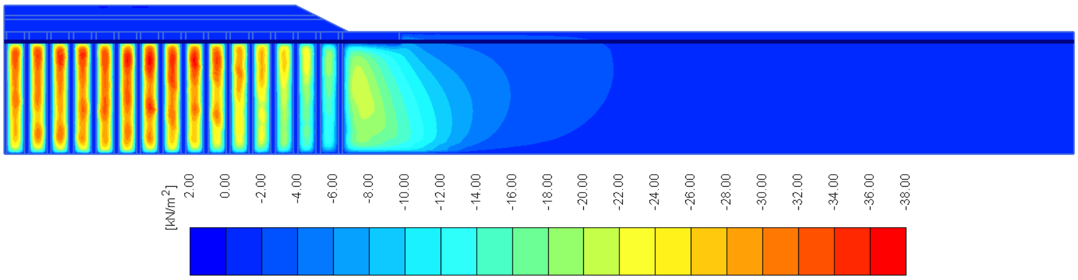

Figure C.16 Phase-7 Pore Pressure Generation for Kebun Case

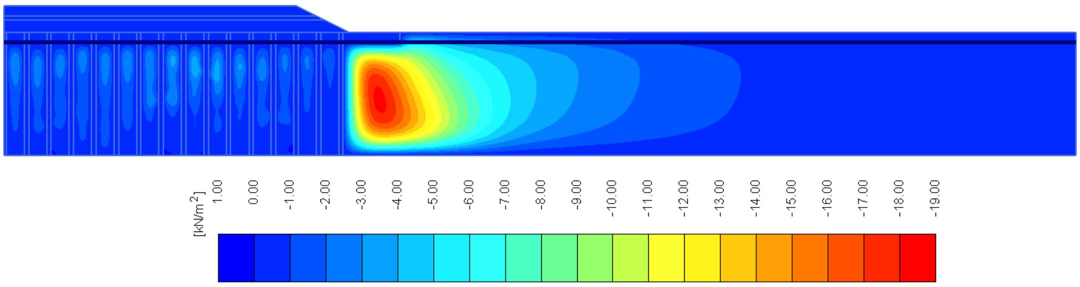

Figure C.17 Phase-8 Pore Pressure Generation for Kebun Case

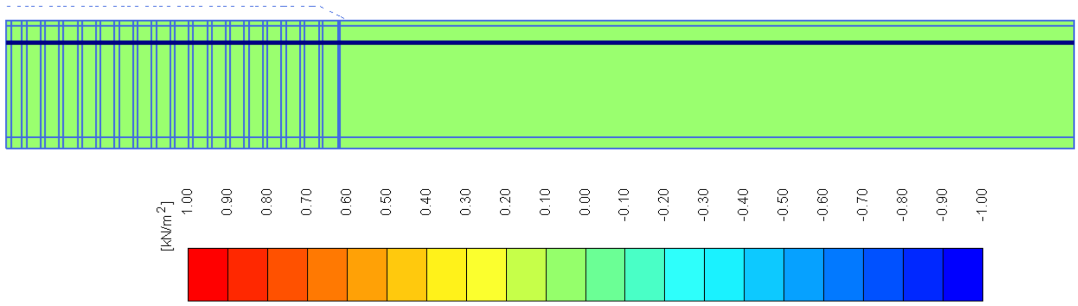

Figure C.18 Initial Phase Pore Pressure Generation for Canvey Island Case

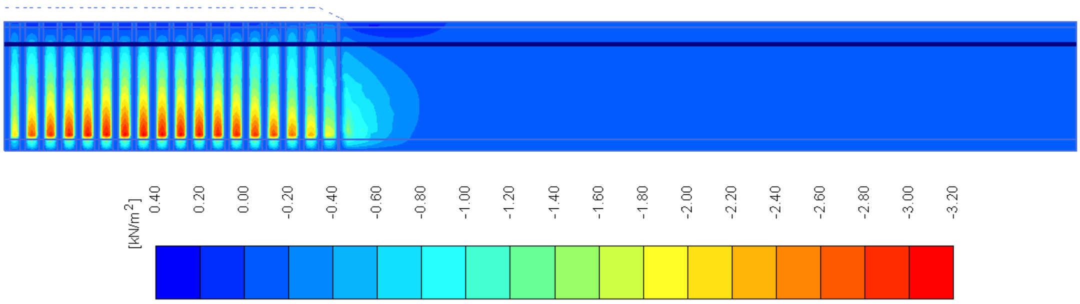

Figure C.19 Phase-1 Pore Pressure Generation for Canvey Island Case

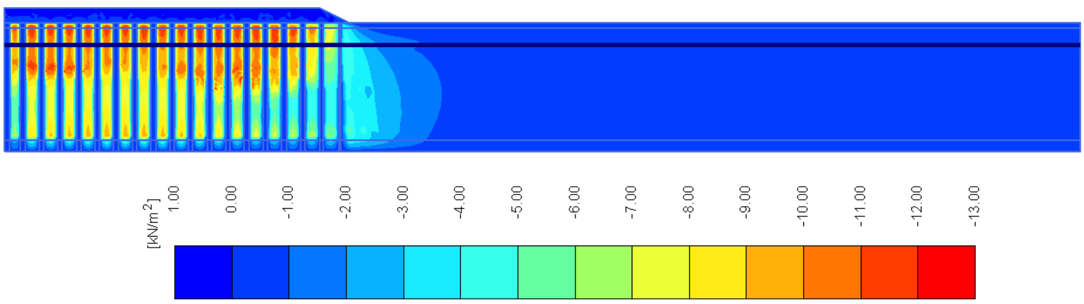

Figure C.20 Phase-2 Pore Pressure Generation for Canvey Island Case

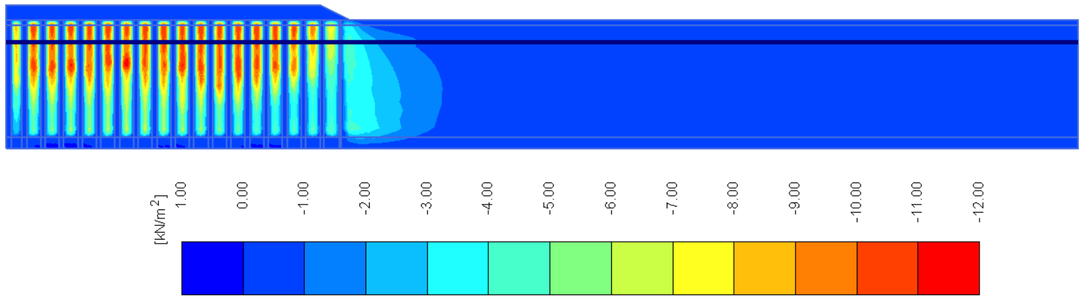

Figure C.21 Phase-3 Pore Pressure Generation for Canvey Island Case

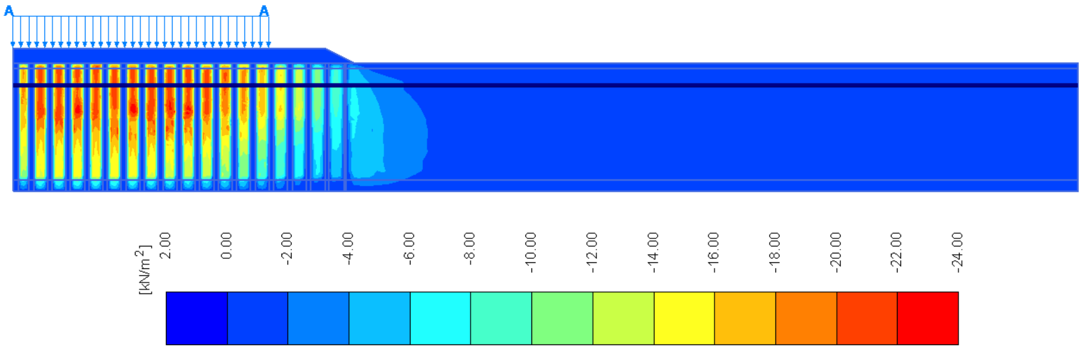

Figure C.22 Phase-4 Pore Pressure Generation for Canvey Island Case

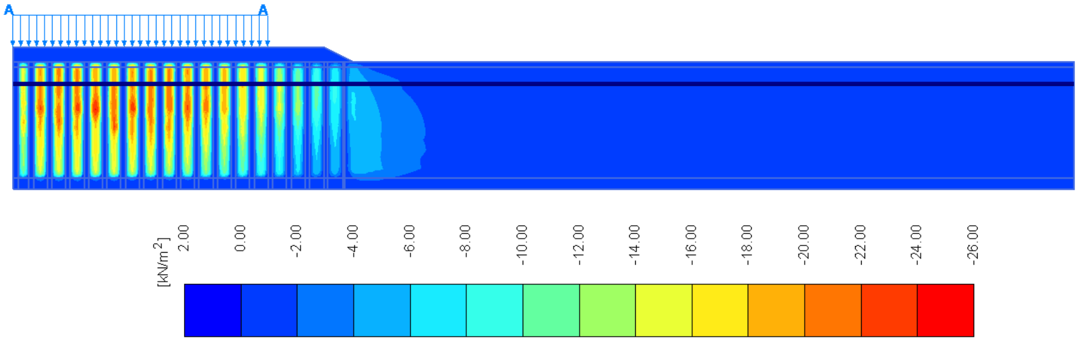

Figure C.23 Phase-5 Pore Pressure Generation for Canvey Island Case

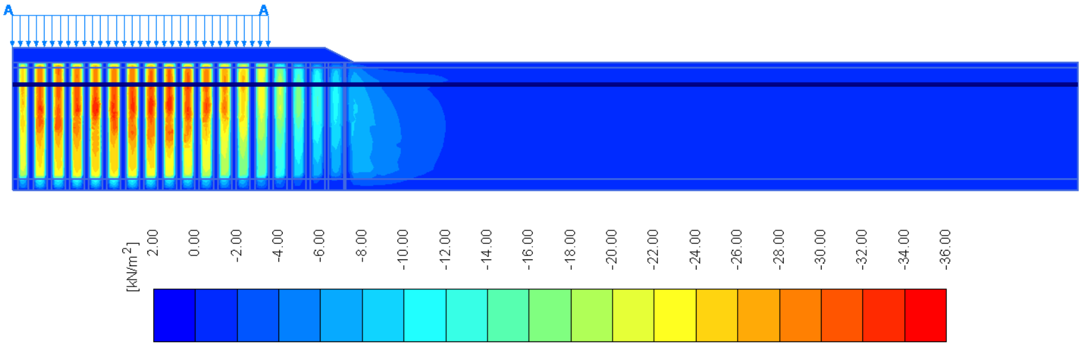

Figure C.24 Phase-6 Pore Pressure Generation for Canvey Island Case

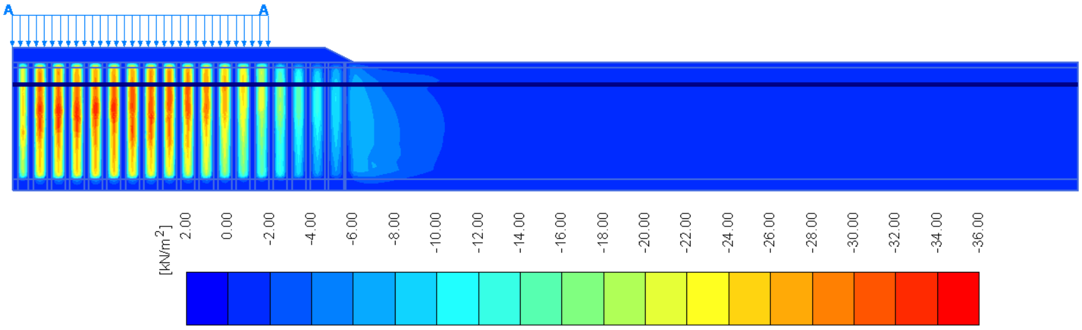

Figure C.25 Phase-7 Pore Pressure Generation for Canvey Island Case

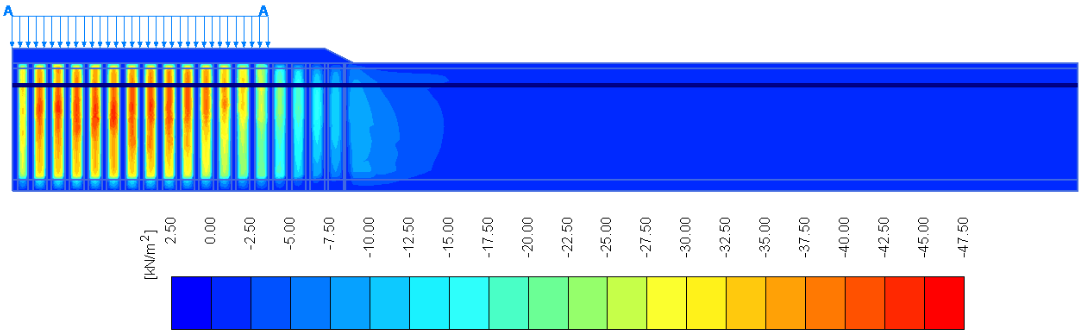

Figure C.26 Phase-8 Pore Pressure Generation for Canvey Island Case

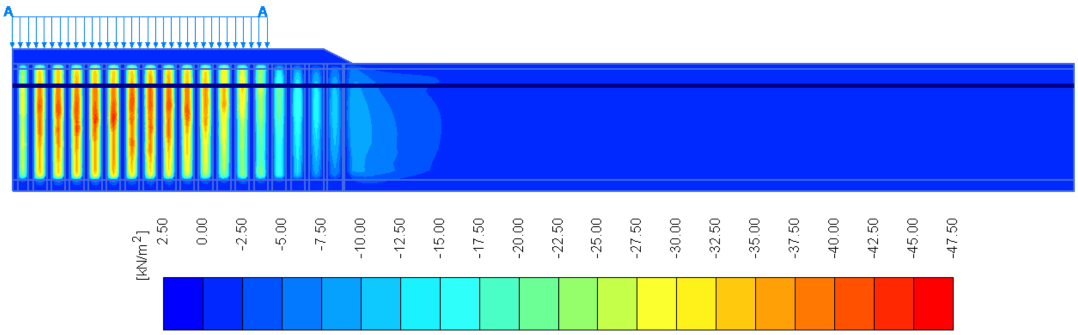

Figure C.27 Phase-9 Pore Pressure Generation for Canvey Island Case

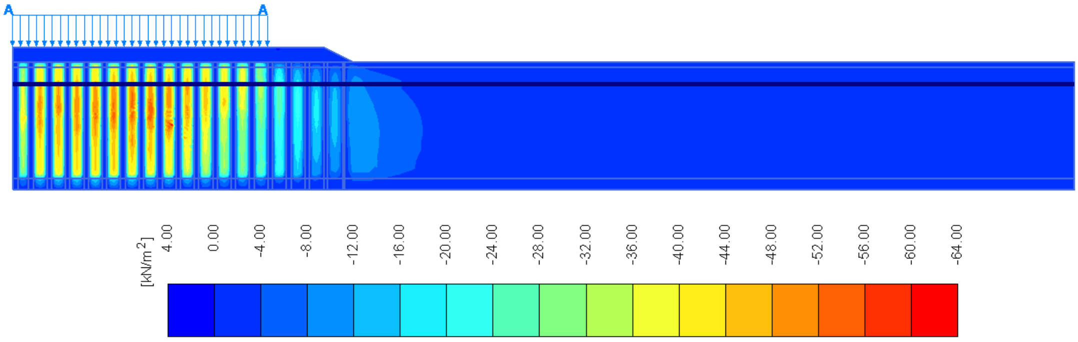

Figure C.28 Phase-10 Pore Pressure Generation for Canvey Island Case

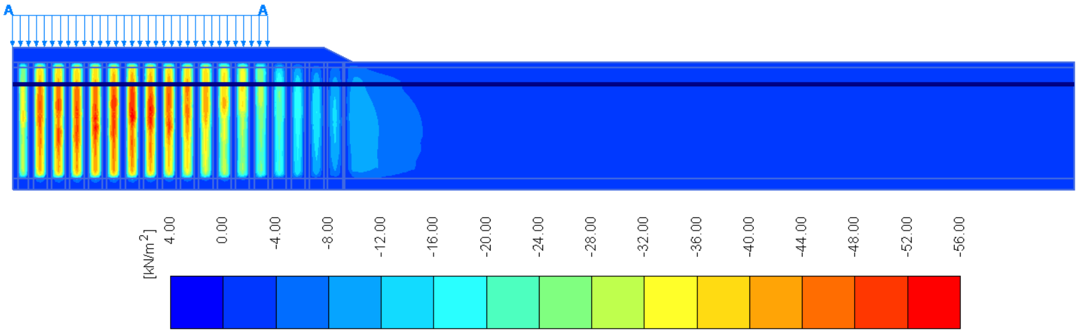

Figure C.29 Phase-11 Pore Pressure Generation for Canvey Island Case

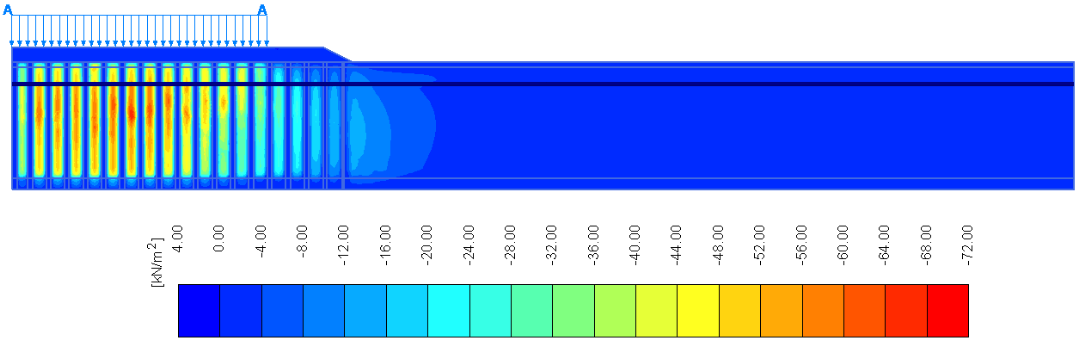

Figure C.30 Phase-12 Pore Pressure Generation for Canvey Island Case

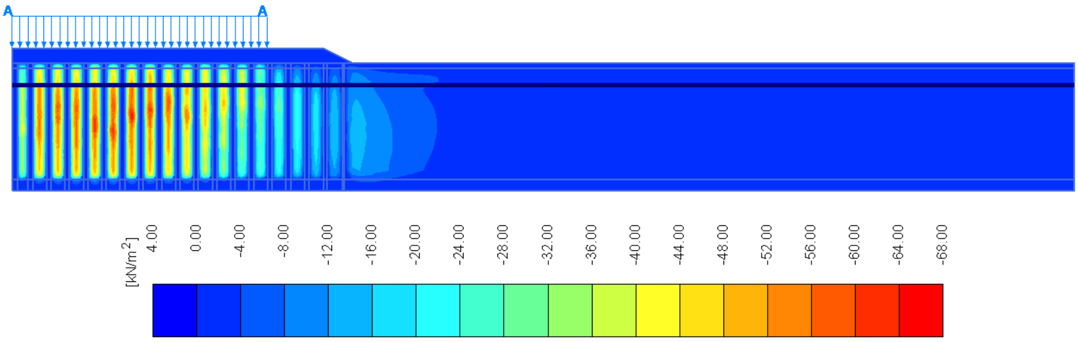

Figure C.31 Phase-13 Pore Pressure Generation for Canvey Island Case

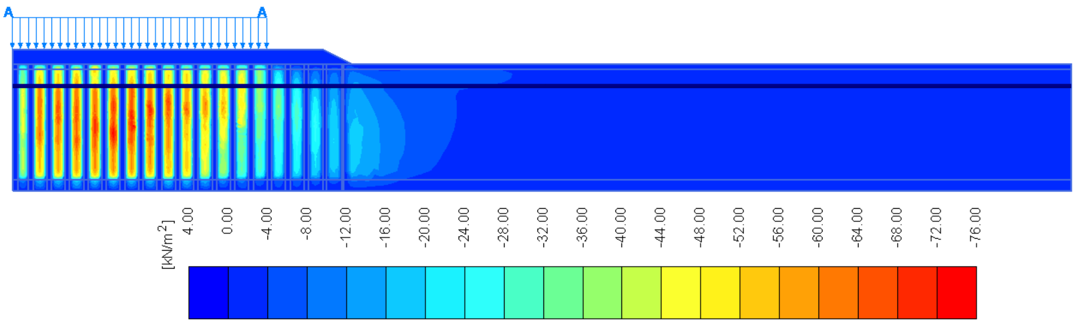

Figure C.32 Phase-14 Pore Pressure Generation for Canvey Island Case

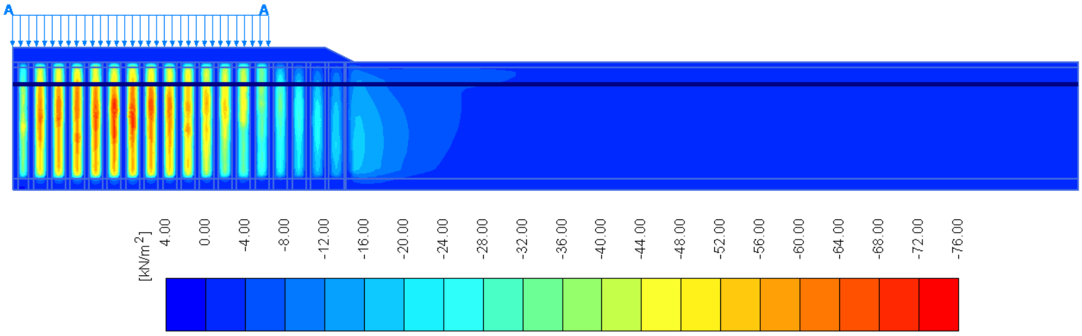

Figure C.33 Phase-15 Pore Pressure Generation for Canvey Island Case

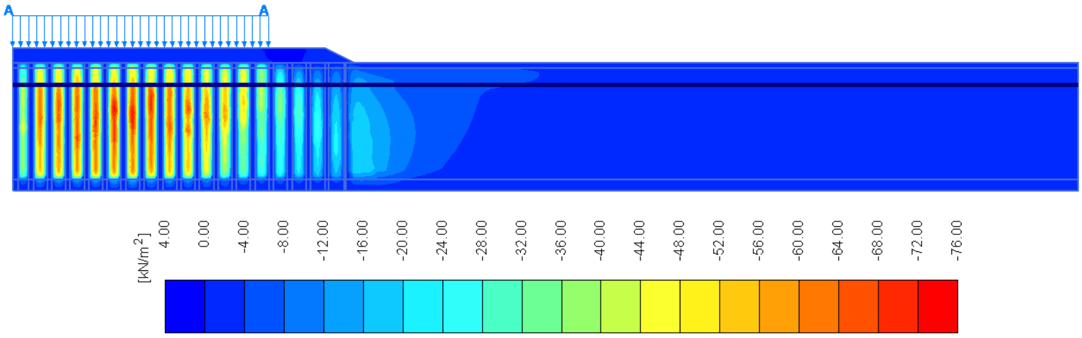

Figure C.34 Phase-16 Pore Pressure Generation for Canvey Island Case

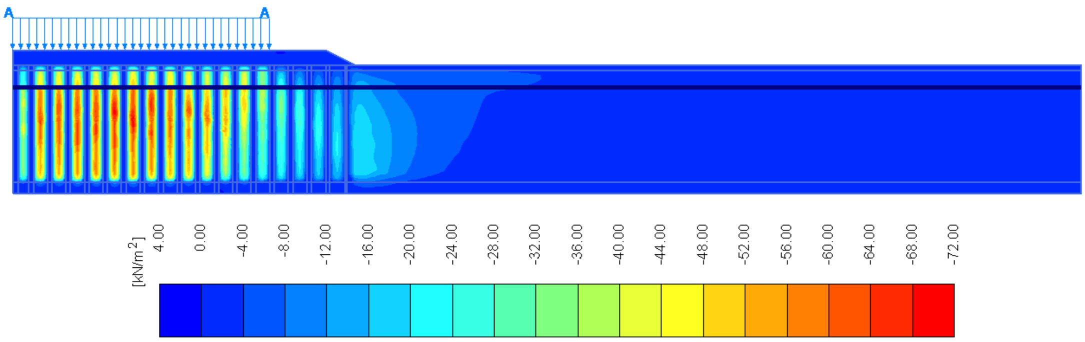

Figure C.35 Phase-17 Pore Pressure Generation for Canvey Island Case